NUCLEONICS VOL. 4, NO. 4, APRIL, 1949

An International Journal for Techniques and Applications of Nuclear Science

TECHNICAL CONSULTANTS

John R. Dunning, Clark Goodman, A. Kalitinsky, R. E. Lapp, W. F. Libby, L. A. Ohlinger, Winfield W. Salisbury, T. I. Taylor, E. O. Wollan

With the cooperation of . . .

THE NETHERLANDS C. J. BAKKER; GREAT BRITAIN E. BRETSCHER; DENMARK and SWEDEN GEORGE HEVESY; GERMANY HANS KOPFERMANN; SWITZERLAND P. SCHERRER; CANADA L. YAFFE

CONTENTS

Crystal Counters—I 2
ROBERT HOFSTADTER

Stack Meteorology and Atmospheric Disposal of Radioactive Wastes 28
NORMAN R. BEERS

Cosmic Rays—I 39
J. M. JAUCH

The Proton Microscope 52
CLAUDE MAGNAN

Gamma-ray Well Logging 67
ROBERT E. FEARON

NUCLEONIC EVENTS 76
BOOKS 79
PRODUCTS AND MATERIALS 81
ABSTRACTS 84

Keith Henney ..... Editor
Jerome D. Luntz ..... Assistant Editor
Ethel Pelzer ..... Assistant Editor
Gladys Montgomery . Washington Editor
S. D. Kirkpatrick ..... Consulting Editor
P. W. Swain ..... Consulting Editor
E. J. Tangerman ..... General Manager

NUCLEONICS (with which is consolidated "Atomic Power" and "Atomic Engineering") April, 1949, Vol. 4, No. 4. Publication Office: 212 East York St., York, Pa. Editorial and Circulation Offices: 330 W. 42nd St., New York 18, N. Y. Published monthly by McGraw-Hill Publishing Company, Inc. Entered as second class matter December 17, 1947, in the Post Office at York Pa., under the act of March 3, 1879. Copyright 1949 by McGraw-Hill Publishing Company, Inc. All rights reserved. James J. McGraw, Jr., President; J. A. Gerardi, Secretary; Curtis W. McGraw, Treasurer. Allow at least ten days for change of address. All communications about subscriptions should be addressed to J. E. Blackburn, Jr., Director of Circulation, 330 W. 42nd St., New York 18, N. Y. Price per copy $1. Subscription rates: United States and U. S. Possessions $10 for 1 year, $16 for 2 years, $20 for 3 years. Canada $15 a year. Latin America $20 a year. All other countries $25 a year. Return postage guaranteed. Member A.B.C.

CRYSTAL COUNTERS—I

One of the first extensive reviews of a field in which there has been considerable activity since publication of Van Heerden's paper in 1945. An active investigator, the author describes his own work and reviews the available literature. Discussed in the first part of two papers are the theory of operation and the properties of crystal counters, the characteristics and methods of preparation of a number of crystals investigated to date, and experimental techniques used

By ROBERT HOFSTADTER

Palmer Physical Laboratory, Princeton University
Princeton, New Jersey

UP TO THE PRESENT TIME, various types of gas-filled particle and photon counters (*1*, *2*) have made possible the accumulation of a vast body of experimental data in the field of nuclear physics. There seemed to have been little need in the past for other types of counters. However, the many new branches of study now being investigated require improved means of counting individual particles or photons.

Such fields as interaction of gamma rays with matter, study of time decays in the disintegration of elementary particles and nuclei, work with large pulsed machines such as the synchrotron and synchrocyclotron, and cosmic ray research require much faster counting mechanisms than have been used previously. The difficulties in using gas counters for such work are due to either long collection times, long deadtimes or small efficiencies of counting.

The development of the "solid counter" at this time is thus most opportune. The "crystal conduction-type counter" and the "scintillation counter" appear to have great promise in the unfolding of new information in the fields mentioned above. It is the purpose of this account to present some of the known facts about the first of these counters, the crystal counter. Unfortunately, relatively little published material is available for study of the crystal counter, and it is therefore with some hesitation that the following survey is presented.

HISTORICAL NOTE

Very early investigations of the effects of ionizing radiation on crystals showed clear indications of induced conductivity. However, the smallness of the observed effects, polarization effects, unfortunate choice of materials (mica, glass, quartz, rocksalt) and the lack of suitable amplifying and counting techniques made discovery of the crystal counter highly improbable. Early workers in this field included W. C. Röntgen and A. Joffé (*3*), H. Schiller (*4*), and G. Jaffé (*5*). A complete bibliography of this very interesting early work is given in the article by Jaffé.

The crystal counter was first described as a practical instrument for detection of single particles by P. J.

van Heerden in a now-famous doctor's dissertation (*6*). Van Heerden's work was accomplished with silver chloride crystals at low temperature. Shortly after van Heerden's discovery, and apparently independently, R. Frerichs and R. Warminsky (*7*) showed that beta particles and gamma rays could be detected by pure, cadmium sulfide crystals. Here, ionization currents caused by the simultaneous entrance of a large number of beta particles or gamma quanta were reported. It was suggested that single particles might be detected in CdS with amplifying means.

The first observation of individual conductivity pulses in solids (diamond) has been described, however, by G. Stetter (*8*), although his observation was not followed up in enough detail to produce a counter. The existence of the early work described by Stetter has been pointed out by W. Jentschke (*9*). In this country the earliest work on the crystal counter was performed by D. E. Wooldridge, A. J. Ahearn and J. A. Burton (*10*) who reported a positive counting effect in diamond. Confirmation and extension of van Heerden's work was performed by J. C. Street (*11*) and R. Hofstadter (*12, 13*). Other investigators also performed similar work but have not reported their findings.

Many groups have since carried on crystal counter work, both for its own sake, and in experiments involving cosmic rays. Among these are D. R. Corson and R. R. Wilson (*2*), L. F. Wouters and R. S. Christian (*14*), L. F. Curtiss and B. W. Brown (*15*), W. L. Whittemore and J. C. Street (*16*), G. T. Reynolds (*17*), and others (*18*).

GENERAL PROPERTIES

Conduction and Counting Phenomenon

The work of van Heerden (*6*) provides an excellent introduction to the subject of crystal counters. The section on gamma-ray counting is of particular interest in the article by Corson and Wilson (*2*). The excellent paper of K. G. McKay (*19*) on the related subject of bombardment conductivity will prove very valuable to a first reader.

The use of a solid as a counter offers certain advantages over a gaseous detector, among which are (a) small size (permits good geometry in experiments), (b) high stopping power (useful both in gamma-ray work and high-energy particle detection), (c) low resolving time (allows both high-speed counting and fast coincidence counting), (d) better conversion of energy into ion pairs than in a gas (provides improved signal-to-noise ratio). Incidentally, most of the above remarks apply to both conduction-type and scintillation-type solid counters.

The advantages of a solid conduction-type counter can be counterbalanced, to some extent, by certain difficulties, described below in detail. It might be mentioned at this point, however, that strains in the crystal, polarization effects, variation in counting efficiency in different regions within the same crystal, annealing procedure and low-temperature requirements in some cases, are among the troublesome characteristics of these new counters. It is not known, at the present time, how many, or which, of the disadvantageous features of the conduction-type crystal counter will ultimately be removed.

The basic operation of a conduction-type crystal counter can be described with the help of Fig. 1. A single particle, for example, a high-speed beta particle, may enter the crystal at the point *A*. The beta particle frees secondary electrons in the body of the crystal until the particle is stopped. In a gas, the analogous process is called ionization, and negative (electrons) and positive ions are produced along the track of the particle. In the crys-

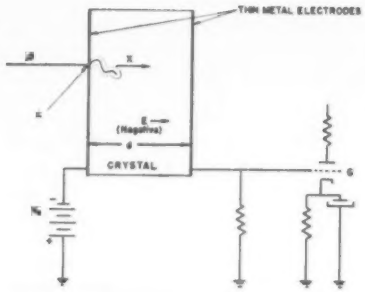

FIG. 1. Schematic diagram of crystal counter

tal, the large number of freed secondary electrons are concentrated along the track of the beta particle.

A number of positive sites, called "holes," equal to the number of freed electrons, are produced at the same time. The holes may be either stationary or mobile. When the holes are stationary we have an obvious difference from the gaseous phenomenon. Let us, for the present time, take the holes to be immobile.* Under these conditions the cloud of freed secondary electrons can now be accelerated by the electric field, E, in the crystal. The motion given to the electrons by the field is superimposed on a random thermal motion which electrons experience by virtue of their collisions or encounters with the ions or atoms of the crystal lattice.† A theory of the collision process has been given by H. Fröhlich and N. F. Mott (*20*). The combined effect of these motions is a drift of the electrons toward the positive electrode.

On the way to the positive electrode, an individual electron may pass near a "trapping center" or, more simply, a "trap."‡ A trap can be an impurity atom, an interstitial atom, a vacancy or other kind of lattice defect, a crack, or perhaps still some other type of irregularity in the lattice. If an electron passes slowly enough and close enough to a trap it will be captured and thereby rendered immobile. Electrons may be released slowly from traps by thermal quanta, but we shall not be concerned with their release at this point because of the slowness of such a process (*22*, *23*).

In a weak field it is therefore true that all electrons will be captured before reaching the positive electrode. In a stronger field the electrons will move with greater drift velocity and hence will not spend as much time in the neighborhood of a trap. They may, therefore, cover the negative-to-positive electrode separation without being captured, but presumably are finally stopped at the crystal-electrode boundary. In this case it is possible for electrons to travel through the entire thickness of the crystal. It is clear that further increase of field strength will have no result other than to increase the drift velocity of secondary electrons.§ The number of electrons "collected" will tend to approach a constant.

The process by which secondary electrons are released in an insulating crystal by an ionizing particle may be thought of in the simple manner suggested by the present energy band theory of the solid state. Such a description is analogous to the qualitative theory of photoconduction in crystals (*21*, *23*, *24*). One supposes, referring to Fig. 2, that, in an insulator, a quasi-continuous band of possible

* This is the case for AgCl at low temperatures, which has been shown by W. Lehfeldt in an elegant experiment in photoconductivity (*28*).

† More exactly, by collisions with the vibrational modes of the lattice.

‡ Discussion of traps in solids may be found in reference *21*. The possibility of surfaces acting as trapping states has been envisaged by I. Tamm, *Physik. Z. Sowjetunion* **1**, 733 (1932). See also W. Shockley, *Phys. Rev.* **56**, 317 (1939).

§ We do not consider multiplication processes at this point. Multiplication, however, has been observed by Kallmann and Warminsky (*40*).

energy states at A is completely filled under normal circumstances, in conformity with the exclusion principle of Pauli. When a beta particle enters the lattice its near approach to electrons in these states excites the electrons into higher states in the normally unfilled band of states D (the "conduction band"). In this band an electron is in a semi-free state and can accept energy from the electric field E, causing it to rise from level G to some higher unoccupied level H.

It is probably true that the electron rapidly drops close to the bottom of the conduction band before moving any large distance from the position at which it was set free. Under these conditions G and H are to be considered close to the bottom of the conduction band D. Since an electron does not already occupy the state H, the freed electron may rise into this level without violating the Pauli exclusion principle. By such a process the electron moves semi-freely in the general direction of the field, gaining energy as it moves. This process does not continue indefinitely since the electron makes numerous collisions with the ions or atoms of the lattice. After collision has occurred, it is imagined that the moving electron has given up to the lattice its recently acquired electrical (now kinetic) energy. It is therefore ready to go through this process once again and the motion is pictured as a succession of small jumps with a recurring component of motion in the direction of the electric field.

It has been supposed that the electron remains in the energy band D during these jumps. This will be so if there is no other process tending to take the electron from this band. However, during one of the small jumps the electron may pass very near a trapping center, such as F in Fig. 2, or perhaps a vacant impurity state at C in the neighborhood of an impurity atom.

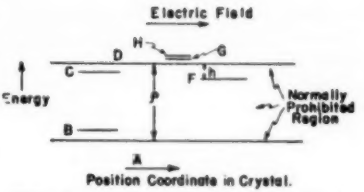

FIG. 2. Energy band diagram for insulating crystal, having traps (F) and impurity atoms (BC)

In such cases the electron may be captured and held at F (or C). The length of time that the electron is held at F depends on the energy depth of the trap, h, and the temperature (*22*). If the electron is captured at C, a luminescent quantum may be emitted (*23*) when the electron-impurity system makes a transition to its ground state B.

In order that the state B be empty, one may suppose that "holes" in the band A, which are left by electrons raised to state D by the beta particle, rapidly migrate to impurity atoms and electrons drop from states B to these holes. Such a process may also be used to explain a possible behavior in some scintillation-type counting materials (alkali halides). It is to be noticed, however, that motion of the holes is postulated in this case, and it is by no means certain that motion of holes occurs in the general scintillation material. In AgCl at low temperatures, the holes do not seem to move.

It is, of course, also possible that an electron may be released from the trapping center by thermal excitation, after which migration brings it into the neighborhood of another empty state B. The electron may drop into this state, again emitting a light quantum (*23*). This type of luminescence may show a long duration, since considerable time will be required to oust the electron from trap F.

The secondary electrons, produced by light or by a beta particle, are captured

by a process which has been described phenomenologically by K. Hecht (*25*). Hecht has confirmed his analysis by photoconductivity experiments with AgCl. The substance of Hecht's analysis is as follows: We suppose that an electron remains free for an average time, T seconds, which does not depend on field strength. The electron therefore avoids a trap for an average time T. The chance that the electron is captured is proportional to dt/T where dt is a small interval of time. If there are n free electrons at time t, in time dt, $dn = ndt/T$ of these will be trapped. The number of electrons remaining free after any time t is, therefore,

$$n = n_0 e^{-\frac{t}{T}} \tag{1}$$

if n_0 is the number present at time $t = 0$.

The average distance that electrons cover before being captured will clearly be

$$\delta = vET \tag{2}$$

where E is the field strength and v the "mobility" or drift velocity per unit electric field.* Theoretical values of the mobility may be obtained from the work of Fröhlich and Mott (*20*) for polar crystals and Seitz (*26*) for non-polar crystals. The quantity δ, sometimes called the "Schubweg," is a most important figure in work with crystal counters and photoconductivity. The reason for this is that an electron contributes to the measured voltage or charge pulse only an amount proportional to the length traveled in the direction of the field. Thus, an electron does not necessarily contribute the full electronic charge e (4.80×10^{-10} esu) to the induced charge on the grid G of Fig. 1. In fact, it may be expected on theoretical grounds (*27*) that an electron which moves a distance Δx in a crystal of thickness d contributes to the charge induced on the grid G an amount

$$q_{eff} = e\Delta x/d \tag{3}$$

Hecht's work confirms this equation. If the hole moves also, the charge induced will be

$$q_{eff} = e\,\frac{\Delta x_- + \Delta x_+}{d} \tag{4}$$

Δx_- and Δx_+ refer to the distances moved before trapping of the electron and hole, respectively. Accordingly, for the case when the holes are stationary, the voltage signal is

$$V_{eff} = \frac{e\Delta x}{Cd} \tag{5}$$

where C is the capacitance to ground of the system which comprises the grid, crystal, and distributed and stray capacitances of connections to these elements.

We can make sample calculations for the case where the bombarding particle penetrates a very small fraction of the crystal thickness. For example, consider that alpha particles enter the crystal at A, in Fig. 1, and penetrate a distance of the order of 10 microns. In general, such a small penetration is negligible with respect to the thickness of the crystal, which may be one or a few millimeters. Thus, n_0 secondary electrons are produced within a very small distance of the negative electrode, defined by $x = 0$. Each of the n_0 secondary electrons may travel a different distance x before being trapped. The number which have traveled a distance in the range dx at x is

$$dn = \frac{n_0}{\delta} e^{-\frac{t}{T}} dx$$

by Eqs. 1 and 2 and the equation

$$x = vEt \tag{6}$$

Expressed as a function of x we can write

$$dn = \frac{n_0}{\delta} e^{-\frac{x}{\delta}} dx$$

Electrons captured in the range dx at x

* The drift velocity is assumed to be small compared with the thermal velocity of electrons.

contribute an effective charge

$$dq_{eff} = \frac{ex}{d}\,dn = \frac{exn_0}{\delta d}\,e^{-\frac{x}{\delta}}\,dx$$

and, therefore,

$$q_{eff} = \frac{\delta n_0 e}{d}\int_0^d \frac{x}{\delta}\,e^{-\frac{x}{\delta}}\frac{dx}{\delta}$$

summing over all electrons which travel distances between $x = 0$ and $x = d$. Those electrons which might have traveled larger distances $d < x < \infty$ each contribute a charge e. The contribution from such electrons is added to q_{eff} to give Q_{eff}. Hence

$$Q_{eff} = \frac{\delta n_0 e}{d}\left(\int_0^d \frac{x}{\delta}\,e^{-\frac{x}{\delta}}\frac{dx}{\delta} + \frac{d}{\delta}\int_d^\infty e^{-\frac{x}{\delta}}\frac{dx}{\delta}\right)$$

or

$$\frac{Q_{eff}}{n_0 e} = \frac{\delta}{d}\left(1 - e^{-\frac{d}{\delta}}\right) = F\left(\frac{\delta}{d}\right) = \frac{\bar{x}}{d} \quad (7)$$

A graph of this function is given in Fig. 3*a*. The voltage pulse at the grid G of Fig. 1, corresponding to the sudden release of n_0 electrons at the cathode, is, therefore,*

$$V_{eff} = \frac{n_0 e}{C}F\left(\frac{\delta}{d}\right) \quad (7a)$$

which shows that the pulse size is dependent on the value of δ, and in fact shows a characteristic saturation behavior. The curve is often more conveniently plotted against electric field E rather than δ. Equation 2 shows that δ is proportional to E. By making such a plot from experimental data it is possible, in principle, to find a value for δ. Such determinations have been made by Lehfeldt (*28*) in studies of photoconductivity. However, it must be known or otherwise assumed, that electrons are not stopped by a barrier, such as a crack, before reaching the positive electrode. In other words, a determination of δ requires that the only cause of electron stoppage is due to traps distributed at random throughout the crystal. This distribution is usually called a homogeneous distribution of traps. If one assumes, for example, a barrier such as a plane separating two contiguous crystals, the effective charge, Q_{eff} will be

$$Q_{eff} = n_0 e\,\frac{\delta}{d}\left(1 - e^{-\frac{S}{\delta}}\right) \quad (8)$$

where S is the distance between cathode and barrier. The saturation value of Q_{eff} is, in this case,

$$Q_{eff} = n_0 e\,S/d \quad (9)$$

whereas in the previous case (barrier absent) Q_{eff} is $n_0 e$. It should be emphasized at this point that the mere fact that saturation behavior is observed does not imply that electrons travel the entire distance between

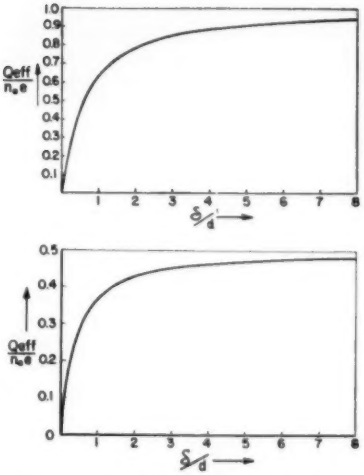

FIG. 3. (*a*) **Charge pulse for particle with small penetration plotted against δ/d, according to Eq. 7. δ is proportional to the electric field;** (*b*) **Charge pulse for particle, penetrating crystal and ionizing uniformly, plotted against δ/d, according to Eq. 7*b*. δ is proportional to the electric field**

* When the bombarding particles penetrate a small average distance b, Eqs. 7 and 7*a* can obviously be amended to take this into account by subtracting b from d in the exponential function.

electrodes. If the value of n_0 is known, making the maximum possible charge n_0e, saturation at this value of charge definitely established the fact that electrons have traversed the entire thickness of the crystal.

It is worthwhile to give the expression for the pulse size in the case where the bombarding particle is a penetrating one, such as a high-energy electron, proton or meson. In this case the secondary, or ionization, electrons will be produced along the track of the particle in the solid. In other words, a sheath of free electrons and holes will surround the particle's track. If we assume that the particle ionizes uniformly throughout its path, the resulting pulse can either be calculated directly by considerations of the type leading to Eq. 7, or else can be taken with small modification from a formula of Mott and Gurney (p. 122, *21*). The charge pulse is therefore

$$\frac{Q_{eff}}{n_0e} = \frac{\delta}{d}\left[1 - \frac{\delta}{d}\left(1 - e^{-\frac{d}{\delta}}\right)\right] \quad (7b)$$

where n_0, as before, is the total number of secondary electrons freed by the ionizing particle within the solid. A plot of this function is given in Fig. 3*b*. When $\delta \to \infty$, it can be seen that the pulse size shows saturation at a value $n_0e/2$, if again the assumption is made that no barriers exist other than randomly located traps. If the holes are equally mobile, the pulse size will be doubled.

In passing, it should be noticed that the supply voltage which produces saturation is proportional to the square of the thickness of the crystal. This arises from the fact that, to attain a given fraction of the saturation pulse size, the value of δ must be proportional to d. However, δ is itself proportional to V_0/d. Hence V_0 must be proportional to d^2. Experimental verification of this behavior may be found in the work of Flechsig (*29*).

Discussion of δ

It is relevant, at this point, to discuss the quantity δ for this quantity is of great significance in determining whether any material will behave as a crystal counter. In the event that δ is small it is highly improbable that a crystal will make an efficient counter under the normal circumstances in which moderate voltage gradients are used. We can see that, under these conditions, the exponential in Eq. 7 can be neglected, resulting in

$$Q_{eff} = n_0e\frac{\delta}{d} \quad (10)$$

and with δ small, Q_{eff} is small. It is worthwhile noticing also that quite another condition may prevent a crystal from being an efficient counter, namely, if barriers are present such that $\frac{S}{d} \ll 1$. (See Eq. 9.) This point will be discussed later.

The Schubweg, δ, which is a mean-free-path relative to trapping centers, may be expressed as follows:*

$$\frac{\delta}{E} = \frac{e}{6kT}\frac{l}{P\sigma} \quad (11)$$

where T is the absolute temperature, l is the mean-free-path with respect to the lattice vibrations and is connected closely with the mobility, P is the number of randomly distributed trapping centers per unit volume and σ is the cross section for capture of an electron by a trapping center. As Mott and Gurney have pointed out, little is known of the value σ, even if it is assumed to be a constant, independent of electron speed. Under most conditions little is known about the value P for the large majority of crystals (P may depend on previous treatment). On the other hand, values of l are found in the theories of Fröhlich and Mott (*20*), and Seitz (*26*). Values of l for various representative substances have been calculated from the expression of Fröhlich and Mott and

* See ref. *21*, p. 131.

TABLE 1

Material	T Temperature (°K)	λ (microns) Absorption wavelength	K Dielectric constant (Static)	K_0 Dielectric constant (High freq.)	θ (°K)	v Mobility (cm²/volt-sec)	l (A.U.)
AgCl	77	87	12.3	4.01	503	1570	530
AgBr	77	124	13.1	4.62	356	296	100
TlBr	77	157 (estimated)	29.8	5.41	460	880	294
LiF	300	32.6	9.27	1.92	1280	216	145
KCl	77	70.7	4.68	2.13	382	478	160
KCl	300	70.7	4.68	2.13	382	10*	7*
KBr	77	88.3	4.78	2.33	302	196	66
KBr	300	88.3	4.78	2.33	302	7*	4*
NaCl	77	61.1	5.62	2.25	491	1580	532
NaCl	300	61.1	5.62	2.25	491	15*	10*
Diamond	300	—	16.5	5.5	—	156	—

* Denotes order of magnitude.

Fröhlich-Mott:

$$v = 2\sqrt{\frac{3}{\pi m k \theta}}\, e a_0 \,(e^{\frac{\theta}{T}} - 1)\,\frac{K - K_0 + 1}{K - K_0} \qquad a_0 = \text{radius of first Bohr orbit}$$

$$\theta = \frac{hc}{k\lambda}\,(K - K_0 + 1)^{1/2} \qquad l = \frac{1}{e}\sqrt{3mkT}\; v$$

λ = absorption eigen-wavelength $\qquad$ T = absolute temperature

The effective mass of the electron in the conduction band is taken equal to the mass of the free electron.

collected in Table 1. The Fröhlich-Mott formula and defined quantities are given below Table 1. The theoretical relation between l and v is also given below Table 1. The values of dielectric constants have been taken from the book of Mott and Gurney.

Table 1 will be used to prepare a table of values for δ. To do this we require values of σ and P, both of which are difficult to find. Mott and Gurney use a value $\sigma \cong 3 \times 10^{-15}$ cm² for AgCl. We will adopt this value in our calculations although it is likely to be revised as more information becomes available. A value for P has been estimated for AgBr from the data of Lehfeldt for (δ/E) and from our calculated value of l, which appears to be in reasonable agreement with the experimental facts. We will arbitrarily choose values of P for AgCl and TlBr as equal to the value chosen for AgBr. With respect to the alkali halides of Table 1, it is possible to place an upper limit on estimates of P if it is assumed that the effective trapping mechanism is an F-center,* namely, a position in the lattice where an electron has replaced a negative halogen ion (*30*). The calculation of Smakula (*31*) has been employed in finding P. Smakula† gives an expression for the optical absorption coefficient in terms of the density of trapping centers, the oscillator strength, and the width of the absorption band due to F-centers in the alkali halide crystals. By examining the absorption of clear LiF, KCl,

* We have assumed that the effective trapping mechanism is an F-center because the Schubweg or range decreases inversely as the concentration of F-centers. See ref. *21*, p. 127, Fig. 43.

† See also Seitz (*30*), page 386.

TABLE 2

Material	*T* (°K)	*l* (*A.U.*)	*Absorption coefficient* (cm^{-1})	*P* (cm^{-3})	*E* (*volts/cm*)	δ (*cm*)
AgCl	77	530	—	2×10^{13}	5×10^{3}	11.0
AgBr	77	100	—	2×10^{13}	5×10^{3}	2.1
TlBr	77	294	—	2×10^{13}	5×10^{3}	6.2
LiF	77	very large	0.1	11.3×10^{14}	1×10^{4}	> 10.0
LiF	300	145	0.1	11.3×10^{14}	1×10^{4}	0.11
KCl	77	160	0.1	4.8×10^{14}	1×10^{4}	0.28
KCl	300	7	0.1	4.8×10^{14}	1×10^{4}	0.003
KBr	77	66	0.1	8.5×10^{14}	1×10^{4}	0.07
NaCl	77	532	0.1	7.5×10^{14}	1×10^{4}	0.60

NOTE: $\sigma = 3 \times 10^{-15}$ cm^2 assumed for all trap cross sections.

KBr and NaCl crystals in the neighborhood of the *F*-center bands we can place upper limits on the *P* values for such samples. Values of δ, calculated with such data and Eq. 11, are shown in Table 2.

In the table it has been assumed that an oscillator strength of 0.75 can serve for our rough calculations of δ, except in those cases, such as KCl, where the oscillator strength has actually been measured. From Table 2 it can be seen that many values of δ are reasonably large at low temperatures (0.2–10.0 cm). Many crystals, such as the alkali halide type with such values of δ, have not been observed to act as counters. It cannot be claimed that the value of δ is too small in these cases for it is of the same order as in AgBr at low temperatures. One must look for other causes. We will return to this point later.

Discussion of n_0

In addition to the two lengths, δ and *l*, which are important quantities for crystal counters, it is evident that n_0, or the number of secondary electrons, is quite significant. The pulse size is directly proportional to n_0, as can be seen from Eq. **7**, **7***a*, and **7***b*. The quantity n_0 is clearly related to the question of how the excitation energy of the bombarding particle is distributed to the crystal lattice and to the "semi-free" electrons which are advanced to the conduction band. It is probable that a very large number of electrons is produced initially by the ionizing particle. The number of such electrons probably corresponds, in order of magnitude, to the energy of the particle divided by the energy gap ρ of Fig. 2. The duration of the ionization process is of the order of 10^{-12} second. The electrons may recombine with their holes after the completion of this time to give Frenkel "excitons" (*32*) or may give their energy to the lattice in some other manner, perhaps by several collisions (*6*). In any case, free electrons may be removed from the conduction band and their energy is given in some way to the lattice. The result of this behavior is that electrons are not free long enough to engage in a conduction process—of the order of magnitude of one microsecond. We can summarize these remarks by noting that if a

large share of the bombarding particle's energy is spent in (eventual) thermal excitation of the lattice, little energy will be left over for producing free electrons and few electrons will be produced.

A measure of the efficiency of production of conduction electrons is the so-called "energy per ion pair" or "energy per free electron." It is well known that the corresponding figure is about 30 electron volts for a gas and that this value is unaffected by variations in type of gas. Although van Heerden has found the analogous figure for AgCl to be 7.6 electron volts, which is an impressively lower value than that for a gas, there are apparently no theoretical calculations for polar or non-polar crystals with which the experiments can be compared. Therefore one must treat the question empirically at the present time.

In this regard, one can express the number of secondary electrons set free by an ionizing particle which spends all its energy in the crystal as a coefficient ψ times the ratio of particle energy to the smallest possible value of the energy per ion pair, namely ρ, or the energy gap between the filled band and the conduction band. With this convention, the number of secondary electrons is

$$n_0 = \frac{H}{\rho}\psi \qquad (12)$$

where H is the initial energy of the particle. If ψ is unity, energy is not "wasted" thermally. The results of van Heerden indicate that ψ is about 0.6 in AgCl. Additional results on ψ will be reported in Part 2.

Polarization Effects

It has been noticed by numerous observers (*33*, *34*, *35*) that polarization phenomena occur when electric currents pass through insulating crystals. It can be expected that such effects will also appear in crystals used as counters (*6*). It is therefore not surprising to find references to polarization in some of the early experimental literature on crystal counters (*14*, *16*). At the present time such information is not well coordinated or explained in terms of a mechanism. It is the purpose here to present a simple theory of some polarization phenomena, which may help to explain some of the observed facts.

A polarization effect in crystal counters can usually be detected by a gradual decrease in pulse size as the number of counted events increases. The obvious explanation of this fact is that the displacement of charge, effected by the electric field, results in a field opposed to the applied one. Electrons therefore move shorter distances before being trapped since δ, which depends on the actual field present, decreases as the number of counted events increases. It is clear that we must assume that trapped electrons or "holes" are stationary. It is on the basis of such ideas that we may look for an explanation. It is quite possible to treat polarization effects when holes move, as in diamond, and are subsequently trapped. However, we will treat the simplest case only, that apparently corresponding to AgCl, in which electrons move until trapped and the holes or positive sites are immobile.

We will assume that the process of ionization by incoming particles, and the subsequent drift of electrons in the crystal, produces a resultant separation of positive and negative charges, as shown in Fig. 4. The model illustrated in Fig. 4 is, of course, a simplification of the actual charge distribution since the positive charge, resulting from stationary holes, and the negative trapped electron charge are assumed to be concentrated in plane sheets parallel to the crystal faces (or electrodes). A closer approximation to the actual charge distribution, produced by monoenergetic beta or alpha particles entering an ideal

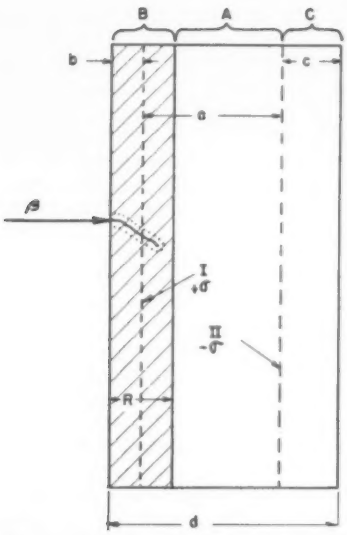

FIG. 4. Simple model representing polarization charges within crystal. Positive holes in shaded region are replaced by a positively charged plane (I) having surface charge density $+\sigma$. Electrons are trapped at plane barrier (II) where the surface charge density is $-\sigma$. R is the average range of the incident particle

crystal at the left electrode, would consist of a more or less uniform distribution of positive charge (holes) in the region B of the above figure and an exponentially decreasing negative charge distribution in the remainder of the crystal. Our model has been intentionally made different from the actual distribution, so that the ideas can be presented more clearly. Our case also covers the situation in which a crack or crystal boundary occurs between regions A and C. The distance b in the case of our model is of the order of half the average range of beta or alpha particles in the crystal material.

A discussion of polarization effects for the more accurate representation of the charge distribution will be left for a later time. The model in Fig. 4 will be used for the present. In this model the continuous distribution of positive charge, in the region B, has been replaced by a sheet of positive charge of density $+\sigma$ at a distance $b = R/2$, where R is the average range of the monoenergetic beta or alpha particles. The layer of equal negative charge separating regions A and C will be produced whenever the electric field is large and when a barrier exists which acts as a region of electron traps, for example, such as a crack or boundary, as previously mentioned. In the special case of an ideal crystal, without traps or other barriers, the layer of negative charge will form in the crystal at the positive electrode ($a = d - b$). Our assumption is that electrons do not leave the crystal to enter the metallic surface of the electrode.* If the crystal is not ideal, e.g., a AgCl crystal with traps, the above conditions are approximately satisfied when the electric field is large.

It is apparent, furthermore, that in the particular case of alpha particles or fission fragments, where the penetration into the crystal is negligible (10 microns or less), the layer of positive charge is resident practically at the negative electrode. The situation evidently recalls the introduction of a polarizable dielectric between the plates of a condenser. If the voltage across such a condenser is maintained by a battery (EMF = V_0), the electric field in the dielectric is given by

$$E = V_0/d \qquad (13)$$

just as in the case where a dielectric is not present. The charges appearing at the electrodes, due to the polarization of atoms or molecules of the dielectric, are neutralized by charges removed from the battery and sent to the metallic condenser plates.

*It is not known whether this is so for diamond.

In the circumstance that we have described, in which the ionizing particles are alpha particles or fission fragments, the charge layers I and II appear practically at the electrodes (large applied field, no barrier) and the polarization of the crystal, due to accumulation of charges at the electrodes, is of little consequence. The field in the crystal remains $E = V_0/d$, to the approximation that b/d is negligible.* As a result, a very large number of heavy particles (perhaps 10^8 or more) may be counted in a small crystal before reduction of pulse size is noticeable. In the case of an actual crystal with a barrier, polarization can occur more quickly.

Polarization by beta particles. When particles penetrate significantly into the crystal from the left side, such as beta particles in Fig. 4, the polarization of the crystal is marked and the electric field is no longer given by Eq. 13. A simple calculation in electrostatics, neglecting end effects, shows that the fields in regions a, b, c are given by

$$E_a = \frac{V_0}{d} + \frac{4\pi\sigma}{K}\left(1 - \frac{a}{d}\right) \quad (14)$$

$$E_b = \frac{V_0}{d} - \frac{4\pi\sigma}{K} \times \frac{a}{d} \quad (15)$$

$$E_c = \frac{V_0}{d} - \frac{4\pi\sigma}{K} \times \frac{a}{d} = E_b \quad (16)$$

where σ is the charge per unit area and K the static dielectric constant of the crystal. It can be seen from Eqs. 14, 15 and 16 that there are supplementary fields due to polarization with different behaviors in the different regions. In region b the supplementary field is aiding, in region a opposing, and in region c aiding. Region c is not important since electrons do not cross the plane II. The effect of these polarization fields in determining pulse size will now be considered.

The charge density σ in the above formulas can be expressed in terms of the number of ionizing events and the energy associated with each event. If N particles, each of energy H, enter the crystal uniformly over its area A, and if, further, the energy per ion pair conversion is ϵ, the positive charge density is

$$\sigma = \frac{NH}{\epsilon A}e \quad (17)$$

where e is the absolute value of the electronic charge. Inserting this expression for σ in Eq. 14 and solving for the case where the original field E_a is reduced to the fractional value $f\frac{V_0}{d}$, one obtains

$$N_f = \frac{V_0 \epsilon KA}{4\pi dHe} \frac{f - 1}{1 - \frac{a}{d}} = n \frac{1 - f}{1 - \frac{a}{d}} \quad (18)$$

where

$$n = -\frac{V_0 \epsilon KA}{4\pi dHe} \quad (19)$$

In these equations V_0 is a negative potential and N_f, therefore, a positive number, giving the number of pulses required to reduce the field to fractional value fV_0/d. By way of example, the electric field will be reduced to $\frac{1}{2}$, $\frac{1}{5}$ and $\frac{1}{10}$ of its original intensity for values of N_f equal, respectively, to

$$0.5\frac{n}{1 - \frac{a}{d}}, \quad 0.8\frac{n}{1 - \frac{a}{d}}, \quad 0.9\frac{n}{1 - \frac{a}{d}} \quad (19a)$$

Equation 7 now gives the pulse magnitude as a function of the field E_a, since δ is directly proportional to E_a, by Eq. 2. It is, therefore, clear that pulse magnitude obtained from Eqs. 2 and 7 will fall off as N increases. It will be shown directly below that, with large

* If one assumes a continuous positive space charge distribution in region B, and if $(b/d) \ll 1$, it may be shown that secondary electrons, produced in this region by ionizing particles, will be subjected to a supplementary polarization field aiding the applied field. There is a narrow sub-region in B, of width $b^2/2d$, close to the dividing plane I, where the supplementary field is opposed to the applied field and of the same order of magnitude as in region A. The region A may therefore be thought of effectively as a little wider than indicated in the figure.

fields and small values of N, the decrease will be small at first. Larger values of N will subsequently reduce the pulse size abruptly.

It is desirable, in many applications of crystal counters, to utilize strong fields, thus assuring saturation of pulse size. We can therefore reason that a reduction of the field by a factor of two will, in general, produce only a small decrease in pulse size due to the saturation character of Eq. 7 or Fig. 3*a*,*b*. However, a reduction of the field by a factor of five will almost certainly produce a marked decrease in pulse size; one then travels down the knee of the curve in Fig. 3*a*,*b*. Moreover, it can be seen from the expressions in (19*a*) that only small increments in the number of counted events are sufficient to produce large relative changes in the effective field strength in region *a*.

We can take a numerical example as follows: Assume that our source of beta particles to be P^{32} in which case the average energy is 660 electron kilovolts. The range of such particles in a silver chloride crystal is about 0.05 cm. Thus, b can be taken to be 0.025 cm. If we assume that a barrier or crack does not exist within the crystal (homogeneous trap distribution), $a = d - b$ or $c = 0$, then the negative layer forms principally at the positive electrode.* Consequently, for a crystal 0.5 cm thick, $a = 0.475$ cm. We can take V_0/d to be 5,000 volts/cm and $K = 12$ for silver chloride. With $A = 1.0$ cm^2 and $\epsilon = 7.6$ electron volts/ion pair, we find $N_{0.5}$, $N_{0.2}$, $N_{0.1} = 3.8 \times 10^6$, 6.1×10^6, 6.8×10^6 particles. Therefore, noticeable decrease in pulse size would occur in the interval between 3.8 and 6.1 million counts under the assumed conditions. This is not a large number of counts compared with the life of a G-M counter (10^8–10^{10} counts). Unless means are found to reduce the effects of polarization, the short life will prove a serious limitation in the use of such a counter for fast counting. On the other hand, warming of the crystal releases the trapped charges and, on recooling, the crystal is ready again for use. Perhaps irradiation with visible or infrared light may achieve the same effect.

Polarization produced by penetrating radiation (space charge effects). If the polarization is produced throughout the volume of the crystal, for example, by homogeneous gamma-ray bombardment, a positive space charge is produced in the crystal by the removal to the positive electrode of the secondary electrons. A saturation field will be assumed again. Let N be the number of (gamma) pulses counted by a crystal of volume τ. Each gamma quantum is assumed to provide, on the average, H/ϵ secondary electrons. The positive space charge per unit volume is

$$\rho_0 = \frac{NH}{\epsilon\tau}\,e \qquad (20)$$

assuming that the absorption of the radiation is small in a crystal of the size contemplated (0.5 cm thick). For this case of uniform space charge it can be shown that the effective field is

$$E = \frac{V_0}{d} - \frac{2\pi\rho_0}{K}(d - 2x) \qquad (21)$$

where x represents distance from the negative electrode. A plot of relation (21) is shown in Fig. 5. It may be noticed that the effective field is numerically larger than the applied field for $x < d/2$, smaller than the applied field in the region $x > d/2$, and equal to the applied field at $x = d/2$. Consequently, polarization effects will occur at first in the region $x > d/2$. A reverse field will gradually build up in this region so that more and more trapping

* We make no allowance for the case of electrons being trapped in the region between layer I and the positive electrode. Such trapping certainly occurs but our order of magnitude calculation will not require its appraisal. The accurate charge distribution discussed earlier is dependent on this assembly of trapped electrons.

will take place as ρ_0 increases, or as the number of counted pulses increases. Representative figures can be taken as follows: Let $V_0/d = 5{,}000$ volts/cm, $\tau = 0.5$ cm^3, $d = 0.5$ cm, $K = 12$, $\epsilon = 7.6$ electron volts/ion pair, $H = 0.5$ Mev. The number of pulses required to reduce the effective field to one fifth of the applied field, at the point $x = \frac{3}{4}d$, becomes 1.6×10^6. It is difficult to discuss this case in greater detail since the pulse size is dependent on the energy transfer in the Compton encounter, the place of appearance of the secondary electrons, as well as on the polarization field already present.

Further remarks on polarization effects. (*a*) It is possible and sometimes advantageous to use a small field in making the secondary electrons drift through the crystal. In this case the field is not large enough to move secondary electrons to the positive electrode with the exception of those produced near the positive electrode. Such might be the situation if one uses energetic protons or mesons which may lose much energy in the crystal and produce a proportionately large number of secondary electrons. In this case, a signal much greater than noise will be obtained even though the electrons do not move far. Under these conditions the secondary electrons are freed as usual but travel only a short distance before being trapped. The positive sites are again assumed to be stationary, thus resulting in a polarization field in the crystal. The effect of polarization produced by such displacement of charges can be overcome by displacing a similar number of elementary charges in the reverse direction. Such a displacement can be achieved by reversing the applied field for a time during which a number of pulses is counted equal to the number producing the polarization. Such repeated reversals have already been reported by Wouters and Christian (*14*) and achieve the desired effect. It is not clear, however, how many times the reversals can be made without producing new effects.

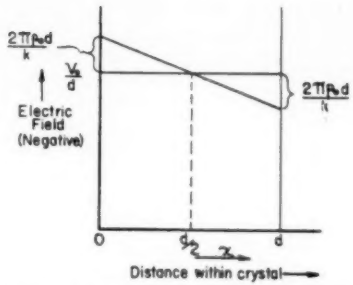

FIG. 5. Plot of electric field within crystal (inclined line) when positive space charge of volume density $+\rho_0$ has been produced uniformly in the crystal by penetrating radiation, for example, by gamma rays. Electrons have been swept to boundary ($x = d$) where they do not contribute to the polarization field. K is the dielectric constant. The horizontal line represents the initial electric field

$$\left(E = \frac{V_0}{d}\right)$$

It is clear that this procedure should be effective for ionization which occurs throughout the volume of the crystal and not so effective for beta particle counting, where the incident particles have a rather low energy and traverse only a small part of the crystal near the negative electrode and where a saturation field is usually required. Electrons, which can travel in the reverse direction when reverse field is applied, are not available beyond the range of the beta particles.

(*b*) It is also to be noticed that the effective field in the region B of Fig. 4 (or in the region $x < d/2$ for the case of space charge) is larger than the applied field. It is conceivable that the field can become large enough to permit electrons to enter the crystal from the negative electrode. Effects of this kind have been noticed in experiments

by Lehfeldt (*28*).* Perhaps some of the peculiar behavior noted by Whittemore and Street (*16*) with crystal counters can be ascribed to similar polarization effects.

Lehfeldt observed that crystals of silver chloride become conducting at low temperatures after irradiation by a large quantity of light. Mott and Gurney (*21*) have attributed this conductivity obtained by the photoeffect to the passage of electrons into the crystal from the electrode due to the presence of a double charge layer at the negative electrode (*21*, p. 186).

Whittemore and Street have observed quite large and irregular pulses after long irradiation by gamma rays. In this case such pulses may be due to fluctuations of d-c current which enters the crystal at the negative electrode. It is perhaps worth pointing out that spurious pulses in some crystals (termed "hash") have been observed at higher voltages and are probably not to be ascribed to polarization effects. Such spurious pulses have been reported in TlBr-TlI (*36*) and are believed to be due to impurities in the crystal samples. Subsequent work on pure crystal samples, grown synthetically at Princeton, indicates very few, if any, spurious pulses except at extremely high gradients or after prolonged exposure of crystals to ionizing radiation.

(*c*) If our picture is a correct one and the applied field is turned off (former high-voltage electrode connected to ground) after polarization has occurred, we can expect the following behavior:

(1) If beta particles are used, as in Fig. 4, no large pulses of opposite sign will appear. If, however, gamma rays are used following a beta particle exposure, reversed pulses are to be expected.

(2) If gamma rays are used throughout the experiment (while the field is on and after it is turned off), pulses of both signs may be expected depending on whether the Compton electrons, etc., are freed in one half of the crystal or the other. The polarization field is zero at the center of the crystal and has opposite signs in the two halves. A single crystal is required in this experiment.

Corson and Wilson (*2*) have described pulses of opposite sign which occur after the applied field has been removed. The author has also observed such reversed pulses in AgCl while using gamma rays. However, no experiments have been made by the Princeton group to look for or test the above conclusions. Experiments with solid argon (*42*) may have a bearing on such matters although it may well be that the behavior in that case is more complex.

(*d*) On the preceding pages, we calculated the effects due to the positive sites remaining fixed. In reality, trapping of the negative space charge occurs also, as we have pointed out. However, in the early stages of polarization the negative charges are trapped almost entirely near the positive electrode and hence contribute very little to the observed effects. At a later time when the applied field has been reduced to a low value, trapping of negative charge occurs throughout the crystal on a large scale. The approximations break down for this concentration of negative charge. However, we see that the field must already be small for this behavior to occur and, therefore, that the negative space charge can be neglected when the initial polarization behavior is obtained.

TECHNIQUE AND APPARATUS

Materials

The materials which are known to be capable of detecting single ionization events are AgCl (*6*), AgBr (*37*), C (diamond) (*8*, *10*, *15*), ZnS (*38*),

* Also in experiments on CdS by Kallmann and Warminsky (*40*).

TlBr-TlI (*36*), CdS (*39, 40*), and liquid and solid argon (*41, 42*). Diamond, ZnS and CdS can be operated at room temperatures. AgCl, AgBr, TlBr-TlI require low temperatures since these materials are ionic conductors at room temperature. It should be noticed that an alkali halide crystal has not been reported as a successful counter.

Preparation of Crystals

Crystals of diamond, ZnS and CdS require no treatment except perhaps cleaning before use. Diamonds which count are, of course, natural crystals. Ahearn's ZnS crystals (sphalerite and wurtzite) were also natural samples. CdS crystals have been made artificially by Frerichs (*39*), and must be very pure in order to count. Heat treatment or annealing of the room temperature variety of crystal counters does not seem to have been studied with regard to its effect on counting.

The crystals AgCl, AgBr and TlBr-TlI require careful heat treatment (*6, 13, 37*), and careful handling before good operation can be expected. Annealing is a clear requirement in some cases (*36*) where counting is not observed before the annealing treatment but is observed after the treatment. Van Heerden was the first to show that heat treatment is necessary with AgCl crystal counters. In AgCl crystals, colloidal silver specks appear in the crystal after exposure to light, and behave as electron traps. The colloidal specks give the crystals a characteristic bluish cast which may be removed entirely by maintaining the crystal at a temperature of 400° C for a few hours. The object of van Heerden's treatment was the removal of the colloid specks. The work of Haynes (*43*) on AgCl single crystals makes it appear quite probable that electron trapping also occurs in regions of mechanical strain. It is therefore quite probable that an additional result of van Heerden's heat treatment was to anneal the crystal, making it relatively free of strain. A clear proof of the effectiveness of strained regions acting as traps at low temperatures has yet to be given although such a behavior seems very reasonable.

Haynes has described in detail a procedure by which large unstrained single crystals of AgCl can be prepared. As far as the author knows, the complete Haynes preparation has not been applied to counting crystals. In this regard it can be pointed out that even after a crystal has been prepared strain-free, further contact with fingers usually allows enough heat flow into the crystal to produce strains. Such strains are recognized by examination in polarized light. To avoid the introduction of strains in handling and mounting the crystal a new procedure has been used (see below) in which the crystal is not touched after insertion in the crystal holder.

In any case, heat treatment and annealing of silver and thallium halides definitely improves the behavior of these materials as crystal counters. In the following section a part of the material is devoted to the apparatus and annealing technique which has been successfully employed with silver halide crystals.

Crystal Samples

The crystals used in solid conduction counter work have been selected from natural crystals in the case of the room temperature variety (diamond, ZnS) and have been grown synthetically in the case of the silver and thallium halides. Small synthetic crystals of CdS have also been made by Frerichs.

Diamond. Not all diamonds will count. Up to the present time there have been no physical criteria used in selecting "counting" diamonds other than the counting property itself. H. Friedman, L. S. Birks and H. P. Gauvin

(*44*) have attempted to correlate ultraviolet transmission data with the gamma-ray counting property. The results of this investigation indicate that the gamma-ray counting diamonds are of the ultraviolet transparent variety (Type II). An explanation of this behavior was suggested by the writer (*45*). However, the experimental observations are rather incomplete and no certain conclusion can be drawn at the present time. A study of the occurrence of gamma-ray counting diamonds has been made by L. S. Birks, H. P. Gauvin and E. J. Brooks (*46*) with the result that there appears to be a tendency for gamma counting diamonds to be of gem quality and clear and white. This result is not in agreement with the work reported by Corson and Wilson (*2*) who state that there is "no correlation (of counting) with quality." It appears that much more experimental work is required before good physical criteria are known for selecting gamma counting diamonds, although such criteria have been suggested (*45*).

Diamonds which count alpha particles are much easier to find (*47*). It is disappointing that tests have not been carried out to determine the connection between alpha-particle counting diamonds and gamma-ray counting diamonds. However, it has been pointed out by the writer (*45*) and Ahearn (*47*) that there is a much greater probability for observing alpha particle pulses than gamma-ray pulses in small diamonds. The reason is essentially that an alpha particle may lose all its energy in a small diamond while a Compton electron, set free by a gamma ray, may lose only a fraction of its energy in the crystal. A further discussion of diamond counters will be given in Part 2 of this paper.

ZnS. Very little information is available in the case of ZnS crystals. Alpha particle pulses in ZnS are generally a good deal smaller than those in diamond (*38*) which makes the counting property difficult to study. It has been stated that synthetic ZnS (wurtzite) crystals have been grown by Jauch, although it is not known whether these crystals count. An interesting result of Ahearn's investigation is that ZnS crystals (sphalerite) with an impurity content as high as 0.1 percent, mainly germanium, were observed to count. It therefore appears that certain impurities, in moderate amounts, may not be deleterious to the counting property.

CdS. H. Kallmann and R. Warminsky (*48*) have studied the behavior of both non-luminescent and luminescent CdS crystals. In the first case the usual type of crystal counter behavior is observed at room temperature, i.e., pulses due to alpha particles and electrons are of a size consistent with the assumption that the freed secondary electrons drift to the anode without multiplication. With crystals of the luminescent type, amplification of the pulses by 10^3 has been reported within the crystal, and pulses of magnitude 2 volts have been obtained from single alpha particles! However, in the latter case, the pulses last for about 0.05 seconds. It is clear that secondary effects occur in the latter type of crystal while primary effects are important in the first type. Crystals previously irradiated by infrared light lost all amplification properties. Visible light irradiation (volume effect) restored the amplification property. The luminescence of those crystals showing secondary effects seems to be in the red and infrared. Kallmann and Warminsky have also carried on experiments with beta particles and gamma rays with interesting results of the type previously found in AgCl.

Silver and thallium halides. The crystals used in research on silver and thallium halides have all been prepared synthetically. Van Heerden prepared AgCl crystals by the well-known method

of Kyropoulos (*49*). In this country silver chloride crystals have been produced for infrared work by the Harshaw Chemical Company (Cleveland, Ohio) (*50*) by Bridgman's (*51*) method. Most published investigations in this country have been performed with Harshaw crystals (*12, 14, 16*).

In order to understand better the connection between the conditions of crystal growth and purity with the counting property, it was decided to grow silver halide crystals in the Princeton laboratory by Bridgman's method. Yamakawa (*37*) and Harrison (*52*) have successfully grown crystals of AgBr and AgCl by this method. It appears from this work that single crystals of high purity and uniform condition can be prepared so that reproducible counter results can be obtained. In connection with the purity of the crystal samples the experimental and theoretical results of McFee (*53*) on impurities in synthetically grown NaCl may be referred to. McFee has shown quantitatively how the crystallization process removes impurities from a crystal growing out of a melt.

In the Bridgman method of crystal growth the halide powder is placed in a circular pyrex tube drawn to a point at one end, as shown at the left of Fig. 6 and shown in position in Fig. 7. The tube is suspended by a fine Nichrome* wire connected to a halter wound around the top of the tube. The powder is melted in the furnace and more is added later to make up the desired volume of liquid. The temperature of the upper half of the furnace is kept at a value about 10°C above the melting temperature. The tube is lowered slowly into the furnace by a motor and gear train at a rate of about one half to one inch a day. As the melt is lowered through the furnace it passes through a temperature zone at which the liquid freezes (AgCl 455°C, AgBr 434°C). The crystal is formed, layer by layer, as the sample passes through this zone. To keep a constant temperature and temperature gradient in the furnace it has been sufficient to use a constant voltage transformer for the supply voltage, although even better results might be obtained with more careful temperature regulation.

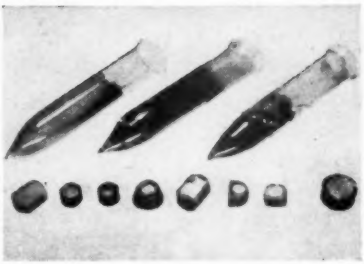

FIG. 6. Above, glass molds and synthetically grown crystals of silver halides. Below, crystal counter specimens cut from molds and ingots of the type shown above

After the crystal has been lowered through the freezing zone, the temperature in the furnace is reduced steadily until the furnace reaches room temperature. In the case of AgBr a clear yellow solid will be formed starting with a seed at the tip. Near the top of the solid the color is generally darker and sometimes even black. This is the region of impurity. The lower portions of the crystal can now be remelted and a recrystallization performed. This time the solid is a uniform pale yellow except at the very top.

With such doubly and triply crystallized samples excellent results have been obtained. It is an easy matter to make a moderately large counting specimen in the form of a cylinder, for example, as at the far right of Fig. 6. One merely grinds through the glass and crystal with a carborundum glassblower's saw and then presses the crystal out of the glass ring. Sometimes

* Platinum is more desirable and avoids corrosion by AgCl vapor.

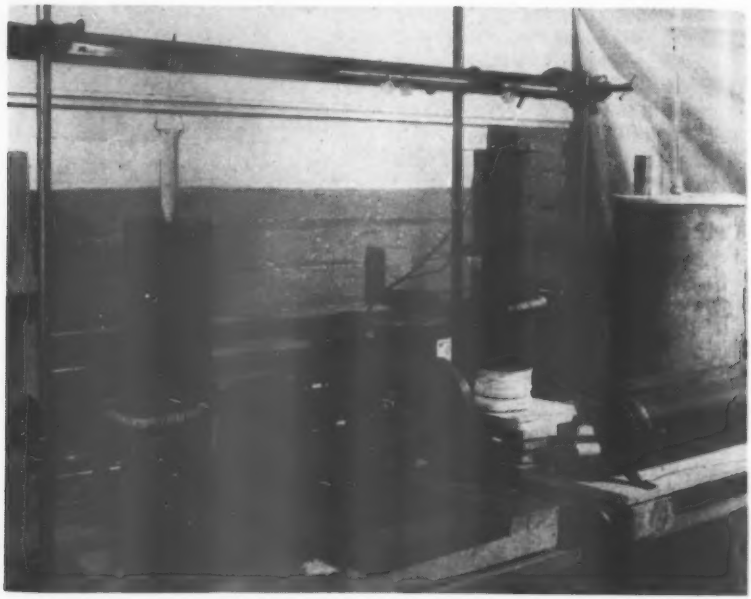

FIG. 7. Furnace, gear train and mold shown in position prior to lowering mold into furnace (Bridgman method)

hypo will aid the removal of a specimen from the glass ring. Such specimens have fairly good surfaces, which can be etched slightly with hypo to remove carborundum dust and to relieve strains, and washed carefully to remove hypo. They are then ready for electrodes, which can be put on with conventional sputtering or evaporation technique or by treatment with a special developer (*43*). Paper developer has also been used successfully. Aquadag electrodes have also been used.

Crystals grown at a slow rate seem to show smooth surfaces in contact with the pyrex glass mold. Crystals grown rapidly generally show irregular pitting and bubbles at the glass-crystal interface. Recently, Harrison has grown quite perfect, large AgCl crystals (1.5-in. diameter, 2.5 in. long) using a new furnace with 4-in. diameter core. This furnace is provided with two heating coils and three thermocouples for measuring the temperature above, below and at the level of crystal growth and also, therefore, the temperature gradient at the liquid-solid interface. The most recent samples have been grown in vacuum. The vacuum procedure may prove valuable if it is desired to introduce impurities in the crystal sample which may be volatile at high temperatures. Counter studies of the vacuum-grown samples have unfortunately not been made at the present writing.

An attempt has been made to grow crystals in a square pyrex tube so that subsequent machining of the sample might be kept to a minimum. Instead of obtaining a single crystal a polycrystal was formed, many small crystals growing out of the corners. Experi-

ments with rounded corners are contemplated but have not yet been attempted.

The AgBr samples prepared by the Bridgman method have been shown by etch tests to be made up of large regions in which the material is in the form of "single" crystals. The macroscopic etch test gives, of course, no indications as to the microscopic structure of the crystal. Etch figures can easily be seen on rolled Harshaw specimens, as in the case of Fig. 8. The crystals grown by Yamakawa and Harrison show little etch structure, except in the impurity regions on top of the crystallized ingot specimens. The crystals can also be examined under polarized light in looking for strains and crystal boundaries. Although this test is convenient and simple, strain colors confuse the pattern and the etch test is probably more reliable when it is desired to look for crystal boundaries. Correlation between counting specimens and their X-ray patterns would probably provide the most accurate index to the counting property.

Samples grown and cut by the methods outlined above are shown below the tubes in Fig. 6. Such crystals show no electrolytic or electronic conduction at low temperatures, i.e., they are insulators. Samples taken from the upper parts of the crystal or prepared from impure material will show conductivity even at low temperatures and such crystals are useless as counters. Occasional commercial crystals of AgCl show such conductivity. Spurious pulses due to such conductivity may appear at high voltage gradients in impure samples, and it is believed that impurities therefore furnish at least one contribution to the cause of spurious pulses observed in crystal counters of the silver or thallium halide types (*36*).

It is quite interesting that pure crystals of AgCl and AgBr prepared by recrystallization show less darkening

FIG. 8. Etch pattern of a commercial rolled specimen of AgCl showing many small crystal faces. Diameter of specimen is $1\frac{1}{4}$ inches

when exposed to (fluorescent) light at room temperature than impure samples. The indications are therefore that the darkening is connected in some way with impurities.

A crystal taken directly from the mold (presumably strained by contact with the glass walls) will generally not count well, if it counts at all. Annealing of such a sample always produces a counting sample. It is therefore felt that this method of crystal growth and preparation is reasonably successful for production of crystal counters. There may be other schemes equally good or better for preparing counting specimens. However, the lack of published results does not permit of comparison.

The eutectic (KRS-5) thallium iodide (60%) - thallium bromide (40%) has also been prepared by Harshaw and the National Bureau of Standards. This material has great promise because of its high density (> 7.00) and temperature at which it can presumably be made to count when pure ($-70°$ C). However, the dielectric constant is rather large (~ 30) compared with AgCl (~ 12) and the capacitance of the crystal is thus rather high compared with AgCl or AgBr. The pulse size may be smaller on this account. Polarization effects in these salts should be

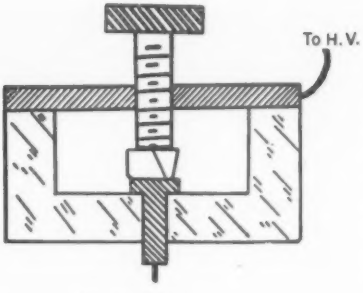

FIG. 9. Diamond crystal holder (Curtiss and Brown)

smaller than in the silver halides because of the large dielectric constants.

Solid and liquid argon. Extremely interesting experiments have been made recently by N. Davidson and A. E. Larsh (*41*) and by A. W. Hutchinson (*42*) which show that both solid and liquid argon can be made to count ionizing radiation. Davidson and Larsh have used alpha particles whereas Hutchinson has employed gamma rays. In this work the argon was carefully purified in order to remove oxygen atoms. Less than 1% of dissolved oxygen quenches all pulses. Considerable quantities of dissolved nitrogen do not affect the pulses, although liquid nitrogen apparently does not count when pure. n-Heptane and hexane do not give observable pulses. Further discussion of argon counters is given in Part 2.

Apparatus

A typical crystal holder used by Curtiss (*15*) in work with diamond crystals is shown in Fig. 9. A simple holder of this type suffices for work at room temperature. Although not used by Curtiss, it may be advisable to use a vacuum chamber surrounding the holder, to prevent atmospheric water vapor from affecting the results. Spurious counts, due to ionization of the air between the electrodes, can also be avoided by such means.

For work at low temperatures (77° K) a vacuum chamber appears to be a necessity. A typical apparatus is one used by the author and shown in Fig. 10. This photograph shows a vacuum chamber and the lower end of a dewar vessel held within it. "Micalex" terminals, electrode clips, crystal, positive circular electrode (rear), rectangular crystalline quartz insulating plate and electrode bushings can all be seen in the photograph. The shield, shown out of position and below the chamber, is usually placed over the crystal holder. A thermocouple is fastened to the outside of the shield. To the left, on the cover plate, a radioactive button of P^{32} is shown together with a brass shutter which is moved in or out of the beta particle beam by a "Hermeflex" bellows seal. A schematic diagram of the crystal holder is also shown in Fig. 11.

An over-all view of the apparatus used in studying crystal counters is shown in Fig. 12. The vacuum chamber, pumping system, amplifier, sweep circuit, voltage supply and oscilloscope are all shown in the photograph. Not all the apparatus shown is required for simple counting measurements. A camera is shown attached at the left port of the vacuum chamber (right port of Fig. 10). This camera has been used by K. A. Yamakawa to photograph strain patterns in AgBr crystals at various temperatures. The ports on either side of the vacuum chamber can be used for measurements involving the introduction of light, such as strain measurements or experiments on photoconductivity. The oscilloscope at the right has been used for photographing pulse shapes.* To the left, on the

* The laboratory oscilloscope of V. Fitch and E. W. Titterton, *Rev. Sci. Instr.* **18**, 821 (1947) is more satisfactory for photographic work.

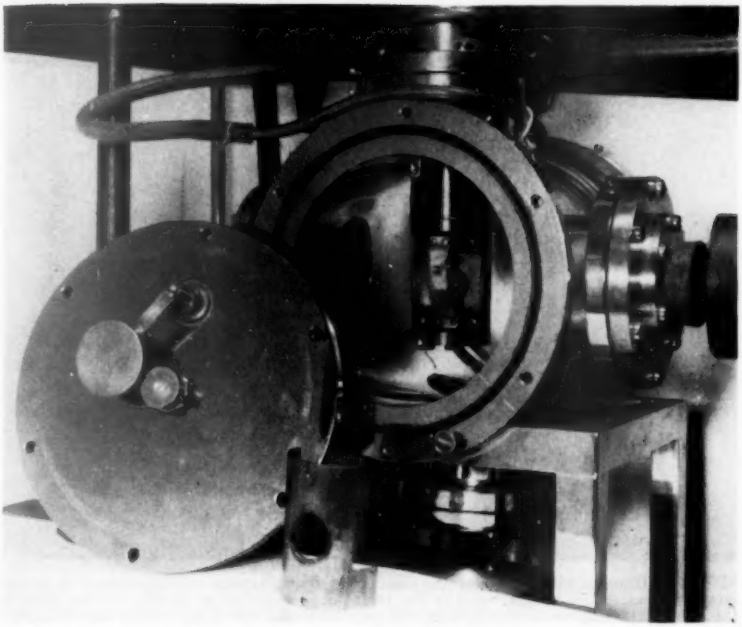

FIG. 10. Vacuum chamber, dewar and crystal holder used in studying silver and thallium halide crystal counters at low temperatures. Radioactive source and shutter are shown at left on the inside face of the cover plate

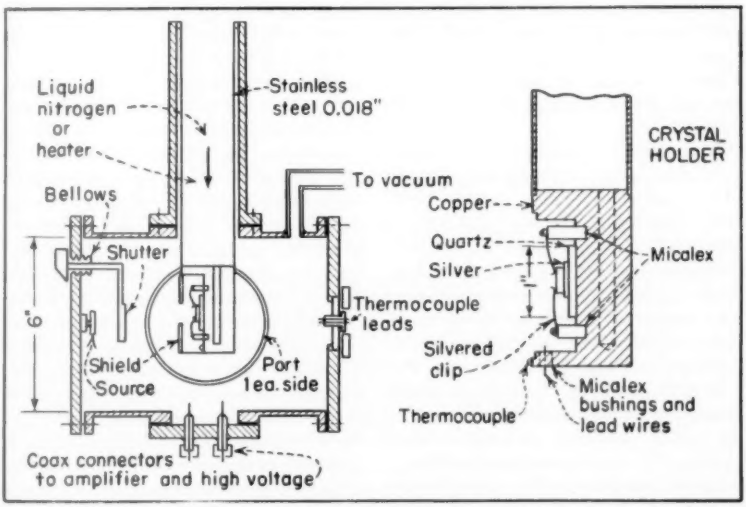

FIG. 11. Diagram of the vacuum chamber, dewar and crystal holder shown in Fig. 10

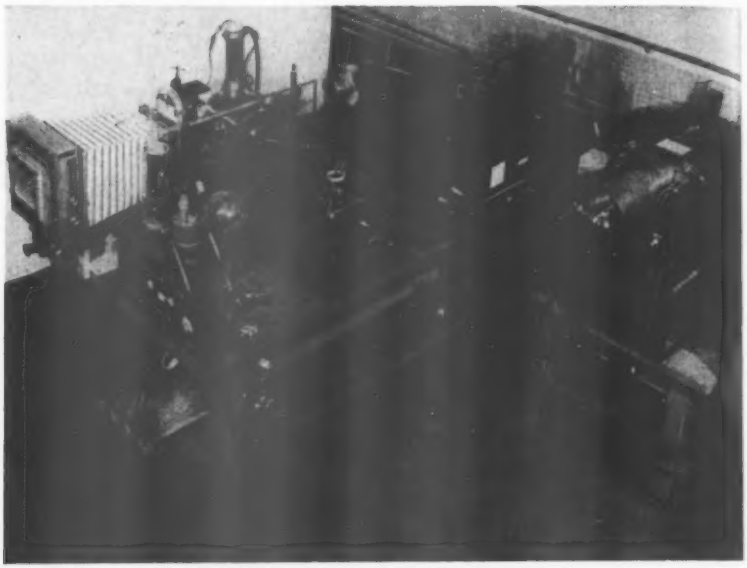

FIG. 12. General view of apparatus used in studying crystal counter operation at low temperatures. The heater, used in the annealing operation, is shown inserted within the dewar. Water cooling coils keep the outside of the dewar near room temperature. Camera at left was used to photograph strain patterns

lower shelf of the table, a motor and gear train are shown with a mechanical connection to a Variac. This auxiliary equipment is used in annealing crystals and will be discussed at the end of this section.

A schematic diagram of the above apparatus is shown in Fig. 13. A variable voltage supply is shown at the left. The positive electrode (at ground potential) is brought to a "Model 501" preamplifier (*54*). The two output leads of the amplifier are conventionally connected as shown so that one drives a sweep and the other feeds the oscilloscope through a delay line. The "Model 260 Sweep" is a trigger sweep circuit and discriminator, designed by M. Sands (*55*), and provides a sweep voltage for each pulse greater than a selected bias level. This arrangement is quite satisfactory but it is certain that many equivalent schemes can be used.

The crystal counter can be expected to provide a larger signal than the gas ionization chamber because of a lower energy/ion pair figure. Even though the pulse obtained is larger than that in an ionization chamber, the pulse is still small enough ($\sim$1–2 millivolts) to require large amplification for studies of pulse size and counting. The large amplification necessarily brings with it the appearance of (shot) tube noise and resistor noise. A discussion of noise is obviously beyond the scope of this survey. However, thorough discussions of this topic have been given by van Heerden (*6*) and Elmore (*56*). It is shown in these considerations that the signal-to-noise ratio takes an optimum

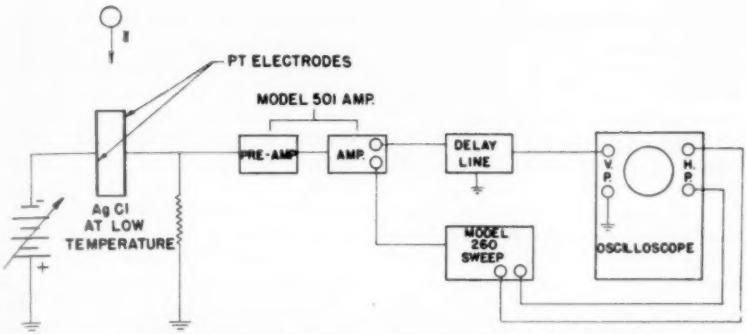

FIG. 13. Schematic diagram of apparatus shown in Fig. 12

value, for any given input tube, when the amplifier frequency characteristic has certain special features. For example, Elmore shows that a minimum detectable pulse of 100 electrons at the grid of a 6AK5 tube can be observed when the rise time and "clipping time" of the amplifier are 40 microseconds and 16 microseconds, respectively. A pulse giving 100 secondary electrons at the 6AK5 grid would correspond to a 760 electron volt beta particle (in AgCl) under the best conditions. It is quite probable that 5–10 electron kilovolt beta particles can be detected in present practice by a crystal counter without great difficulty.

With such an amplifier one can count 160 random pulses per second with only 1% loss of counts. This counting rate is adequate for a large number of problems and, in particular, does not have to be exceeded if one is merely searching for new crystal counting material or if one is studying energy/ion pair. Under these conditions the "slow" amplifier described above, having optimum signal-noise ratio, is highly desirable. In other applications, e.g., coincidence counting, measurement of short time intervals, measurement of mobility, etc., it is necessary to have a more rapid rise time than 40 microseconds. In fact, with crystal mobilities of the order of 250 cm^2/volt-sec, it is possible to obtain crystal rise times of 0.5 microsecond or less. With these conditions a large amplifier bandwidth is required and the signal-noise ratio suffers. Unless such fast amplifiers are necessary it is wiser to use longer rise times, although one must then take precautions against "microphonics" to make full use of the available gain.

At Princeton all studies have been made with the 501 amplifier, which is relatively fast. Its rise time is 0.15 microsecond and gain 3×10^5. The noise level equivalent is a little less than fifty electron kilovolts. In searching for gamma-ray counting diamonds the slower amplifier is definitely more suitable.

In order to photograph the rise of a voltage pulse a delay line is required to delay the pulse while the sweep starts. A Sickles delay line having a 1.1 microsecond delay and 0.25 microsecond rise time was used in early work. However, a more useful delay is given by a Western Electric line having a delay of about 4.8 microseconds and 0.15 microsecond rise time.

With the apparatus of Figs. 10–13, the crystal can be studied with alpha,

beta or gamma-ray sources. As mentioned above, careful handling and heating (annealing) are required for successful operation (*57*). Both ends can be attained simultaneously by the following simple procedure which has been used by the author and K. A. Yamakawa. The object of this procedure will be seen to be that no further handling of the crystal is necessary after insertion of the crystal in the crystal holder.

The crystal is prepared with thin metal electrodes before introduction into the vacuum chamber. The prepared crystal is mounted in the chamber as shown in Fig. 10. No great precautions need be taken other than to keep the crystal clean and to avoid excessive pressure at the contacts. The vacuum chamber is closed and evacuated to a pressure between 10^{-4} mm and 10^{-5} mm Hg. A small heater is placed in the interior of the dewar vessel where liquid nitrogen is usually introduced. The heater is therefore in air and is used to bring the crystal holder and crystal to a temperature of about 400°C for AgCl and about 380°C for AgBr. After the dewar is held at this temperature for a few hours the temperature is gradually reduced automatically by the Variac, motor and gear train previously referred to. Seventeen hours, or perhaps less, are sufficient for the entire annealing process in a small crystal, although tests on the optimum duration have not been made. After reduction of the dewar and crystal to room temperature the dewar is filled gradually during a period of a few hours with liquid nitrogen and the temperature is thereby reduced to 77° K*. The crystal will be sensitive to ionizing radiations at this temperature after such treatment. In this way consistent and reproducible counting behavior has been obtained. It is not necessary to perform the operation of annealing before each use of the crystal. If the crystal is kept in the dark, subsequent cooling to low temperature seems to give the same pulse shapes and pulse heights. A study by Yamakawa has shown that several successive coolings do not change the strain pattern in the crystal, at least when the cooling operation is performed in a half hour period or longer.

The above apparatus might be improved by placing heater coils directly in the crystal holder. Water cooling on the outside of the vacuum chamber is desirable, since the metal walls get warm and may damage the rubber gaskets used for vacuum seals. With the arrangement described above it is important to use electrode terminals which will withstand high temperatures. "Micalex" appears to be satisfactory in this respect.

Some final words of caution may help one avoid some of the troubles usually experienced:

A field should not be placed across the crystal unless it is at very low temperatures—or otherwise permanent changes will take place in the crystal. All (!) light must be excluded from the vacuum chamber during the time that a field is placed on the specimen. It is a good idea to keep light away from the crystal at all times after it has been placed in the vacuum chamber. If it is necessary to view the crystal, orange or red light is probably satisfactory if the field is turned off. Too high temperatures should not be used in annealing since the crystal material will evaporate into the vacuum. As van Heerden has pointed out, only silver, platinum and gold may be used for contact with the crystal. Chemical substitution occurs with other metals. The capacitance of crystal connections and preamplifier input should be kept as low as possible to obtain the best signal to noise ratio.

* Van Heerden has used less than an hour for the cooling process.

EDITOR'S NOTE: Part 2 of this paper, which will be published next month, will contain detailed descriptions of the experimental results of the author and other investigators, a discussion of the results, and an evaluation of the present status of the field and the future possibilities.

BIBLIOGRAPHY

1. For information on such counters, see S. Korff, "Electron and Nuclear Counters," (D. Van Nostrand Co., New York, 1946)
2. D. R. Corson, R. R. Wilson. Particle and Quantum Counters, *Rev. Sci. Instr.* **19,** 207 (1948)
3. W. C. Röntgen, A. Joffé; *Ann. Physik* **41,** 449 (1913); **64,** 1 (1921)
4. H. Schiller, *Ann. Physik* **81,** 32 (1926)
5. G. Jaffé, *Physik. Z.* **33,** 393 (1932)
6. P. J. van Heerden, The Crystal Counter. Utrecht Dissertation, 1945
7. R. Frerichs, R. Warminsky, *Naturwissenschaften* **33,** 251 (1946); R. Frerichs, *Naturwissenschaften* **33,** 281 (1946)
8. G. Stetter, *Verhandl. deut. physik. Ges.* **22,** 13 (1941) in which the work of J. Kosmata, K. Huber and W. Jentschke was reported
9. W. Jentschke, *Phys. Rev.* **73,** 77 (1948)
10. D. E. Wooldridge, A. J. Ahearn, J. A. Burton, *Phys. Rev.* **71,** 913 (1947)
11. J. C. Street, Letter to J. A. Wheeler; see also Brookhaven Conference Report on High Speed Counters, August 14–15, 1947
12. R. Hofstadter, *Phys. Rev.* **72,** 747 (1947)
13. R. Hofstadter, J. C. Street, Brookhaven Conference Report on High Speed Counters (August 14–15, 1947)
14. L. F. Wouters, R. S. Christian, *Phys. Rev.* **72,** 1127 (1947)
15. L. F. Curtiss, B. W. Brown, *Phys. Rev.* **72,** 643 (1947)
16. W. L. Whittemore, J. C. Street, *Phys. Rev.* **73,** 543 (1948)
17. G. T. Reynolds, unpublished
18. R. Hofstadter, J. C. D. Milton, S. L. Ridgway, *Phys. Rev.* **72,** 997 (1947)
19. K. G. McKay, *Phys. Rev.* **74,** 1606 (1948)
20. H. Fröhlich, N. F. Mott, *Proc. Roy. Soc.* **171A,** 496 (1939)
21. N. F. Mott, R. W. Gurney, "Electronic Processes in Ionic Crystals," (Oxford University Press, New York, 1940)
22. J. T. Randall, M. H. F. Wilkins, *Proc. Roy. Soc.* **184A,** 366 (1945)
23. R. P. Johnson, *J. Optical Soc. Am.* **29,** 387 (1939)
24. F. Seitz, R. P. Johnson, *J. Applied Phys.* **8,** 84, 186, 246 (1937)
25. K. Hecht, *Z. Physik.* **77,** 235 (1932); see also ref. *21*, p. 121
26. F. Seitz, *Phys. Rev.* **73,** 549 (1948)
27. W. Shockley, *J. Applied Phys.* **9,** 635 (1938)
28. W. Lehfeldt, *Nachr. Ges. Wiss. Göttingen,* N. F. Fach, **2,** 171 (1935)
29. W. Flechsig, *Z. Physik* **46,** 788 (1928)
30. F. Seitz, *Revs. Modern Phys.* **18,** 384 (1946)
31. A. Smakula, *Z. Physik* **59,** 603 (1930)
32. J. Frenkel, *Physik. Z. Sowjetunion* **8,** 185 (1935)
33. B. Gudden, R. Pohl, *Z. Physik* **16,** 170 (1923)
34. R. C. Herman, R. Hofstadter, *Phys. Rev.* **59,** 79 (1941)
35. A. L. Hughes, L. A. Du Bridge, "Photoelectric Phenomena," pp. 308 ff., (McGraw-Hill Book Co., Inc., New York, 1932)
36. R. Hofstadter, *Phys. Rev.* **72,** 1120 (1947)
37. K. A. Yamakawa, Thesis, Princeton (1949)
38. A. J. Ahearn, *Phys. Rev.* **73,** 524 (1948)
39. R. Frerichs, *Phys. Rev.* **72,** 594 (1947)
40. H. Kallmann, R. Warminsky, *Ann. Physik* **4,** 69 (1948)
41. N. Davidson, A. E. Larsh, Jr. *Phys. Rev.* **74,** 220 (1948)
42. A. W. Hutchinson, *Nature* **162,** 610 (1948)
43. J. R. Haynes, *Rev. Sci. Instr.* **19,** 51 (1948)
44. H. Friedman, L. S. Birks, H. P. Gauvin, *Phys. Rev.* **73,** 186 (1948)
45. R. Hofstadter, *Phys. Rev.* **73,** 631 (1948)
46. L. S. Birks, H. P. Gauvin, E. J. Brooks, memorandum, Naval Research Laboratory, June 4, 1948
47. A. J. Ahearn, *Phys. Rev.* **73,** 1113 (1948)
48. H. Kallmann, R Warminsky: An abstract of this article has been obtained. The article itself (*40*) is in *Ann. Physik* **4,** 69 (1948) and has not been available
49. S. Kyropoulos, *Z. Physik* **63,** 849 (1930)
50. H. C. Kremers, *J. Optical Soc. Am.* **37,** 337 (1947)
51. P. W. Bridgman, *Proc. Am. Acad. Arts Sci.* **60,** 305 (1925)
52. F. B. Harrison, unpublished
53. R. H. McFee, *J. Chem. Phys.* **15,** 856 (1947)
54. W. C. Elmore, to be published
55. M. Sands, to be published
56. W. C. Elmore, NUCLEONICS, **2,** No. 3, 16 (1948)
57. J. C. Street, Brookhaven Conference Report on High Speed Counters (August 14–15, 1947)

Stack Meteorology and Atmospheric Disposal of Radioactive Waste

By NORMAN R. BEERS
Brookhaven National Laboratory, Upton, New York

"Two strange towers have recently been completed at Brookhaven. They are needed for study of air currents high above the laboratory so that the operators of the nuclear reactor will know where its exhaust gases are going. One of them is 420 feet tall—highest structure on Long Island—and has a pipe running all the way to the top. When weather observations are going on, the smoke from a standard Army smoke generator released through the pipe creates a small cloud, which can sometimes be seen for miles around."

—Fifth Semiannual Report of the Atomic Energy Commission

In common with other industries, the new atomic-energy industry presently disposes of certain waste products into the atmosphere by the use of high stacks. As pointed out by W. A. Rodger, of the Chemical Engineering Division of Argonne National Laboratory, speaking in Washington at the recent Waste Disposal Symposium (*1*), "The stated aim of the Atomic Energy Commission is to discharge no activity to nature. Practically this is a very difficult thing to do. Tolerances will be set probably at or near the natural backgrounds for the areas involved."

Another participant in the symposium, Roger S. Warner, director of the AEC's Division of Engineering, remarked that gaseous, liquid and solid wastes appear at each of the various hot steps, and the "expedients for disposal used to date have at least stood the test of time." The ultimate goal is improvements in basic design which will if perfected do away with waste disposal problems by changes in the sources so that no waste ever appears.

The general facts of ordinary waste disposal to the atmosphere are obvious to anyone who has lived in or near an industrial city. Only the more severe days of smog or the occurrence of a Donora disaster serves to arouse more than casual interest; in fact, the general apathy of the public toward the problems of smoke in the atmosphere is not unconnected with its very prevalence.

No such apathy exists either publicly, or in the Commission or with its contractors, when radioactive waste is considered. David E. Lilienthal, AEC's Chairman, has set the task ahead by remarking that we must learn to live with radiation, that radiation has become a kind of fourth "R," and that the "waste disposal problem is a part of this general business of learning how to live with radiation."

The proposed radioactive waste disposal at Brookhaven that resulted in

Oil-fog smoke, seen trailing from the taller of the two Brookhaven National Laboratory meteorology towers, is used in experiments to collect data on safe atmospheric disposal of radioactive waste from the 320-foot reactor stack

the construction of meterological towers and field test installation of oil-fog smoke is inherent in the choice of cooling fluid (air from the surrounding atmosphere) for the nuclear reactor or pile. After passing through the reactor, ducts, fanhouse, cooling tower and 320-foot stack, the cooling air will contain a small quantity of radioactive argon. The stack will discharge its effluent at a speed and temperature considerably in excess of the surrounding air, and the effluent will then be dispersed to insignificant concentrations by atmospheric turbulence. Even on leaving the stack, the concentration of argon-41 will be small. Of the total mass of atmosphere, only 1.28% is argon, and of the total mass of argon only a very minor fraction becomes radioactive as the air passes through the reactor.

Reactor-cooling air will be filtered before and after delivery to the pile to remove dust which may be radioactive. Carbon-14 may occasionally be discharged in very small amounts, so small as to have no public health significance according to Arthur E. Gorman (*1*). The reason for a meteorologist's interest in the physical nature of the effluent is that required conditions of atmospheric turbulence, serving to disperse the effluent to harmless concentrations, differ according to whether the pollutant contained has a long or short half-life, is washed out by rain or snow, is deposited or adsorbed on or by vegetation and other obstacles, is gaseous or particulate, *etc.*.

Meteorological tower showing first three booms with thermohms, Aerovanes, and Gurley wind transmitter

The meteorologist must also inform himself, from public health authorities or others, of the tolerances or maximum permissible operating levels set for the different pollutants that may appear. From a practical point of view, these tolerances are and must be set so that the instantaneous concentrations will not exceed a certain maximum and that the time mean of concentration, sometimes over a rather long period of time,

will be attainable in practice. One would not permit even small atmospheric concentrations of certain odors, for example, to persist for as long as ten minutes, whereas an equal concentration of argon-41 surrounding the person would in that time pass completely unnoticed and would cause no harm whatever.

The argon problem lends itself to a second illustrative example with equal force. Argon-41 has a half-life of 110 minutes and is a gaseous constituent of the atmosphere. Consider the effluent from a high stack when the wind at stack top is light and variable in direction. Under the very light atmospheric turbulence assumed, and provided the vertical structure of temperature shows an inversion (*i.e.*, warm air overlying cold), then, by the time molecular diffusion has carried the argon-41 to ground, its concentration in curies per cubic meter will be so small, due to decay alone, as to be harmless, if the concentration at stack top is small enough to permit operation of the reactor normally. If, on the other hand, the effluent should contain particulate matter either of long half-life or of sufficient size and mass to fall out quickly, then persons within a few stack heights of the plant will probably be exposed to danger unless the effluent is curtailed or stopped.

Stack Meteorology

From the preceding paragraphs, it is obvious that for best results the stack meteorologist will need to be consulted even during the plant-planning stage. Some of the more important parameters which determine the control regime to be adopted for a particular waste disposal installation are as follows:

Design parameters of source(s)—
- Height and diameter of stack.
- Temperature, effluent speed, physical nature, and mass rate of stack effluent.
- Nature of surrounding structures and terrain.

Meteorological parameters—
- Wind—speed, direction, gustiness, persistence, and their derivatives.
- Temperature—air temperature and its derivatives.
- Humidity and precipitation.

Usually the general plant location is settled by considerations beyond the scope of meteorology, although when atmospheric waste disposal is contemplated this procedure is subject to criticism. The location of stacks in valleys will, other things being equal, result in larger concentrations of pollutants near the ground than would result if the stacks were on level country or on knolls. Each case of plant location must be examined on its merits, with attention being paid waste disposal problems as well as availability of water, raw materials, *etc.*

High stacks are usually desirable not only because they produce increased draft, but also because the maximum ground concentration of effluent from the stacks varies inversely as the square of stack height, if the top of the stack is above the chaotic turbulence found near rough structures such as buildings. This requires, in general, that the stack be at least 2½ times the height of structures that are within 20 stack heights of it, although in order to be certain one sometimes resorts to tests of models in wind tunnels. Such tests were performed for the Brookhaven Laboratory by the Cornell Aeronautical Laboratory in their new variable-density wind tunnel in Buffalo.

High stacks also raise the effluent source above the lower layers of the atmosphere in which wind speed decreases at night on the average. The height to which one must build to attain a level where the wind speed not infrequently increases will vary with plant location and the surrounding terrain; at Upton, where the general

topography is slightly rolling and covered with small trees up to about 30 feet in height, experience shows that wind speeds at about 300 feet above the surface will usually increase at night and may decrease during the day if the pressure gradient remains about constant, and if there are few or no clouds.

Stack diameter is important when one considers that sufficient diluting air must be forced through with the pollutant so that the concentration at stack top will not be too great to be endured for short periods at the ground level. For when there is a temperature lapse (*i.e.*, cold air overlying warm), the atmosphere is filled with large eddies, three-dimensional in character, which carry effluent from the stack top to ground from one to perhaps ten stacks heights away from the base of stack. The concentration at stack-top level is brought with little additional dilution to ground and, while the condition may not persist longer than a few minutes, it generally recurs throughout a longer period, *e.g.*, the whole of a sunny day.

Hot stack gases rise of their own buoyancy well above the structural height of the stack, provided their effluent speed is not much lower than the speed of the wind. Even the warmest gases will go off almost horizontally when the wind speed exceeds three times the effluent speed, for within a very short distance of the stack opening the hot gas is cooled by mixing with the surrounding atmosphere. With light wind and an almost isothermal atmosphere, stack gases may rise several hundred feet above stack top; thus the value of maximum ground concentration may be quartered, for example, if the effective height of stack is thus doubled.

Once the design parameters of the source(s) are fixed and certain generally acceptable simplifying assumptions are made in regard to the nature of atmospheric turbulence, one may refer to a formula by Sutton (*2*) for the concentration of pollutant downwind from a continuously emitting point source. Sutton finds that

$$\chi(x,y,z) = \frac{Q \exp\left(-y^2/C_y^2 x^{2-n}\right)}{\pi C_y C_z u x^{2-n}} \left[\exp\left\{ -\frac{(z-h)^2}{C_z^2 x^{2-n}} \right\} + \exp\left\{ -\frac{(z+h)^2}{C_z^2 x^{2-n}} \right\} \right]$$

to an adequate first approximation where

x, y, z = axes along the direction of the mean wind, across wind, and vertical; $z = 0$ at the ground

χ = concentration of smoke or gas (gm/cm^3)—or curies/cm^3

Q = strength of source (gm/sec)—or curies/sec

u = mean wind speed, assumed invariable with height (cm/sec)

C_y, C_z = virtual diffusion coefficients for y- and z-directions

n = pure number lying between 0 and 1, a parameter related to the diffusing power of the atmosphere

h = effective stack height

Sutton proceeds to give formulas for C_y and C_z in terms of the kinematic viscosity of the air, n, u, and the eddy velocities v' and w', thus relating these coefficients to observable meteorological entities without reliance in any way upon observations of the diffusion of matter. Some changes of consequence are suggested by Sutton himself in recent lectures given at the Weather Bureau in Washington; others have been promised in a forthcoming publication.

Considerations of probability and statistics alone clearly demonstrate that the functional form of Sutton's equation for concentration of effluent pollution in the atmosphere has a validity greater than may be ascribed to his further efforts to associate it with

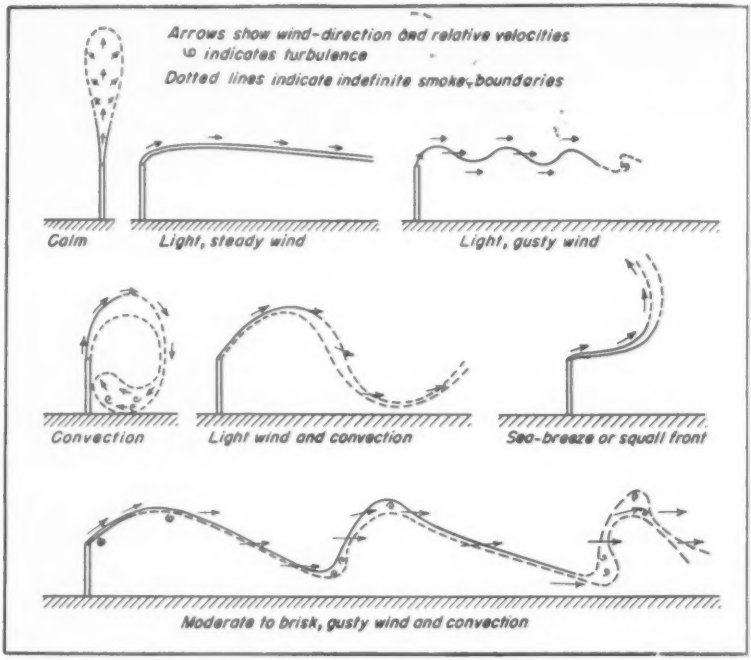

Smoke forms following Etkes and Brooks (7)

meteorological entities alone. Moreover, it is difficult with any apparatus to determine what the eddy velocities v' and w' are, and, in any case, such equipment as has been used (both American and British bivanes essentially) is not available as a catalog item.

Even if the eddy velocities are determinable as meteorological entities, and this may be argued, one may adopt an entirely different course of investigation, as has been done at Brookhaven.* This is to seek relations among effluent concentration as observed and those meteorological entities that appear on the daily weather map. The seeking is greatly facilitated by using relations derived from Sutton's equation (or another of similar form developed at Brookhaven), *e.g.*, to devote special attention to measuring the maximum ground concentration. Thus one seeks to determine C_y, C_z, and n in terms of isobaric or frontal configurations of the Norwegian school essentially, or to determine the minimum additional regular data needed in special cases.

The course of investigation actually adopted at Brookhaven from July 1947 onwards seems also to fit very well the description of what is desirable in a second special field, namely, *radio meteorology*. According to Booker (*3*), "There is, of course, no particular difficulty in measuring the profiles of temperature and humidity as required above at a particular location by means

*Research carried out at Brookhaven National Laboratory under the auspices of the Atomic Energy Commission.

of meteorological instruments attached to towers, balloons, kites, aircraft, *etc.* Important as such experiments are, however, they do not by themselves constitute an adequate understanding of the problem for radio meteorological purposes. *The real problem is to be able to specify the profiles of temperature and humidity sufficiently accurately purely from the weather data ordinarily available in synoptic meteorology.*" The italics are the present author's. The quotation will serve to illustrate some differences as well as similarities between stack and radio meteorology.

Quite aside from the relative advantages or disadvantages of seeking values for the diffusion coefficients as functions of eddy velocities or of more macroscopic entities such as cyclones and frontal slopes, one must still investigate the fit between theory and observed values of effluent concentration in the atmosphere. Thus Sutton's work was released for publication only some years after its execution since, in the last analysis, it has to stand on observations, and in his case the observations were reported in certain fundamental and but recently secret experimental data emanating from the Chemical Defense Experimental Station (Ministry of Supply, England). An equally comprehensive set of experiments for the case of an elevated source has yet to be performed.

It is to obtain data from such experiments that the meteorological installation at Brookhaven was planned and constructed. Work of a somewhat similar nature was carried on at the Hanford Engineer Works by Church (*4*) during war years. Both Church and Sutton concerned themselves with an effluent assumed gaseous in character, *i.e.*, an effluent in which particulate matter remained indefinitely in suspension. The agglomeration of test matter was omitted from consideration. As a result of these and other considerations, it appears clearly that considerable research into the nature of atmospheric turbulence, its relations with synoptic weather, and the behavior of aerosols all are warranted, from the point of view held not only by those responsible for the disposal of radioactive (or other) wastes but equally by those who wish to maintain a certain minimum concentration of some effluent in the atmosphere, *e.g.*, in the control of insects by the dissemination of DDT.

Oil-fog Smoke Tests

The field test station in the Brookhaven tower consists of an Army M-1 smoke generator modified so as to vaporize as little as 18 gallons of special fuel oil per hour. The generator manifold with its jets is mounted near the ground and at the base of a 350-foot high, 20-inch diameter, steel pipe supported in one vertex of the 420-foot triangular steel tower. A 30-horsepower blower forces up to 10,000 cubic feet of clean air per minute past the jets. As oil vapor at about 850° F flows out of $^3/_{16}$-inch nozzles and cools rapidly in the stream of cold air, oil droplets of rather uniform particle size (0.6 microns diameter) are formed. These generators were due originally to Langmuir and Schaeffer, and developed for the U. S. Chemical Warfare Service (*5*).

When the generator is operating, one sees a dense white cloud of oil-fog "smoke" effluent from the 20-inch stack. The mass rate of flow is determined by measurement of oil consumption by the generator. Samples of the admixed oil-fog and clean air are drawn into the chamber of a photometric densitometer, which was constructed by the Electronics Division at Brookhaven on reports received from du Pont engineers who had made such a device for Church at Hanford. The densitometer is placed appropriately in the oil-fog either at the ground or aloft (up to now in a small aircraft) and used to

Typical Oil-fog Smoke Dispersion During Inverse Conditions

Trail, at sunrise, extended to east-southeast for several miles at 400 feet above ground; wind speed was about 10 mph; inversion was about 5° C between 410 and 18 feet

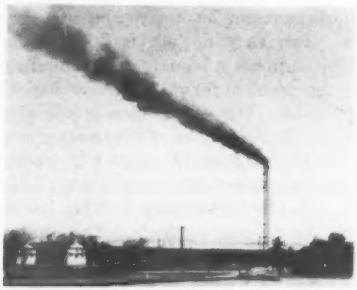

Early morning view of effluent seen from a distance of 2000 feet; wind was from west-northwest at 12 mph; inversion of approximately 4° C persisted between 410 and 18 feet

obtain an indication of the concentration of oil-fog smoke in the air.

Calibration of the densitometer was achieved by Church through use of repeated sampling and admixture of known volumes of stack effluent and clean air as measured by a double-barreled pump. The calibration at Brookhaven is carried on in a smoke-filled room wherein both densitometers and observers (wearing gas masks) operate. The smoke is provided for convenience by a miniature generator which vaporizes a few ounces of oil per hour. Results have been remarkably uniform from test to test considering the inherent instability of the densitometers used.

The photometric densitometers operate on the principle of small-angle scattering of visible light. The particle size selected is that best for obscuration in the visible spectrum. A check on the method is also provided by an air sampler which draws about 0.02 cubic meters per minute of the mixture through Whatman No. 41 filter paper. The filter paper is weighed on a sensitive balance both before and after the run. Background count of dust is accounted for in the photometric densitometer by zeroing of the indicating needle and in the filter by one run when the oil-fog smoke is not present. The photometric densitometers are necessary to observe very low concentrations of oil-fog, the design requested and received being such that normal dust background in the country at about 15 feet above surface would not interfere with measurements. The observation may be made in a few seconds. The filter paper air sampler, on the other hand, is useful for obtaining integrated values, *i.e.*, concentration times time, and may be used with accuracy only when the total mass collected on the filter is several times larger than the limiting sensitivity of the balance used.

The field test program must operate not once but several times in each of many different weather conditions. Outstanding types for investigation are (1) inversion, (2) lapse, and (3) change-over from inversion to lapse. As stated previously, an inversion or stable case exists when warm air overlies cold, on a hazy or frosty morning, for example, after a clear night. The lapse condition occurs whenever cold air overlies warm. Such a condition is

Typical Oil-fog Smoke Dispersion During Lapse Conditions

Effluent from 350-foot stack in the 420-foot meteorology tower. The reactor stack, seen to the right in the distance, lies 3000 feet east of meteorology building which appears in the left foreground. A fresh northwesterly wind under strong lapse (2° C) conditions dispersed the effluent into low concentrations

This oil-fog smoke was photographed on a bright sunny morning at the time of change-over from inversion to lapse conditions. As typical of light winds and variable temperatures, effluent periodically rose several hundred feet above top of tower and then descended, dispersing itself throughout the atmosphere

almost universal on a bright sunny day, for solar insolation heats the earth's surface more than the air above it. During lapse, the lower layers of atmosphere are being continuously replaced by air from aloft; there is an interchange of rather large masses, or one may say the atmosphere becomes thoroughly mixed, or that the atmosphere is turbulent. Flight in an airplane is bumpy during such times of lapse, and smooth during inversions.

Change-over from lapse to inversion occurs normally each evening after sundown, and change-over from inversion to lapse each morning shortly after sunup. The importance of the morning change-over is apparent when one considers that the pollutant effluent during night inversion generally remains in a narrow stream aloft without any great change in concentration from what the concentration was at stack top, except for decay or fallout. When change-over occurs, usually within a few minutes, the entire area under the plume of pollutant aloft will be fumigated by the resultant mixing. It is rather as if a thin layer of oil, say, lying above a layer of water in static equilibrium were mixed into the water by vigorous stirring. Hewson (*6*) studied this phenomenon at Trail, British Columbia, to apply a control regime to the smelter operations there.

The Brookhaven meteorological towers perform two major functions: a source for testing atmospheric dispersion of oil-fog smoke, as it is released from an elevated point; and a support for various instruments to measure meteorological quantities.

A 160-foot triangular cross section tower is located 900 feet from the 420-foot tower. The shorter tower is North-60°-West from the taller; the two are connected by electrified wires about 100 feet above surface. The connecting wires will support a cage in which is to be mounted an electric motor for power to move the cage along this elevated trolley; the cage will carry various instruments to determine, as it transits the 900 feet, the variation of wind, temperature, and humidity along the horizontal. Brook-

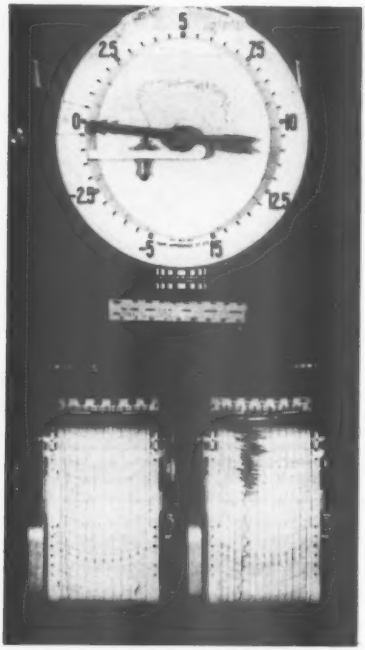

Temperature difference between 410 and 18 feet on meteorological tower. Wind speed and direction at 410 feet. The three traces show quick change-over from inversion to lapse conditions. Effluent dispersion changes character as the wind traces change from inversion to lapse type **(see righthand picture on page 35).**

haven's two towers and provision for instrumentation between them above the surface give the first opportunity to investigate whether the usual assumption of horizontal isotropy is justified. This is of practical importance since meteorological observations have to be extrapolated from the towers to the reactor stack, about 3,000 feet away.

The 420-foot tower was constructed to this height so that observations of wind and temperature up to about 50 feet above the level of nuclear reactor stack top could be obtained continuously. The 160-foot tower stopped at its height because horizontal gradients of meteorological variables are believed to be small or constant above it. Each tower is equipped with an instrument hoist or dumbwaiter sturdy enough to carry 500 pounds; the devices operate at 100 feet per minute on a-c motors. Each tower has a platform for working space at 9, 18, 37, 75, and 150 feet above surface; the tall tower has additional platforms at 300, 355, and 410 feet above surface. The hoist cage is operated from controls located on the platforms and can be stopped at any level by an operator at that or any other level.

When not in use, the hoist cages can be lowered into pits beneath the respective towers. These pits contain the hoist motors and controls, electric panels, and aspirator pumps and motors for thermometers on the various levels. At each platform is mounted a counterbalanced boom long enough to support temperature and wind transmitters some 20 feet from the tower structure. The booms extend in different directions on the two towers so that correct wind speeds are obtainable irrespective of wind direction. Bendix-Friez Aerovanes and Gurley anemometers and anemoscopes measure wind; Leeds and Northrup 100 ohm copper thermohms measure temperature. The thermohms are aspirated with about 15 cubic feet of air per minute supplied by the pit pumps. All instruments record electrically in the meteorology building 900 feet away from each tower.

The meteorology building houses the recorder panel and provides space for miscellaneous maintenance of meteorological equipment, offices for computers and weather technicians, a vault for original records, teletype receivers for Weather Bureau synoptic data, laboratory space for complete examination of samples, *etc.* The entire installation was designed around the

hard fact that in this new and exploratory field, withal one requiring definite answers to specific questions early in its existence, one must prepare to initiate and indeed execute at least the first steps for many problems. Major attention has been devoted to standard meteorological instrumentation, for example, but personnel and equipment are available to extend cautiously if the need arises.

Meteorological Control

Hewson's pioneer work at Trail, referred to above, provides much of interest, not only in the description of instruments and methods used, but also in being perhaps the first successful application of what has become widely known as meteorological control. By meteorological control is meant, not control of the weather, but determination of plant operations that are most effective and efficient with a given source of pollutant for the variable meteorological conditions that will occur. This may mean, for example, an increase in temperature of the effluent, or a change in blower power for the stack, or even curtailment or shutdown of the source. The type and extent of control acceptable clearly depends on a variety of factors.

At Trail, the control regime adopted to prevent damage from sulphur is seasonal and diurnal and includes contemporary meteorological observations. The release of sulphur to the atmosphere is decreased when atmospheric turbulence, especially as determined by gustiness, falls below predetermined values, which vary also with wind direction. Hewson writes, "Attempts were made to forecast winds in the valley, but the difficulties are great. . . . The forecasting of turbulence is even more difficult and was not even attempted. Over more level terrain, forecasts of both wind and turbulence would doubtless be of value, but at Trail the control regime was of necessity based on contemporary observations."

Brookhaven is located much more advantageously than Trail for weather forecasting and, from the first, plans have been pushed so that "operation of the pile will be subject to an elaborate (*sic*) system of meteorological forecasts and the level of operations will be governed accordingly" (*1*). Similar efforts are made or are being considered at other plants both in the United States and abroad.

The full results of investigations now in progress to control disposal of radioactive wastes to the atmosphere will, it is hoped, prove of inestimable value to the smoke problems of all industry. The compelling factor in radioactive waste disposal is perhaps simply that sources are so few that an increase of radiation intensity at any one place will be correctly blamed on the particular plant that produced it. This simplification is rarely found in a study of atmospheric pollution in any great city. However, the opinion is ventured that unless and until coolants other than air are provided simply and inexpensively, the present course will result in satisfactory operations when carefully applied, with full understanding, to the design and construction of future reactors.

The final evaluation will come after the Brookhaven reactor is in operation. Field tests with oil-fog smoke, or any other agent that may be used, will then occupy second place to monitoring the actual radiation count received at various places. The oil-fog smoke tests will have been successful if they permit an accurate prediction of the places that will receive the maximum radiation and a fair estimate of the exact amount present. By itself, testing with an aerosol can do no more, for the radiation received at a point from a cloud of radioactive argon will depend not only on the concentration of ar-

gon-41 at that point but also on the concentration within a region of space around the point in question. This matter can be and is being examined theoretically, but observations after reactor operations commence are necessary to check the work. The important item is that the maximum value can be tested and observed; this is being done.

For the sake of completeness it may be mentioned that the Brookhaven meterological installation, although designed and installed because of the argon-41 in reactor-cooling air, also finds uses in connection with ecological and crop surveys around Upton. Data are here brought to the site by mobile weather and air sampler units (first fitted to test oil-fog smoke concentration around the countryside); from these data an extensive microclimatology of Upton will be determined.

In addition to the argon-41 problem, which in fact assumes on close examination a relatively minor role because of the 110-minute half-life so that the equilibrium value is small in curies even for an otherwise strong source, one must perforce examine the possibility of other waste. It is known, for example, that under strong inversion conditions the effluent from high stacks may travel in visible concentrations to great distances. This fact is also contained in the theoretical treatment. What then of places tens or even hundreds of miles downwind from the source where, presumably, radiation monitoring devices to report directly to the offending plant are not located? Here reliance must be placed on cooperation between operations and meteorological personnel, the latter to make the best estimate of conditions under which an effluent may continue aloft for many miles downwind and the former to curtail or shutdown the plant even though there is no immediate evidence that accepted levels of radiation are being exceeded.

The problems posed by such speculation are of course recognized as severe enough to warrant extensive and expensive filter or precipitator installations to prevent any such waste reaching the atmosphere. The best equipment is, however, no substitute for knowledge, and no matter how great the reliance placed on devices to can and hold wastes indefinitely, one still must know the areas that will be disturbed in case of accident and the degree of disturbance that will likely result. At the very least, such knowledge will aid in the dispatch of necessary assistance to the right place and in the needed amount. And at the best, one can with forethought undertake those experiments that are hazardous only under (predictable) atmospheric conditions that will certainly provide all the turbulence necessary to perform good dispersion.

Shields Warren (*1*) is credited with the following which makes an excellent closure here. "To sum up the present situation, then, we can say that so far as external ionizing radiation is concerned, there is no hazard with proper methods of disposal. . . . We are striving for as near the ideal as possible; we would like to get as near zero output of radioactivity as we can attain. We have measuring devices that can detect activity at a level that will not be dangerous to humans. We have a means of knowing what our hazard is and of measuring that hazard."

BIBLIOGRAPHY

1. NUCLEONICS **4**, No. 3, 9 (1949); also U. S. Atomic Energy Commission Press Release No. 154 (Supplement), January 27, 1949
2. O. G. Sutton, *Quart. J. Roy. Met. Soc.* **73**, 426 (1947)
3. H. G. Booker, *Quart. J. Roy. Met. Soc.* **74**, 277 (1948)
4. P. E. Church, C. A. Gosline, Jr., MDDC 73
5. I. Langmuir, *Proc. Amer. Phil Soc.* **92**: **3**, 167 (1948)
6. E. W. Hewson, *Quart J. Roy. Met. Soc.* **71**, 266 (1945); see also very extensive report, Bulletin 453, U. S. Bureau of Mines, Govt. Printing Office, Washington 25, D. C. (1944)
7. P. W. Etkes, C. F. Brooks, *Monthly Weather Review* (Oct., 1918)

COSMIC RAYS—I

A review of present knowledge of a field in which a vast amount of research is taking place, together with a report on the status of this research leading to a better understanding of the fundamental properties of the elementary particles

By J. M. JAUCH

Department of Physics, State University of Iowa
Iowa City, Iowa

Discovery and Experimental Methods

EVER SINCE their discovery by V. F. Hess (*1*) in 1911, the phenomena of cosmic rays have been surrounded by mysteries. It is true that since the pioneer days of Hess the interest in cosmic ray research has increased steadily. Today we know so much more about cosmic rays that the early work which led to their discovery appears to us now like a groping in the dark. But it must also be admitted that the greater insight into the nature of cosmic rays which has been gained by the patient and painstaking work of a generation of scientists has resulted in the appearance of new and even greater mysteries. On the other hand, few single fields of research have led in such a short time to such a series of the most astounding discoveries. By means of cosmic rays, nature furnishes us with matter under conditions which could not be realized by any terrestrial experiment. The study of cosmic rays has thus considerably widened our theoretical understanding of the nature and fundamental properties of the elementary particles.

The present state of knowledge in the field of cosmic rays presents thus a very incomplete and fragmentary picture. Large sections hang together and make sense within the framework of our theoretical concepts. But other areas cannot be understood within that framework and even seem to conflict with each other to some extent. In this review we shall not restrict ourselves to the discussion of the well understood and settled questions on cosmic rays but shall also try to summarize our state of knowledge in the incomplete areas. It is hoped that from such a summary there will be gained a better understanding of the purpose and meaning of current research in this field.

The discovery of cosmic rays grew out of the interest in the ionization in gases. After the discovery of radium, it was realized that the radium content of the earth contributed a significant amount to this ionization which was observed in an ionization chamber placed on the surface of the earth. However, Rutherford and his co-workers had observed that shielding of the ionization chamber with lead was not sufficient to remove the ionization completely. In fact, a residual ionization remained even with lead shields sufficient to keep out all radiation due to radioactive materials. A. Gockel (*2*), in 1910, carried an ionization chamber in a balloon to about 4000 m alti-

tude and observed that the ionization decreases somewhat at first, only to increase slightly in higher altitudes. Hess (*1*) subsequently verified these findings with balloon experiments to still higher altitudes. Hess also showed that this radiation, which was responsible for the residual ionization, did not depend on the time of the day or night. He even observed during an eclipse of the sun and could not find the slightest variation. He then was led to postulate the existence of a radiation which entered the atmosphere from outside, which had its origin not in the sun but presumably far removed from the solar system. Hence the name "cosmic rays."

Similar and improved experiments which verified the findings of Hess and Gockel were made by Kolhörster (*3*).

The main results established by these early experimenters were the following: A radiation of unknown nature enters the earth's atmosphere. It produces on sea level an ionization of about 16 ion pairs per cm^3 and per second. This is roughly 10% of the total ionization on the ground due to radioactive sources. With increasing altitude the cosmic rays' intensity increases to many times the ground intensity. No periodic variations of the intensity were observed.

After an interruption of almost ten years, due to World War I, research in cosmic rays was resumed by a large number of physicists. Considerable improvements were made in the experimental technique. Whereas the first discoveries were made exclusively with the ionization chamber, later work was done with the Wilson cloud chamber, the Geiger-Müller counter and, more recently, the photographic plate.

All these research tools operate on the same basic principle. They are merely different devices to detect ionizations produced by fast charged particles or γ-rays. In the ionization chamber the ions are collected on a conductor and the resultant current is measured.

In the counter, the ions which are produced by a fast particle in a gas are used to produce a cascade of electrons and ions in a discharge tube. The most important advantage of the counter is that two or more counters can be set up in such a way that a count is registered only when it occurs nearly simultaneously in all tubes (*4*). With such coincidence arrangement, the background count due to radioactivity can be completely eliminated and the background is thus due entirely to accidental coincidences. It is also possible to arrange counters in anticoincidence. In the more refined modern experiments often a large number of counters are used, partly in coincidence and partly in anticoincidence to register special cosmic ray events. Recently counter arrangements have also been used in delayed coincidences, especially for the investigation of the radioactive decay of the mesotron.

The Wilson cloud chamber uses the tendency of over-saturated water vapor to condense on ions and thus to make the location of these ions visible. Skobelzyn (*5*), who was the first to observe cosmic ray particles in the Wilson chamber, used a magnetic field in the direction of observation to distinguish the charges of the particle. Because of poor statistics, the Wilson chamber is not so useful for large scale quantitative study of cosmic ray events, but the direct visibility of individual events has led to some of the most important discoveries with the Wilson chamber. The Wilson chamber, in recent work, has often been used in combination with the counter in such a way that the chamber mechanism is released by the tripping of a suitably chosen counter system. In such a way events of particular interest can be selected and studied without undue wasteful exposure of the chamber.

Finally, the photographic plate has been used very recently with considerable success for cosmic ray studies. In this case the ions produced by the radiation form the center of a metallic silver crystal, thus leaving a permanent record. The obvious advantage of the photographic plate is its continuous sensitivity and the relative permanence of its recordings.

These four ways of recording ions are the main research tools of the cosmic ray physicist. All the experimental results to be discussed below were obtained with one or several of these tools. It should be mentioned that the physicists are at a great disadvantage in recording the electrically neutral component of the radiation. For the neutrons, this is still relatively easy with the neutron counter, a special adaptation of the ordinary counter, containing boron in the filling gas. However it has so far been impossible to record neutral mesotrons which, according to theoretical consideration, should be present in the cosmic rays in great abundance.

Altitude Dependence of Cosmic Rays

It was observed by the earliest experimenters that the intensity of the cosmic rays increased rapidly with increasing height. In fact from the start this property was considered as one of its main characteristics. The early measurements were all made with the ionization chamber which gives the intensity of the rays entering from all directions. For theoretical interpretations it is more convenient to measure the vertical intensity with a suitable counter arrangement. Rossi (*6*) has recently summarized the best available experiments of the altitude dependence. In Fig. 1 is shown the altitude dependence of the vertical intensity of the total corpuscular radiation. The ordinate is the number of particles crossing one cm^2 in one second per unit solid angle in the vertical direction on a logarithmic scale. The abscissa is the atmospheric depth in gm cm^{-2}. The curve shows an upward curvature from 600 gm cm^{-2} to sea level, a straight section from 300 to 600 gm cm^{-2}, and a pronounced maximum at 140 gm cm^{-2}. From the fact that a maximum occurs, it is seen that the behavior of cosmic rays in the atmosphere is complicated by the production of secondaries. An ordinary absorption, proportional to the intensity of the radiation and the mass of the absorber, would simply lead to a straight line. The maximum indicates that the radiation undergoes a multiplication in addition to the absorption, thus leading to the maximum as observed. The section of the curve near the surface of the earth with the upward curvature, on the other hand, is a first indication of the component structure of cosmic rays; for it shows that one part of the radiation penetrates to great depth with an absorption coefficient different from that of the radiation which is primarily recorded between 300 and 600 gm cm^{-2}. The altitude curve depends on the geomagnetic latitude at which the ascent is made. The curve here reproduced is for geomagnetic latitudes greater than

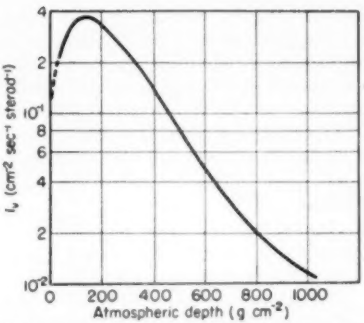

FIG. 1 The vertical intensity of the total corpuscular radiation as a function of altitude

about 45°, beyond which practically no variation is observed. If the curve for the total intensity could be extrapolated to zero depth one could obtain the intensity of the primary radiation. This procedure however is very uncertain because of the large fluctuations of the total intensity curve at high altitudes.

Fortunately, it has recently been possible to measure the primary intensity directly with a counter placed in the nose of a rocket. Van Allen and Tatel (7) report a constant directional intensity of 0.12 particles cm^{-2} sec^{-1} $sterad^{-1}$ for altitudes above 55 km to as high as 161 km. These authors point out however that this figure may not represent the true number of primaries because of the fact that an unknown number of secondaries may be scattered into outer space and circle around in certain orbits determined by the earth's magnetic field and then reenter the top of the atmosphere. Thus the actual number of primaries could be expected to be somewhat lower than this figure.

The Components of Cosmic Rays

A large number of experiments indicate that cosmic rays as observed in the atmosphere are not homogeneous but are composed of several different types of particles. For practical purposes it has become customary to place the different kinds of particles into two groups, which are called the hard and soft components of the radiation.

The two components can be made visible by the simple experimental arrangement indicated in Fig. 2. A lead plate of variable thickness is placed between two counters in coincidence one above and one below the plate. If the counting rate is plotted as a function of the lead thickness, the thick curve in Fig. 2 is obtained. This curve shows a marked change in slope at about 8 to 12 cm of lead. For thickness up to 8 cm the experiment gives the absorption curve for both hard and soft component together. At 12 cm the soft component is practically completely absorbed and what remains is only the hard component with a considerably lower absorption coefficient and hence a more gradual decrease with increasing thickness. One may define the hard component arbitrarily as the radiation which penetrates 12 cm of lead. The part which is absorbed is then the soft component.

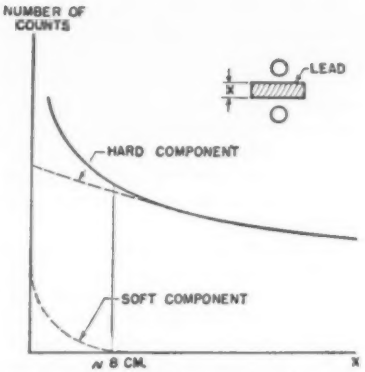

FIG. 2. Experiment for separating hard and soft components

At sea level the soft component is about 23 % of the total intensity. The ratio changes rapidly with altitude. At 630 gm cm^{-2} the two components are about equal in intensity, and at 140 gm cm^{-2}, where the total intensity has a maximum, the soft component is about 78 % of the total radiation. The most remarkable feature however is the fact that the intensity of the hard component keeps on increasing up to the highest altitudes for which measurements were made. Thus the maximum of the curve giving total radiation is entirely due to the maximum of the soft component.

The definition of hard and soft component just given is purely phenome-

nological. This division is, however, useful from the theoretical point of view also, since the so-defined radiations almost coincide with particles of different fundamental properties. Thus the soft component in the lower atmosphere is now known to exist to almost 100% of photons, electrons and positrons. For the purpose of this review we shall identify the soft component of the radiation with these particles. At high altitudes, however, as much as 15% of the soft component as defined above may consist of slow mesotrons. The hard component, on the other hand, consists primarily of mesotrons which are particles of positive and negative charges and a mass of about 200 times the electron mass. Thus, these mesotrons constitute the bulk of the radiation at sea level. Recent work has furnished strong evidence that there exists a different kind of mesotron at higher altitude with a larger mass and probably a different interaction with nuclear matter (*8*). These heavier mesotrons would have to be included in the hard component. Also included are the very small number of protons, neutrons and perhaps other nuclear fragments, since they are also of the penetrating sort.

The Geomagnetic Effects

Before proceeding further with the discussion of the special properties of the soft and hard components, we shall mention here first the effects caused by the magnetic field of the earth. This field is sufficiently strong to influence considerably the primary radiation far outside the atmosphere. To understand these effects it is necessary to enter briefly into a discussion of the motion of a charged particle in a magnetic dipole field such as that of the earth.

We use a Cartesian coordinate system with the origin in the center of the earth and the z-direction pointing to north. The earth's magnetic field is then very nearly represented by a magnetic dipole at the origin pointing south. The magnetic field strength is derivable from a potential function

$$\psi = -\mu z/r^3 \qquad (1)$$

where μ is the strength of the dipole. The magnetic field at any point (x,y,z) is then given by

$$\mathbf{H} = -\nabla\psi \qquad (2)$$

or

$$\begin{aligned} H_x &= -3\mu xz/r^5 \\ H_y &= -3\mu yz/r^5 \\ H_z &= \mu\left(\frac{1}{r^3} - \frac{3z^2}{r^5}\right) \end{aligned} \qquad (3)$$

The equations of motion of a particle with rest mass m_0 and charge e are then

$$\frac{d}{dt}\mathbf{p} = \frac{e}{c}(\mathbf{v} \times \mathbf{H}) \qquad (4)$$

Here $\mathbf{p} = m\mathbf{v}$ is the relativistic value of the momentum of a particle moving with velocity $\mathbf{v}$ and $m = \dfrac{m_0}{\sqrt{1 - v^2}}$ is the effective mass. It is essential to use the relativistic expression for the mass since most of the cosmic ray particles have energies in the extreme relativistic region.

A first integral of Eq. 4 is obtained by taking the scalar product of Eq. 4 with $\mathbf{p}$, which gives zero on the right-hand side thus leading to

$$\mathbf{p} \cdot \frac{d}{dt}\mathbf{p} = \frac{1}{2}\frac{d}{dt}(p^2) = 0$$

The magnitude p of the momentum and thus the speed v is a constant along an actual trajectory of a cosmic ray particle.

A second integral may be obtained in the following way. Writing out the x, y components of Eq. 4 using dots for the time derivatives we have

$$\begin{aligned} m\ddot{x} &= \frac{\mu e}{cr^5}(3yz\dot{z} - 3z^2\dot{y} + r^2\dot{y}) \\ m\ddot{y} &= \frac{\mu e}{cr^5}(-3xz\dot{z} + 3z^2\dot{x} - r^2\dot{x}) \end{aligned} \qquad (5)$$

Multiplying the first equation with y and the second with x and subtracting,

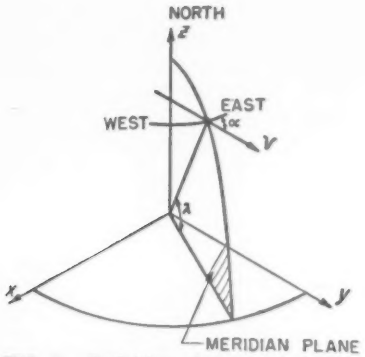

FIG. 3. Definition of geometrical variables in the geomagnetic effect

we obtain after some regrouping of the right-hand side

$$m(\dot{x}y - x\dot{y}) = \frac{\mu e}{c}\frac{d}{dt}\left(\frac{z^2}{r^3} - \frac{1}{r}\right) \quad (6)$$

Integrating with respect to time we see that

$$m(\dot{x}y - x\dot{y}) - \frac{\mu e}{c}\left(\frac{z^2}{r^3} - \frac{1}{r}\right) = C \quad (7)$$

is a second integral of Eq. 4. We introduce now the angles λ and α indicated in Fig. 3: λ is the geomagnetic latitude and α is the angle between the direction of motion of the particle with the west-east direction. Since the first term on the left-hand side of Eq. 7 represents the moment of momentum in the z-direction, it may be written in terms of these angles as

$$m(\dot{x}y - y\dot{x}) = mvr\cos\alpha\cos\lambda \quad (8)$$

We define further the Störmer radius

$$a = \frac{\mu e}{pc} \quad (9)$$

and the dimensionless integration constant

$$\frac{C}{pa} = A \quad (10)$$

Equation 7 may now be written

$$\frac{r}{a}\cos\lambda\cos\alpha + \frac{a}{r}\cos^2\lambda = A \quad (11)$$

To discuss the physical implications of this equation we consider A as a function of r for various values of α and λ. If we let α, λ run through their respective ranges of values

$$\left(0 \leq \alpha \leq \pi;\ -\frac{\pi}{2} \leq \lambda \leq \frac{\pi}{2}\right)$$

we obtain a two-parameter family of curves in the A,r plane, which cover a certain domain in the A,r plane indicated in Fig. 4 as the allowed region. A particle which comes from infinity moves on a line of constant A, since Eq. 11 is an integral of the equations of motion (Eq. 4). If this line represents a real motion, it can never enter a forbidden region; that is, if it reaches the boundary of such a region, the particle does not approach any closer to the earth, but instead turns around and returns to infinity.

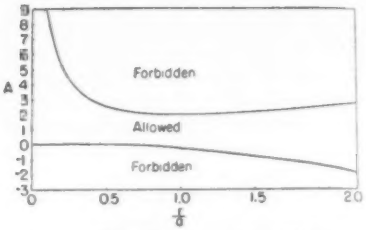

FIG. 4. The allowed and forbidden regions in the plane of A and r/a

Now consider cosmic ray particles which enter the top of the atmosphere at a fixed point $r_0\lambda_0$ and under a definite direction α_0. We see from Fig. 5 that if the energy of these particles is such that $a < r_0$ they may enter at $r_0\lambda_0$ for any direction α_0. However, if $a > r_0$ certain directions α_0 are not accessible for such energies. Since the minimum of the upper forbidden region occurs at $r = a$, $A = 2$, all those orbits are cut off for which

$r_0 < a$ and

$$\frac{r_0}{a}\cos\lambda_0\cos\alpha_0 + \frac{a}{r_0}\cos^2\lambda_0 > 2 \quad (12)$$

The critical angle α_c for which this will occur is thus given by

$$\cos \alpha_c = \frac{2a}{r_0 \cos \lambda_0} - \frac{a^2}{r_0^2} \cos \lambda_0 \quad (13)$$

For a fixed energy no particles will enter at $r_0\lambda_0$ with an angle $\alpha < \alpha_c$. The critical angle α_c is thus half the opening angle of a forbidden cone with its axis normal to the meridian plane. This cone is known as the Störmer cone.

The critical energy, for which the radius of the earth r_0 is equal to the Störmer radius, is 59.6 Bev for electrons and 58.5 Bev for protons.

This elementary theory of the Störmer cone is useful for a first orientation of the effects produced by the earth's magnetic field on the primaries and the phenomena to be expected due to this field. However, for a quantitative study of the geomagnetic effects the theory must be refined. The reason for this is that the elementary theory gives only a value for the lower limit of the energy which can reach the top of the atmosphere in a certain direction. It does not state whether this limit can actually be reached. To decide this it is necessary to know the general solution of the Eq. 4. Since it is not possible to give this solution in analytical form, numerical calculations are needed. Such calculations were carried out by G. Lemaître and M. S. Vallarta (*9*). The results of these calculations for the orbits is that all orbits can reach the surface of the earth for which $A < 1.57712$. There exists therefore a second cone, the main cone, inside which all directions are allowed for a given energy. Between the main cone and the Störmer cone there is a region of alternating bands of allowed and forbidden directions, the so-called "penumbra."

The theory is equally valid for positive and negative charges. The only difference is that East and West need to be interchanged for the two cases.

In cosmic ray research there are two geomagnetic effects which have been extensively studied. They are *the latitude effect* and *the east-west effect.*

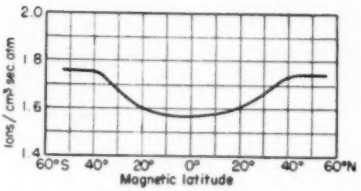

FIG. 5. The latitude effect of the total radiation at sea level

The latitude effect is the variation of the vertical intensity of cosmic rays with the geomagnetic latitude. The effect was discovered by T. Clay (*10*) and later studied by A. H. Compton (*11*) and associates. As a convenient measure of the strength of the effect in per cent we may define

$$l = 100 \frac{I(90°) - I(0°)}{I(90°)} \quad (14)$$

Here we have written $I(\lambda)$ for the vertical intensity at the geomagnetic latitude λ. It is found experimentally that the radiation intensity remains constant for $\lambda > 50°$. The latitude effect of the total radiation at sea level is about 9%. The curve found by Clay is reproduced in Fig. 5.

At high altitudes the latitude effect is much stronger, amounting to about 60–70% at 100 gm cm^{-2} atmospheric depth, with a similar although somewhat less pronounced flattening-out at $\lambda > 50°$.

From these general features we may draw a few qualitative conclusions. First, the existence of the latitude effect proves that an appreciable fraction of the primary radiation carries charge. What the sign of this charge is cannot be decided with the latitude effect alone. Second, the existence of the polar plateau, even at high altitudes, indicates that practically no primaries below about 2 Bev enter the top of the atmosphere. A possible explanation for this is that the magnetic field of the sun has the same effect on primaries as does that

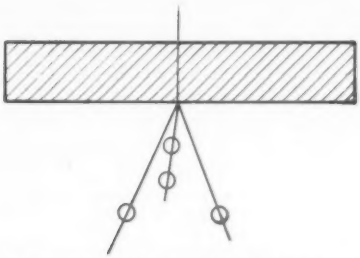

FIG. 6. Counter arrangement for measuring showers behind absorbers

of the earth. The only difference is that it extends much farther into space on account of its greater strength. The calculation shows that the sun's magnetic field would actually begin to cut out protons of 2 Bev if they enter in a vertical direction.

The east-west effect is the variation of intensity at a fixed point for two directions pointing into the eastern and western horizon, respectively, with a fixed zenith angle z. For quantitative measurements one may define the strength of the east-west effect in per cent as

$$a = 200 \frac{I_{west} - I_{east}}{I_{west} + I_{east}} \qquad (15)$$

The effect was predicted by B. Rossi (*12*) and discovered experimentally by T. H. Johnson and J. C. Street (*13*). It is especially pronounced near the geomagnetic equator at high altitudes and for large zenith angles. Since the sign of the asymmetry depends on the sign of the charges of the particles which are responsible for the measured effects, we have a means of determining the sign of the charges of the primaries. The sign of the effect at sea level is such that it would correspond to a positive charge of the primaries responsible for these effects. The maximum value at sea level of about 15% is reached for a zenith angle of about 45° at $\lambda = 0°$ (*15*).

The conclusion that can be drawn from these experiments on the east-west effect is that the radiation observed at sea level which shows any directional asymmetry is due to positive primaries. This experiment is therefore very important because it proves the existence of positive primaries. Of course the existence of negatively charged primaries is thereby not excluded since they may be too strongly absorbed by the atmosphere to reach sea level or since their energy may be too high to have a forbidden cone.

The Soft Component

We have previously defined the soft component as that radiation which is absorbed by 12 cm of lead. For practical purposes, however, the soft component is much easier to distinguish by its property of producing showers. A shower is a sudden simultaneous occurrence of several particles. Cloud chamber studies reveal that such showers consist, on the average, of an equal number of positive and negative particles. Experiments with counters show that showers are more frequent behind a few cm of lead. If for instance the coincidence rate of four counters placed out of line (Fig. 6) is plotted against the thickness of a lead absorber, a curve is obtained which shows a pronounced maximum at about 2 to 3 cm of lead (Fig. 7). A curve of this nature was obtained for the first time by B. Rossi (*16*) and it is usually called the Rossi curve. The explanation of this behavior of the showers is essentially tied up with the existence of the positron, a particle with positive charge but otherwise with the same properties as the electron. It was discovered in 1932 by Anderson (*17*), who could also show that positrons are produced in pairs of an electron and a positron by a neutral γ-quantum. The theory of the production of electron-positron pairs by γ-rays and the production of γ-rays by

fast electrons and positrons (*18*) lead to the interpretation of the shower production as a cascade process. According to this theory a primary electron, for instance, enters an absorber and radiates a γ-quantum because of its collision with a nucleus of the absorber. The γ-quantum in turn can produce an electron-positron pair in the electrostatic field of a nucleus. Both particles of this pair, in addition to the primary particle, may produce additional γ-quanta if their energy is still high enough, and thus the process goes on multiplying the number of particles and photons in a cascade or chain reaction which stops only when the energy of the particles and quanta reaches values too low for the radiation and pair production processes to continue. The quantitative theory of these cascade processes given first by Bhabha and Heitler (*19*) and Carlson and Oppenheimer (*20*) is in good agreement with the experimental results. According to this theory showers should also occur in the atmosphere, and since they have to traverse a considerable thickness of material such showers must contain a large number of particles spread over a relatively large area. These air showers were actually observed by K. Schmeiser and W. Bothe (*21*) and by P. Auger and collaborators (*22*).

Auger was able to detect coincidences with counters several hundred meters apart, corresponding to showers that contain about a million particles. The energy of the primary particles which produce such showers was estimated by Auger to be larger than 10^{15} ev. From the frequency of occurrence of such showers it was estimated that the primaries which have such energy enter the top of the atmosphere at the rate of about 10^{-9} per minute and per cm^2. This value is in good agreement with an integral energy spectrum $N(E) = C/E^{1.5}$, where $N(E)$ represents the number of primaries entering per second and

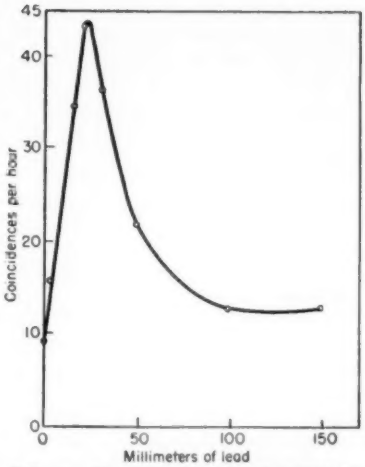

FIG. 7. Shower curve (Rossi curve) for counters arranged as in Fig. 6

cm^2 from all directions with energy larger than E, and C is a numerical factor which, if E is measured in ev, is about 5×10^{16}. This formula for the integral energy spectrum holds very well for all energies higher than about 5 to 6 Bev.

We shall give here a simplified discussion of the quantitative aspects of the shower theory. The two fundamental processes which enter into the shower production are:

(a) The emission of a photon by a fast electron or positron (bremsstrahlung).

(b) The production of an electron-positron pair by a photon.

In addition to these two processes, there exist the Compton effect, the photoelectric effect and the collision loss by ionization. All these effects are entirely negligible in comparison with the first two in the high energy region in which we are working. Only for rather low energy does the ionization loss become more important than the bremsstrahlung. For our simplified theory it is sufficient to assume that the

critical energy E_c for which the two last mentioned processes have equal probability plays essentially the role of a cut off energy. We simply assume that only electrons with an energy larger than E_c contribute anything to the shower-process.

The probabilities for the two processes (a) and (b) can be most conveniently expressed in terms of a characteristic length for the absorber and the particle in question. It is defined by the expression

$$l = \frac{137}{4}\left(\frac{mc^2}{e^2}\right)^2 \frac{1}{NZ^2}\frac{183}{Z^{1/3}} \qquad (16)$$

Here e is the charge of the electron, m its mass and c the velocity of light. The quantity $e^2/(mc^2)$ is the "classical electron radius" and equals 2.8×10^{-13} cm for electrons. N is the number of scattering atoms per cm^3 and Z is the atomic number. For some substances the characteristic shower length has the following values:

Absorber	*l in cm*
Pb	0.51
Fe	1.8
Al	9.6
H_2O	43
Air	33000

For the probability of the emission of photons in the energy range W to $(W + dW)$ by an electron of energy $E \gg mc^2$ $(E > W)$ in a distance dx, the theory of radiation gives the expression

$$dP(W) = \frac{dx}{l}\frac{dW}{W} \qquad (17)$$

A photon of energy W on the other hand creates a pair of energies E, $W - E$ within the energy range dE in a distance dx with a probability

$$dP'(E) = \delta\frac{dx}{l}\frac{dE}{W} \qquad (18)$$

where δ is a numerical factor ($\delta = 7/9$). The theory further predicts that the average angle of emission is very small in both cases so long as the emitting particles or photons have energies large compared to the rest energy mc^2 of the electron. This means that the calculation can be simplified by neglecting in a first approximation the angular spread of the shower.

Consider now an absorber and a certain number of electrons and photons vertically incident. (We use the term "electrons" in the following to denote positrons as well as negative electrons.) We denote $t = x/l$ the depth below the top of the absorber measured in radiation units. Further, let $F(E,t)$ stand for the number of electrons and positrons with energy $> E$ at the depth t and similarly $G(E,t)$ for the number of photons with energy $> E$ at the depth t. The rate of change of these quantities is then given by

$$\frac{\partial G(E,t)}{\partial t} = -\delta G(E,t) + \int_E^\infty \frac{F(E',t)}{E'}\,dE' \qquad (19)$$

$$\frac{\partial F(E,t)}{\partial t} = 2\delta\int_E^\infty G(E',t)\frac{E}{E'^2}\,dE' + \int_E^\infty \frac{\partial F(E',t)}{\partial E'}\ln\frac{E'}{E'-E}\,dE' \qquad (20)$$

The first term on the right of Eq. 19 gives the number of photons lost by pair creation, the second term is the number of photons gained by bremsstrahlung, all in the path length l. The first term follows directly from the definition Eq. 18 for the probability of pair creation. The second term may be obtained in the following way: The number of electrons in the energy interval dE' is $-[(\partial F)/(\partial E')]dE'$. Any one of these electrons may emit, in a distance l, a photon of energy W with a probability $dP = dW/W$. Hence the probable number of photons emitted with energy $W > E$ is given by

$$-\int_E^\infty \frac{\partial F}{\partial E'}\,dE'\int_E^{E'}\frac{dW}{W} = -\int_E^\infty \frac{\partial F}{\partial E'}\ln\frac{E'}{E}\,dE'$$

Integrating by parts and using $F \to 0$ for $E \to \infty$ we obtain the second term

on the right of Eq. 19. By a similar procedure we may verify that the first term on the right of Eq. 20 represents the number of electrons gained by pair creation, whereas the second term stands for the number lost by bremsstrahlung.

Equations 19 and 20 are the fundamental equations of the shower theory. They represent a system of integro-differential equations which must be solved subject to the special conditions which are existing at the boundary of the absorber.

It is easy to obtain a special solution of the equation in the form

$$F(E,t) = f(t)E^{-s}$$
$$G(E,t) = g(t)E^{-s}(s > 0) \qquad (21)$$

If we insert Eq. 21 in Eqs. 19 and 20, we see that we obtain a solution of these equations if $f(b)$ and $g(b)$ satisfy the following differential equations

$$\frac{df}{dt} = -\sigma(s)f + \frac{2\delta}{s+1}g$$
$$\frac{dg}{dt} = \frac{1}{s}f - \delta g \qquad (22)$$

where $\sigma(s)$ is the function

$$\sigma(s) = s\int_1^\infty \frac{1}{y^{s+1}} \ln\frac{y}{y-1}\,dy \qquad (23)$$

Equations 22 are a system of ordinary differential equations with constant coefficients. The solutions of these equations are exponential functions. Thus we write

$$f = ae^{-\alpha t}$$
$$g = be^{-\alpha t} \qquad (24)$$

Inserting these in Eq. 22 we find for a, b, α the equations:

$$-\alpha a = -\sigma a + \frac{2\delta}{s+1}b$$
$$-\alpha b = \frac{1}{s}a - \delta b \qquad (25)$$

This is a homogeneous linear system for the two constants a, b. The condition for α is the vanishing of the determinant, which gives the quadratic equation

$$\alpha^2 - (\delta+\sigma)\alpha + \delta s - \frac{2\delta}{s(s+1)} = 0 \qquad (26)$$

with the two solutions

$$\alpha_{1,2} = \frac{\delta+\sigma}{2} \pm \frac{1}{2}\sqrt{(\delta-\sigma)^2 + \frac{8\delta}{s(s+1)}} \qquad (27)$$

For the ratios of the constants a and b we find then

$$\frac{a}{b} = s(\delta - \alpha) \qquad (28)$$

We have thus for the general solution of Eq. 22

$$f = b_1 s(\delta - \alpha_1)e^{-\alpha_1 t} + b_2 s(\delta - \alpha_2)e^{-\alpha_2 t}$$
$$g = b_1 e^{-\alpha_1 t} + b_2 e^{-\alpha_2 t} \qquad (29)$$

where $b_1 b_2$ are arbitrary integration constants depending on the initial conditions. If we denote with α the smaller of the two roots $\alpha_1 \alpha_2$, then we see that for sufficiently large t only the solution with the α in the exponential will be of importance and we have then approximately

$$f \sim bs(\delta - \alpha)e^{-\alpha t}$$
$$g \sim be^{-\alpha t} \qquad (29')$$

From this result it is seen that the integral energy spectrum Eq. 21 of the electrons and photons remains invariant as the shower develops in the absorber. Furthermore the absorption coefficient at large depth is given by

$$\alpha = \frac{1}{2}(\delta+\sigma) - \frac{1}{2}\sqrt{(\delta-\sigma)^2 + \frac{8\delta}{s(s+1)}} \qquad (30)$$

The measured absorption coefficient of the soft component in air below the maximum is not inconsistent with a value $s = 1.8$. For this value $\sigma = 1.4$ and $\alpha = 0.46$. Thus the radiation decays to $1/e$ of its value for about two radiation units. The special solution just obtained can be used to construct the most general solution of the system. A direct comparison of the theory outlined here with the Rossi curve is complicated by the fact that the energy spectrum of the incident photons or electrons is not very well known and that the directional extension of the shower enters in these measurements. Suffice it to say here that the theory is

in sufficient agreement with experiment to justify the statement made above that the showers normally observed in air and behind absorbers are electron- and photon-showers.

We turn now to the geomagnetic effects of the soft component. The latitude effect may be measured either directly, by measuring the latitude effect of the shower producing radiation, or indirectly, by measuring that effect for the total radiation and the hard component separately and inferring from it the effect for the soft component. The latter method is subject to large uncertainties at sea level since the soft component contributes only about 23% of the total radiation.

From the somewhat sketchy experimental evidence which is available to date one may infer that the latitude effect of the soft component at sea level is somewhat less than that of the hard component, varying probably from 6 to 9%. The only direct contradiction to this value which seems to have been made is by Wilson and Turner (*23*) according to which the latitude effect of the soft component is larger than that of the hard component. This experiment must be interpreted with caution however since it involves just such a difference method as is mentioned above, and is, therefore, not very reliable for the soft component.

At higher altitude the latitude effect of the soft component increases rapidly and amounts to about 70% at an atmospheric depth of 300 gm cm^{-2}.

From this result we may infer two important facts about the nature of the primaries:

a) The majority of the primaries responsible for the soft component are charged.

b) The average energy of the primaries responsible for the soft component at sea level is about 32 Bev and for that at 300 gm cm^{-2} is about 14 Bev, for these are the respective energies of primaries which have latitude effects of about 6% and 70%.

The east-west effect for the soft component has also been measured. As early as 1935, Johnson (*24*) found that the east-west effect of the soft component at zenith angle $z = 35°$, $\lambda = 29°$ (Mexico) and atmospheric depth 600 gm cm^{-2} was only 1% (positive) as compared to 10% for the total radiation under the same conditions. However at $\lambda = 0°$ (Peru) and sea level the effect was found to be 5% for $z = 30°$, as compared to 9% for the total radiation. Johnson himself, as well as other investigators, is inclined to consider the slight positive asymmetry of the soft component at lower altitude as due to the decay electrons from the mesotrons somewhat higher up in the atmosphere. These are expected to form a substantial fraction of the soft component at sea level. It is generally assumed that this fraction is expected to decrease at higher altitude; the east-west effect of the soft component at higher elevation is therefore considered to be more indicative of the charge of the primaries which are directly responsible for the soft component.

An experiment measuring the east-west effect of the total radiation at high altitude was carried out by Johnson and Barry (*25*). At an atmospheric depth of 30–60 gm cm^{-2}, zenith angle $z = 60°$, and geomagnetic latitude $\lambda = 20°$ (Panama Canal Zone), they find an azimuth effect of only 7%. On the other hand these authors estimate that positive primaries alone for the total radiation would lead to an asymmetry of 60% under these conditions. Since, as we shall see below, the primaries of the hard component are largely positive, Johnson and Barry conclude that the primaries of the soft component are positive as well as negative electrons in almost equal number. Neutral rays as primaries for the soft component are excluded on account of

the large latitude effect of the soft component.

Unfortunately, recent experiments fail to detect any electrons as primaries. Schein, Jesse and Wollan (*26*) showed that, at 30 gm cm^{-2} atmospheric depth, only a few percent of the particles of the radiation were electrons which could penetrate more than 4 cm of lead; and recently Hulsizer and Rossi (*27*) showed that the number of primary electrons of all energy is certainly less than 10% of the total incoming radiation. The origin of the soft radiation at high altitude is thus very difficult to understand.

Recent unpublished experiments by Neher (*28*) seem to indicate however that the east-west effect of the soft component at high altitudes may be larger than might be inferred from the above mentioned experiment by Johnson and Barry. According to Neher the effect at $\lambda = 0$, $z = 45°$ and atmospheric depth of about 300 gm cm^{-2} is 25%. This experiment is very difficult to compare with the experiment of Johnson and Barry since all the three parameters, λ, z and atmospheric depth are different in these two experiments and since Johnson and Barry measure only the effect for the total radiation. Moreover, the possibility is not excluded although unlikely that the east-west effect of the soft component might be larger at intermediate heights (300 gm cm^{-2}) than at the extreme heights of the Johnson-Barry experiment (30–60 gm cm^{-2}).

Editor's Note: *In the concluding portion of Dr. Jauch's review, he considers these subjects: The Hard Component, Penetrating Showers and Stars, The Primaries and the Genesis of Cosmic Rays, and Speculations on the Origin of the Primaries. He also lists review papers and books on cosmic rays.*

BIBLIOGRAPHY

The references below and those appearing in the second half of this paper to be published next month are only a small selection of the research papers on cosmic rays.

The principle of selection used follows: In each area some of the early pioneer work and then again the latest work of importance is quoted. Intermediate work is summarized in the text but not quoted.

1. V. F. Hess, *Physik. Z.* **12,** 998 (1911); **13,** 1084 (1912); *Wien. Ber.* IIa **121,** 2001 (1912)
2. A. Gockel, *Physik. Z.* **11,** 280 (1910); **12,** 595 (1911)
3. W. Kolhörster, *Physik. Z.* **14,** 1066 (1913)
4. W. Bothe, W. Kolhörster, *Z. Physik.* **56,** 751 (1929)
5. D. Skobelzyn, *Z. Physik.* **54,** 686 (1929)
6. B. Rossi, *Revs. Mod. Phys.* **20,** 537 (1948). Further references are to be found in this review article.
7. J. A. Van Allen, H. E. Tatel, *Phys. Rev.* **73,** 245 (1948)
8. G. P. S. Occhialini, C. F. Powell, *Nature* **159,** 186 (1947); C. F. Powell, G. P. S. Occhialini, *Nature* **159,** 93 (1947)
9. G. Lemaître, M. S. Vallarta, Univ. of Toronto Studies, Appl. Math. Ser., No. 3, (1938). Summarized by T. H. Johnson, *Revs. Mod. Phys.* **10,** 219 (1938)
10. J. Clay, H. P. Berlage, *Naturwissenschaften* **20,** 687 (1932); J. Clay, *Naturwissenschaften* **21,** 43 (1933); *Proc. Roy. Acad. Amst.* **35,** 1282 (1932); J. Clay, P. M. Van Alphen, G. G. t'Hooft, *Physica* **1,** 363, 829 (1934)
11. A. H. Compton, *Phys. Rev.* **41,** 111 (1932); 681 (1932); **43,** 387 (1933); A. H. Compton, J. M. Benade, P. G. Ledig, *Phys. Rev.* **45,** 294 (1934)
12. B. Rossi, *Phys. Rev.* **36,** 606 (1930)
13. T. H. Johnson, J. C. Street, *Phys. Rev.* **43,** 381 (1933)
14. T. H. Johnson, *Revs. Mod. Phys.* **10,** 193 (1938)
15. T. H. Johnson, *Phys. Rev.* **48,** 287 (1935)
16. B. Rossi, *Naturwissenschaften* **20,** 65 (1932); *Z. Physik.* **82,** 151 (1933).
17. C. D. Anderson, *Science* **76,** 238 (1932)
18. H. A. Bethe, W. Heitler, *Proc. Roy. Soc.* **146,** 83 (1934)
19. H. J. Bhabha, W. Heitler, *Proc. Roy. Soc.* **159,** 432 (1937)
20. J. F. Carlson, J. R. Oppenheimer, *Phys. Rev.* **51,** 220 (1937)
21. K. Schmeiser, W. Bothe, *Ann. Physik* **32,** 161 (1938)
22. P. Auger, R. Maze, T. Grivet-Meyer, *Compt. rend.* **206,** 1721 (1938)
23. V. C. Wilson, R. N. Turner, *Phys. Rev.* **59,** 931 (1941) (A)
24. T. H. Johnson, *Phys. Rev.* **47,** 318 (1935). (Summarized in reference 14).
25. T. H. Johnson, J. G. Barry, *Phys. Rev.* **56,** 219 (1939)
26. M. Schein, W. P. Jesse, E. O. Wollan, *Phys. Rev.* **59,** 615 (1941)
27. R. I. Hulsizer, B. Rossi, *Phys. Rev.* **73,** 1402 (1948)
28. Reported at the International Conference on Cosmic Rays, Pasadena, Calif., June 21–23, 1948, communicated to the author by M. Schein

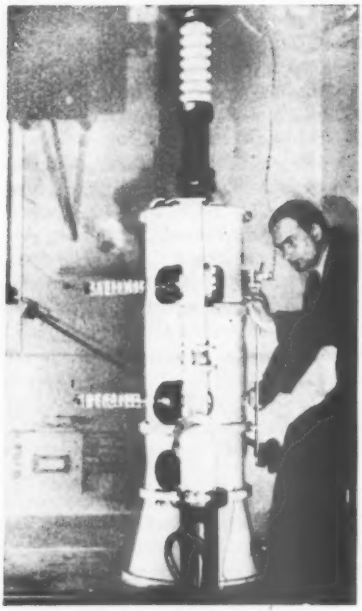

First electrostatic pilot microscope built at Collège de France

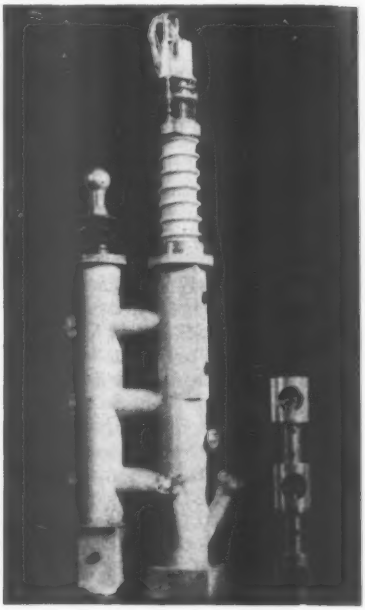

Proton microscope under construction with its three lenses assembled

THE PROTON MICROSCOPE

By CLAUDE MAGNAN

Laboratory of Atomic and Molecular Physics, Collège de France
Paris, France

IT IS KNOWN that the best microscopes which use light can barely develop a magnifying power greater than 3,000 diameters. This limitation is not brought on by the inability to construct apparatus of sufficient geometrical size, but by diffraction effects which cause the images of two near points to form patterns which overlap.

The simple relation below is due to Abbé:

$$d = \frac{\lambda}{n \sin \alpha} \qquad (1)$$

This relates the limit of diffraction resolving power to the wavelength λ of the light used, to the index of refraction n of the object space and to the half-angle α of the light cone which pene-

MICROSCOPES which employ light are limited by diffraction effects to a magnification of about 3,000 diameters. Electrons, whose de Broglie wavelength can be made shorter than that of visible light, have raised this limit to 100,000X. With the use of protons or heavy ions (such as xenon), the wavelengths may be still further reduced. By using the equations of motion for charged particles in an electromagnetic field, the various aberrations may be evaluated. Such particles may increase the resolving so much as to make the possible magnification 600,000X or greater. These microscopes will require new types of ion sources and extremely thin samples. After experiments with an electron microscope, a proton microscope has been built at the Collège de France.

trates the objective. Very often $n \sin \alpha$ is called the numerical aperture.

Thus, with an oil immersion objective, an angle 2α near 180°, a numerical aperture of 1.52 and violet light, a diffraction resolving power of 0.171 μ or 1.710 A.U. is obtained. Since we cannot have a value of 2α greater than 180°, nor values of the index n greater than those of cedar oil used for immersion, nor greater wavelengths for visible light than for violet, we are limited to the magnitude which is compatible with a resolving power of 0.171 μ, i.e., 3,000 times in diameter.

Using electron optics, we can exceed this limit. The fictitious wave that de Broglie associates with a corpuscle in motion has a wavelength λ given by

$$\lambda = h/mv \qquad (2)$$

where h is Planck's constant, m the corpuscle mass and v its velocity. For electrons of 50,000 ev energy, this wavelength has a value of 0.055 A.U. which is 100,000 times smaller than the mean wavelength of visible spectra. Abbé's relation (Eq. 1) gives a resolving power of 2.7 A.U. for electrons of this energy. This value has been calculated for a numerical aperture of 0.02, since, as we shall see later, it is impossible to correct an electron lens as can be done in light optics.

Thus, in spite of the very small apertures used, the diffraction resolving power is 630 times better for electron optical systems than for light optical systems. It would thus seem that an increase in magnification of 630 times would be possible. This is not so, however, since the spherical aberration or aperture aberration limits the resolving power to some millimicrons, in spite of the small aperture of 0.02. Then, finally, the gain over the light optical systems is a coefficient of 40. The limit of magnifying power of an electron microscope will be about 100,000.

The wave-corpuscle duality that de Broglie has shown by comparing the Fermat integral, $\int_A^B n ds = \text{const.}$ along an optical line to the Maupertuis integral $\int_A^B p ds = \text{const.}$ (solution of the Jacobi equation) indicates that the region where there is an electrostatic field is, for a charged corpuscle, equivalent to a medium in which the refractive index n is proportional to the conjugate momentum p.

$$n = \text{const.} \sqrt{v_0^2 + \frac{2e}{m}(V - V_0)} \qquad (3)$$

for $v \ll c$.

If the charged particles form a monoenergetic beam and if the corpuscles, which are charged to the potential V_0, start with a velocity $v_0 = 0$, we obtain

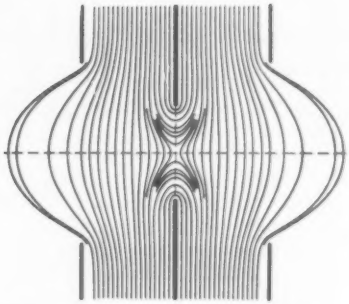

FIG. 1. Equipotential lines between three circular diaphragms

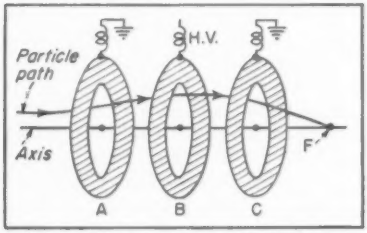

FIG. 2. Model of an electrostatic symmetrical lens

$$n = \text{const.} \sqrt{V} \qquad (4)$$

the index being replaced by the square root of the potential.

Figure 1 shows the equipotential lines between three circular diaphragms whose plane in the illustration is a meridian plane. The central diaphragm is charged to the potential of the corpuscular gun, with the lateral diaphragms at ground potential. The arrangement used, a symmetrical electrostatic lens, is shown in Fig. 2. The study of the distribution of potential is made by an electrolytic trough (*1*). In such a system the index will vary from 0 to $\sqrt{V_{max}}$ and then fall to 0. The optical analogue of such a media is that of a refractive medium of a continuously variable index. We shall see later that the lateral diaphragms have a divergent effect upon the trajectory of particles, whereas the central diaphragm has a convergent effect. It is then possible to compare this electrostatic lens to the juxtaposition of two divergent optical lenses and a convergent lens (Fig. 3).

The optical properties of electrostatic systems are easily deduced from the dynamic equations of a charged particle in a field of electrical forces. In Fig. 4, T is the trajectory of a particle of mass m and charge e, N the perpendicular to the trajectory at point M of coordinates x and y, which is the position of the particle, and α the angle with the x axis of the tangent to the trajectory.

Let us consider the relation

$$m v^2/R = eE_n \qquad (5)$$

where v is the velocity of the particle, R the radius of the trajectory curvature, and E_n the normal component of the electrostatic field. At any point, the centrifugal force mv^2/R is balanced by the electrical force eE_n. Using the classical expressions for v, R, and E_n with respect to the potential V and to its first derivatives, V_x' and V_y', and to the values y, y', y'' of the ordinate and its derivatives, we can write the expression

$$(1 + y'^2)(V_x'y' - V_y') + 2Vy'' = 0 \qquad (6)$$

This equation represents the differential equation of the trajectory for $v \ll c$. Since the equation contains neither m nor e, the trajectory is therefore independent of the mass and of the charge of the particle. An electrostatic lens will have the same optical properties for electrons, protons or for other particles which are heavier or bear greater charge. This is important, as we shall see later.

In electrostatic optics, only the points very near the axis are considered. The values of y will be small and the potential expansion is calculated, in powers of y, keeping only the deriva-

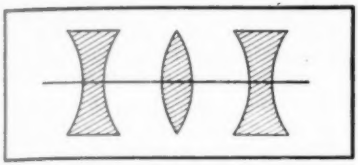

FIG. 3. Optical analogy of an electrostatic symmetrical lens

tives $V_x'(x,0)$, $V_x''(x,0)$, etc. This potential expansion is given by the Laplacian $\Delta V = 0$ and is

$$V(x,y) = V(x,0) - \frac{y^2}{2^2} V_x''(x,0) + \frac{y^4}{2^2 \cdot 4^2} V_x^{IV}(x,0) + \cdots \quad (7)$$

If we substitute the value of $V(x,y)$ and of the successive derivatives in Eq. 6, we obtain

$$(4Vy'' + 2V'y' + yV'') (\tfrac{1}{16}y^3V^{IV} + \tfrac{1}{4}y^2y'V''' + \tfrac{1}{2}y^2y''V'' + 2y'^2y''V) = 0 \quad (8)$$

The first parenthesis gives the particle trajectory at Gauss approximation, i.e., neglecting the terms of the third order.

Electrostatic Optics

The equation

$$4Vy'' + 2V'y' + yV'' = 0 \quad (9)$$

is homogeneous and linear in y and V. Therefore, if $y = Y(x)$ is the equation of a trajectory (solution of Eq. 9), $kY(x)$ is also a solution, where k is a constant. Hence we can deduce that two trajectories, starting from a point on the axis, will intersect it again at the same point. Then an object point will correspond on the axis to an image point. If $y_1 = Y_1(x)$ and $y_2 = Y_2(x)$ are two trajectories (solutions of Eq. 9), the linear combination $y = aY_1(x) + bY_2(x)$ is also a solution. Because of this, two points on the conjugate image plane can correspond to two points on an object plane. In particular, if a trajectory through the lens is parallel to the axis and intersects it in a point F',

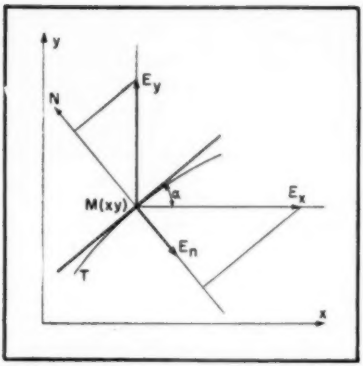

FIG. 4. Representation of a particle in an electrostatic field

all the trajectories parallel to the axis will intersect it at F'. F' will then be the image focus.

From the linearity of Eq. 9, the well-known relations of light optics can easily be obtained.

$$\frac{1}{p} + \frac{1}{p'} = \frac{1}{f}; \qquad \pi\pi' = f^2; \qquad \frac{I}{0} = \frac{p'}{p} \quad (10)$$

Figure 5 shows how, in the lens L_IL_{II}, the principal planes n' and n'' are determined. The focus is given by

$$f = y_0/y_s'$$

Calculation of Focal Lengths

If Eq. 9 is integrated with respect to x, and if $f = y_0/y_s'$, we obtain

$$\frac{1}{f} = -\frac{1}{4\sqrt{V}} \int_{x_c}^{x_s} \frac{yV''}{\sqrt{V}}\, dx \quad (11)$$

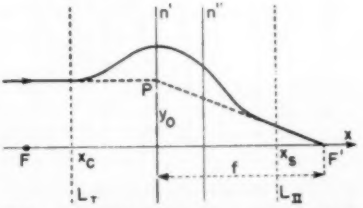

FIG. 5. Determination of principal planes of lens

The electrolytic trough gives the values of V and V'' at all the points on the axis, and the Picard-Scherzer (*2*) successive integrations method gives focal lengths of an electrostatic lens for different values of the parameters δ_1, δ_2 and σ, which are the central diaphragm and lateral diaphragm diameters and the distance between diaphragms, respectively. The curves of Fig. 6, which were established by Chanson, Ertaud and the writer (*3*), show focal lengths for different values of δ_1 and δ_2 for a value of σ of 1.7 mm corresponding to a 60-kv voltage between electrodes in vacuum. The Δ line limits the region on the right, where the focus is in the vanished field, as is generally necessary in corpuscular microscopy.

These curves bear out the important fact that the diameter of the central diaphragm has a great influence on the focal length. Focal length is generally determined by the empirical formula

$$f = 0.06 \times \frac{\delta_1 \sigma}{\delta_2 + e}$$

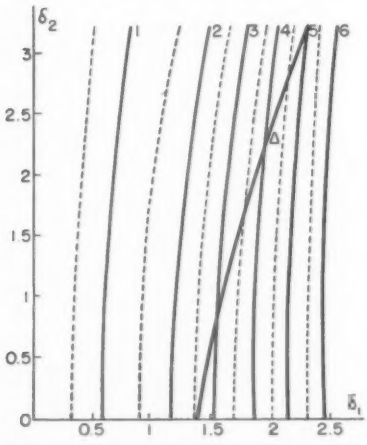

FIG. 6. Curves showing the relation between the focal length and the diameters of the diaphragms of an electrostatic symmetrical lens

where e is the central diaphragm thickness.

Spherical Aberration

We have seen that Eq. 9 contained the Gauss approximation and omitted the aberration terms of third order. The terms in the second parenthesis in Eq. 8 are used to calculate the aperture aberration or spherical aberration. By calculation similar to that for focal length we can find the spherical aberration in the image plane. Shown

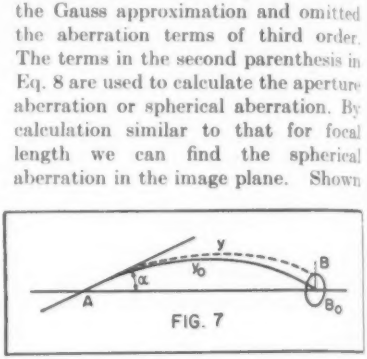

FIG. 7

in Fig. 7 is the aberration disk with a radius of B_0B. Scherzer (*4*) has shown that the aberration expression in Eq. 8 can be written as the sum of square terms of which one $\left(\frac{V''}{V}\right)^2 \sqrt{V} y^4$ represents 97% of the total.

Chanson (*5*) studied, in the electrolytic trough, the expression

$$S_2 = \frac{5f^3}{64\sqrt{V_a}} \int_a^b \sqrt{V} \left(\frac{V''}{V}\right)^2 \left(\frac{y}{y_0}\right)^4 dx \qquad (13)$$

with respect to the diameters δ_1 and δ_2 of the central and lateral diaphragms of the electrostatic lens. Figure 8 gives the values of S_2 for a distance $\sigma = 1.7$ mm between electrodes and different values of δ_1 and δ_2. As far as focal lengths are concerned, the influence of δ_1 is preponderant. The Δ line represents the limit of lenses in which the focus is in the vanished field.

The expression for S_2 shows that spherical aberration cannot be corrected, as in light optics, since the expression in the integral cannot be balanced by any other negative term. A lens with minimum spherical aberration can be sought but there will still be

some spherical aberration. To obtain an aberration of several millimicrons, it will be necessary to use apertures as small as 0.002.

Other Aberrations

In addition to the main aberration (spherical aberration) additional aberrations affect electron or ion optics, and we shall now consider them.

Chromatism. When emitted by a cathode, electrons can have speeds varying between definite limits principally because of the thermal velocity of the electrons in the hot filament of the cathode. The electron speed also varies when passing through the preparation.

If Δu is the potential variation corresponding to a velocity variation Δv, it can be shown that a focal length variation Δf is obtained such that

$$\frac{\Delta f}{f} = k\frac{\Delta u}{u} \qquad (14)$$

where k is a constant. The chromatic aberration will be

$$A_c = 2\Delta f\alpha = 2kf\frac{\Delta u}{u}\alpha \qquad (15)$$

where α is the angle of the trajectory with the axis. For a 5 mm focus, a variation $\Delta u/u$ of 10^{-5}, an angle of $\frac{1}{200}$ and a value of 2 for k (obtained from lens calculations in the electrolytic trough), we obtain $A_c = 1$ mμ. This value is approximately that for aperture aberration.

Relativity aberration. In Eq. 9, which gives the particle trajectory to the Gaussian approximation, we have assumed that the particle speed was very small compared to that of light. But for 50,000-ev electrons this is no longer true. There appears a term, called the relativity term, which is similar to the aberration term in this equation. Chanson and the writer (*3*) have called it *relativity aberration.* We have calculated, by the classical methods for the evaluation of aberrations, that, for 100,000-ev electrons,

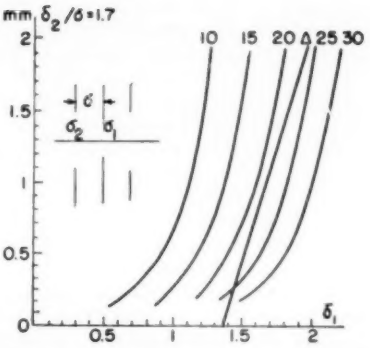

FIG. 8. Curves showing the relation between the aberration constant and the diameters of the diaphragms of an electrostatic symmetrical lens

a voltage instability of $\frac{1}{100}$ caused an aberration of 4 mμ. This is absolutely negligible for particles heavier than electrons, such as protons, where the velocity is small compared with that of light, for several hundred kv.

Ellipticity aberration. Bertein and Regenstreif (*7*) have shown that ellipticity of the central diaphragm of an electrostatic lens caused an aberration in the image plane. They called this *ellipticity aberration.* The aberration picture in the conjugate image plane is a circle of radius ρ given by

$$\rho = 5\delta_{max}\alpha \qquad (16)$$

where δ_{max} designates the maximum geometrical ellipticity of the diaphragm with regard to an ideal circle, and α the beam aperture. If Δa, the difference between the two axes of the elliptical diaphragm, is introduced, then we can write

$$\rho = \Delta a\alpha \qquad (17)$$

Thus, for a value 1 μ of Δa and an aperture of 10^{-3}, we should have $\rho = 1$ mμ. This aberration has some importance. We shall see that the optimum aperture of a proton objective is 0.39, which is less than that for an electron objective. However, it is

necessary to obtain an ellipticity less than a micron, if it is desired to obtain a better resolving power.

Minimum aberration of an electrostatic electron system. We have seen that, in corpuscular lenses, the aperture imperfection cannot be corrected. Different from light lenses, by reduction of the aperture of this type of lens to values of about 0.002, this imperfection can be brought to several millimicrons. Regardless of the associated short wavelength, the diffraction aberration for such apertures is appreciable. A compromise between these aberrations must be reached so that if one decreases the other increases. From the de Broglie formula (Eq. 2) and the Abbé formula (Eq. 1) the diffraction aberration is written

$$a_d = \frac{0.61\lambda}{\alpha} \qquad (18)$$

Spherical aberration is, as seen above,

$$a_s = S_2 f \alpha^3 \qquad (19)$$

Relative to these two phenomena, the total aberration is

$$A = a_d + a_s = \frac{0.61\lambda}{\alpha} + S_2 f \alpha^3 \qquad (20)$$

The aberration will be a minimum for $\frac{dA}{d\alpha} = 0$, i.e. for

$$\alpha_m = 0.67 \sqrt[4]{\frac{\lambda}{fS_2}} \qquad (21)$$

and its value

$$A_m = 1.2\,\lambda \sqrt[4]{fS_2/\lambda} \qquad (22)$$

Thus, for 40,000-ev electrons and a lens calculated with $S_2 = 18$ and a focal length of 4 mm, we have

$$\alpha_m = 2 \times 10^{-2}; \qquad A_m = 2.5\ \text{m}\mu$$

The diaphragm diameter would then be $D = 2\alpha f = 1.6 \times 10^{-2}$ mm. This corresponds to electrostatic electron microscopes already built in France (*8*, *9*) and in Germany (*10*). The value, 2.5 mμ, is a limit below which it is impossible to go, for, if we decrease spherical aberration by decreasing aperture, the diffraction aberration is increased. Other aberrations—chromatism, relativity and ellipticity—add to this minimum 2.5 mμ aberration. Although technical improvements will decrease the effect of these aberrations, it is not expected that the theoretical resolving power will exceed 2.5 mμ for the electrostatic electron microscope.

The magnetic electron microscope is also limited by the same considerations. The theoretical limit of its resolving power is about 1 mμ. This is a better value because the aberration constant S_2 is smaller for a magnetic microscope than for an electrostatic one, but here again, there is a conflict between spherical and diffraction aberrations.

For the electron microscope, then, we are limited to a resolving power of about 1 mμ for the magnetic type and 2.5 mμ for the electrostatic type; for the light microscope, it is 170 mμ. Practically speaking, microscopes generally used often have resolving powers less than these theoretical values, but they never exceed them. The actual magnitudes scarcely reach 100,000 times.

THE PROTON MICROSCOPE

As stated previously, diffraction aberration limits electron microscopes as it does light microscopes. According to the de Broglie formula (Eq. 2), it seemed possible to solve this problem by decreasing λ by means of increasing the mass m. Chanson and the writer (*11*), in 1942, thought of using protons, which have a mass 1,840 times greater than that of electrons. In Germany, Boersch (*12*) also noted this possibility by studying the emissions of an oxide cathode with an ion lens.

We have shown that electrostatic lenses have optical properties independent of the charge and the mass of the particle used; thus they are convenient for proton beams. Chanson and the writer investigated the possibility of obtaining a better resolving

power by utilizing protons instead of electrons, and also what this improvement would be.

The optimum aperture angle, given by Eq. 21, and the optimum aberration, given by Eq. 22, will vary with the wavelength λ, since the focal length f and the aberration constant S_2 do not depend on the kind of particle. For electrons, we have

$$\frac{1}{2}mv^2 = eV; \qquad \lambda_e = \frac{h}{mv} = \frac{h}{\sqrt{2emV}} \tag{23}$$

For protons of mass M, we have, at the same energy,

$$\lambda_p = \frac{h}{\sqrt{2eMV}} \tag{24}$$

If α_e and α_p are the optimum aperture angles for electrons and protons, respectively, and A_e and A_p the corresponding optimum aberrations, we have (*13*) from Eqs. 23 and 24

$$\frac{\alpha_p}{\alpha_e} = \left(\frac{m}{M}\right)^{1/4}; \qquad \frac{A_p}{A_e} = \left(\frac{m}{M}\right)^{3/4} \tag{25}$$

Since $M = 1{,}840m$,

$$\alpha_p = 0.39\alpha_e; \qquad A_p = 0.06A_e$$

The optimum aberration will be 16 times smaller for an electrostatic proton microscope than for an electrostatic electron microscope. If compared to the best magnetic microscope, which, as we saw, is two times as good as an electrostatic one, the gain is still 8. Then, for 40,000-ev protons, we have

$$\alpha_p = 0.8 \times 10^{-2}; \qquad A_p = 0.15 \text{ m}\mu$$

If we consider the human eye's resolving power, a theoretical magnitude of 600,000 can be foreseen.

The proton microscope does not suffer relativity aberration but is affected by ellipticity aberration, which must be reduced to a minimum. The technological problem of obtaining diaphragms whose ellipticity is less than 0.1 μ may be solved. However, the chromatic aberration resulting from the passage of the particles through the preparations offers more difficulties.

Travel of Protons Through Preparations

Absorption. In electron microscopes, preparations are made of a collodion, Formvar, and aluminum membranes, of about 10 mμ thickness, on which are placed objects such as bacteria, microcrystals, or fibers. When the electron beams pass through these preparations, they suffer absorption and diffusion effects which cannot be examined separately.

In passing through matter, electrons suffer a loss of energy and velocity. When they leave the preparation, there is a statistical distribution of energy loss suffered by the beam, and, of course, a chromatic aberration. This energy loss can be calculated from the formula given by Bothe (*14*):

$$\frac{du}{dx} = 510 \times \frac{\beta}{(1-\beta^2)^{3/2}} \times \frac{d\beta}{dx} \tag{26}$$

where $\beta = v/c$. Thus, for a 10 mμ object carrier and an electron beam of 100,000 ev, the most probable energy loss is $\Delta u = 6.3$ ev.

Bothe's formula cannot be used for protons. From Bloch's formula (*15*), which is based on the average ionization potential, we can calculate rather precisely the energy lost per unit path length for electrons, protons and other particles. But this formula is convenient only for heavy particles with a high energy, about several Mev. For protons with an energy less than 300,000 volts, it gives doubtful results. This can be explained if, as Chanson (*16*) points out, we note that 100,000-volt protons have the same velocity as 54-volt electrons, the energy of which is lower than the average ionization potential.

For 300,000-volt protons, we have, from Bloch's formula, $\Delta u = 896$ ev for a 10 mμ thickness. As far as the absorption of 100,000- to 300,000-ev protons in collodion foils of several millimicrons thickness is concerned, no experimental results have yet been

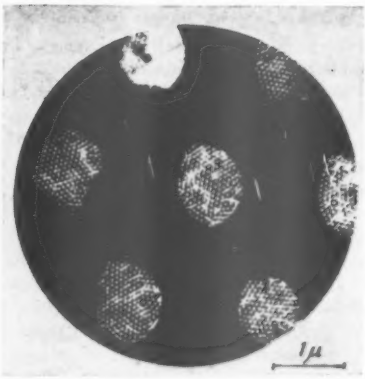

FIG. 9. Photograph of diatom holes

obtained. We can measure the energy lost by 100-kv to 300-kv protons in collodion foils several millimicrons thick, but, from values given by Bloch's formula, we can already state that, for passage through 10 mμ collodion, chromatic aberration is, for 300,000-volt protons, thirty times greater than chromatic aberration for 100,000-volt electrons in the same foil. In fact, since the theoretical resolving power of the proton microscope is about a tenth millimicron, preparations should be about 0.1 mμ thick to give a maximum. But such membranes cannot be made. Thus, other carriers, where only objects about 0.1 mμ thick are illuminated by protons, are used.

Spatial dispersion. Since spatial dispersion engenders contrast, it is important in obtaining the images of the internal structure of objects. However, it causes a chromatic aberration which must be estimated. From Bothe's formula for very small angles, we obtain, for total aberration,

$$d = 2\Delta x \tan \theta \qquad (27)$$

where Δx is the thickness in units of 10^{-3} mm and θ is the most probable angle of dispersion. For $V = 100{,}000$ volts and $\Delta x = 10$ mμ, $d = 0.3$ mμ.

Using α-particles of RaC′ in gold foil 4 μ thick, Geiger successfully verified the formula which gives dispersion angle. Therefore it can be applied to protons by multiplying the value for the electrons at rest by 1,840. We then have $d = 0.27$ mμ which is a value near that for electrons.

The aberration caused by absorption is preponderant. To make this aberration as small as possible, it seems possible to use object carriers, such as diatoms, which have regularly lined holes of very small diameter, as shown in Fig. 9. This photograph has been obtained with a magnetic electron microscope by G. Dupouy at Touloues University.

The diatoms placed on a fine grid are used as an object carrier grid which can be illuminated by protons. The object thickness only will be traversed. Object carrier membranes are avoided.

Description of Proton Microscope

We have seen that, regardless of the particles used, electrostatic lenses have the same optical properties; however, for magnetic lenses, the focal lengths depend on the mass of the particles. In the proton microscope, the electrostatic lenses are the same as in the electron type with only the polarity being different. The main characteristic of the proton microscope is the proton gun.

Proton Sources

The proton beam must be formed by atomic ions and must be monoenergetic to avoid chromatic aberration caused by velocities varying in great proportion. Last year, studies on proton sources, on deuteron sources utilized in high-voltage ion accelerators, and studies on mass spectrography, yielded several models of ion sources, which have some of these characteristics. In our laboratory, we have built and tried an ion source with oscillating electrons.

the type which was suggested in Germany by Hans Heil (*17*) and applied by V. Ardenne (*18*) to ion production in a Van de Graaff generator.

Protons are obtained by hydrogen ionization by an oscillating electron beam. A potential difference of 300 volts exists between two hot tungsten filaments F_1 and F_2 and the gas box G (Fig. 10). This potential difference causes electrons emitted by filament F_1 to enter the gas box. On reaching the vicinity of filament F_2, the electrons suffer an inverse acceleration and reverse their paths, being accelerated between F_2 and G. They suffer another repulsion near F_1 and a new acceleration before G, and so on. Electrons then oscillate between the two filaments F_1 and F_2, under a pressure of about 0.1 dyne per sq cm and a range of 2 cm. They perform about 200 oscillations before vanishing and after having ionized a gas molecule.

To avoid having electrons reach the box walls, the electrons can be concentrated following the plane containing F_1 and F_2 by use of a magnetic field. Electrodes E_1 and E_2 act as mirrors for the electrons. A grid is used for removing ions formed in the gas box in a direction perpendicular to the oscillating electron beam. The ionization will be 80%.

The ions formed in the gas box from gas molecules move with a thermal energy of 0.03 ev and undergo no action by which their average kinetic energy varies beyond this value. Emitted in a region of no field, they leave the gas box G under the bias of the first extraction electrode. As in the case of the box, the voltage on this electrode is low so that the extraction field does not penetrate too strongly into the box where it might interfere with the oscillation of the electrons. We will then have a source of ions with equal velocities which will easily give 1,200-μa protons.

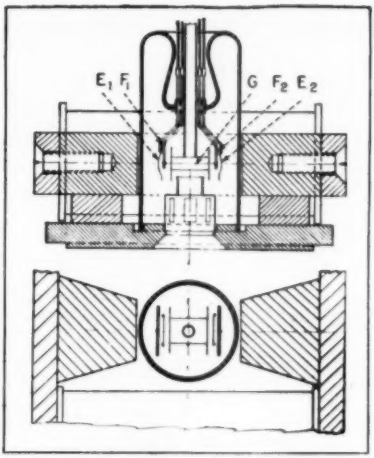

FIG. 10. Diagram of the Heil-type ion source built for the proton microscope of the Collége de France

The proportion of molecular ions is about 30%, which is still too much. Therefore, we considered the use of a mass monochromator, of the type built by V. Ardenne (*18*), in order to obtain a monoenergetic beam of deuterons. This apparatus consists of a magnetic lens which, for a given mass, gives an image of a diaphragm, other mass ions following diverging trajectories intercepted by convenient diaphragms.

Figure 11 shows Heil's source, built by the author, without its magnet. We are now building another ion source of oscillating electrons based on one built by Finkelstein (*19*). In this, the electrons oscillate between the filament and the electrode, which repels electrons and attracts ions.

We now consider a very recent type of ion source, built by Rutherglen (*20*) in England, to be the best. It uses a high frequency field to ionize the gas. There are no heated filaments, and beams, from which molecular ions are practically eliminated, can be obtained. With a 200-Mc frequency and a pres-

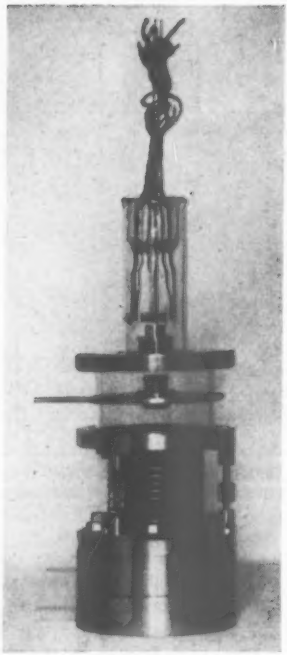

FIG. 11. Photograph of ion source using oscillating electrons

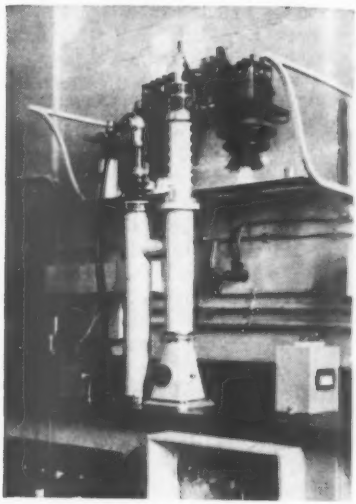

FIG. 12. Proton lens used for experimenting on ion sources and proton images

sure of 0.001 mm mercury, this source yielded an ion current of approximately 1 ma.

Figure 12 shows the proton lens used for experimenting on ion sources and proton images. The proton gun of the microscope was made first of an ion source of Heil's type, which has the same function as the hot filament of the electron gun and the other group of acceleration electrodes, analogous to those of electron guns (see upper part of Fig. 15).

Electrostatic Lenses

The first electrostatic lenses which were built were for the model microscope (see Fig. 13). Of the Ardenne type (*21*), the lenses are symmetrical, consisting of three coaxial diaphragms. The central diaphragm has a 1 mm hole, the lateral 2.5 mm holes, with the distance between diaphragms being 3 mm. Each of these diaphragms has been made round and has been accurately polished and chrome-plated. The focal length is 5 mm and the voltage 50,000 volts.

The proton microscope electrostatic lenses can be compared with the Mahl (*10*) and Grivet (*9*) type. Formed by three circular, coaxial diaphragms, the latter have a cupola shape and are held in place by an annular insulator. Their focal length is 4 mm and they are designed to withstand 100,000 volts. Figure 14 shows one of these lenses disassembled.

The first electrostatic microscope built in the Collège de France, in 1942, was a model designed to verify its operation as an electron microscope and to prepare its conversion into a proton microscope. It contains two Ardenne-

type lenses and has a resolving power for electrons of 8 mμ and a direct magnification of 10,000 times. Direct photographs can be studied by photographic enlargement.

The apparatus is shown on p. 52. In the upper part can be seen the electron gun. In the middle is the object carrier gun, with the lens insulators opposite it. The vacuum manifold, which permits pumping at the level of each lens, can be seen extending along the microscope. In the lower part is the photographic camera and high-voltage potentiometer by which the lens voltage can be varied. And, of course, the focus can be varied according to the preparation.

Knowledge obtained from the building of the first microscope permitted less complicated construction in later models and more precise manufacture of some of the main pieces. Particularly, the condition of the surfaces of the electrodes and the ellipticity of the central diaphragm hole were greatly improved.

However, much more must be done to reach the theoretical resolving power. For electrons, the theoretical resolving power of this apparatus is 2.5 mμ; for protons, it is 0.15 mμ. For protons, the theoretical magnification, with respect to the normal resolving power of the human eye, might then be 600,000 times. To obtain this result, aberrations, especially sphericity, must be eliminated. The first resolving power obtained will probably be better than that of the magnetic electron microscope, but worse than that theoretically possible. Difficulties will not come from the quality of the proton gun, which is good, nor from spherical aberration, which is practically negligible, but rather more from aberrations of unknown magnitude which are anticipated. One such aberration is caused by electrostatic repulsion between protons in the beam.

With its three lenses, the proton microscope has a direct magnification

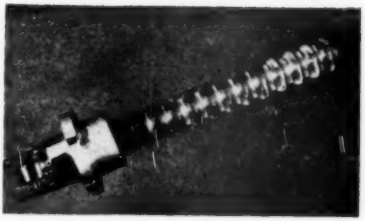

FIG. 13. Electrostatic lens used in microscope model

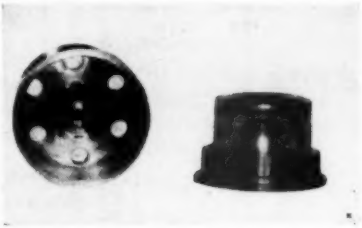

FIG. 14. Grivet-type electrostatic lens disassembled

of 80,000 times. Photographs will be studied by photographic enlargement to the limit of the real resolving power of the apparatus.

The microscope consists of a vacuum enclosure made of a single piece and containing the three lens assemblies. The vacuum manifold is also used as a duct for the conduction of high voltage to each lens. Hence, the operator is protected against high tension on the upper part of the apparatus. The total height is 1.6 meters.

In the upper part of the right photograph on p. 52, there can be distinguished the proton gun insulator and the bearer of the object carriers with adjusters. Immediately below are the objective diaphragm lock and its adjusters. In the lower part are the observation windows, photographic camera and the vacuum lock of the manifold.

Figure 15 shows the construction of the proton microscope. The purpose of this apparatus is the study of the images of such objects as diatoms, placed on a

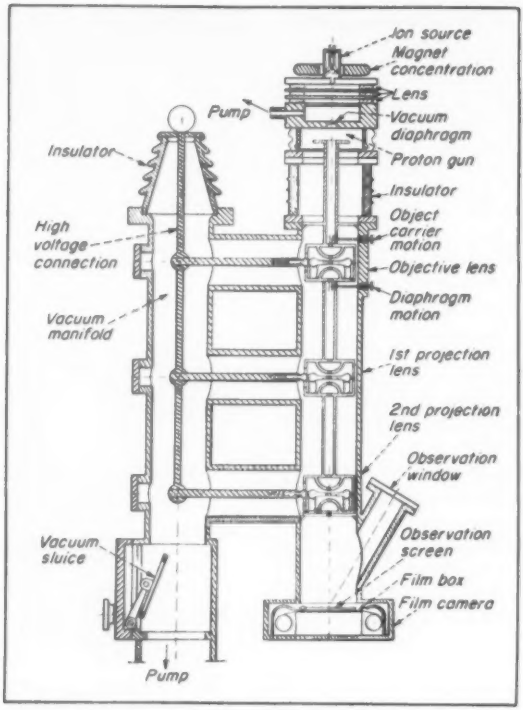

FIG. 15. Diagram of the proton microscope

thin grid, to determine the theoretical resolving power. Then this instrument will be used as a model for a third microscope operating at 300,000 volts, the construction of which has scarcely begun. The latter will be an enlarged reproduction of the first proton microscope.

Limits of Corpuscular Microscopes

The resolving power of 1.5×10^{-8} cm of the proton microscope approaches the diameter of the atom. By the specific volume calculation for solids, the diameter of the *M* electronic shell of the uranium atom is calculated as 0.12×10^{-8} cm and the external diameter of this atom as several Angstroms.

From this, there follows the possibility of an additional increase in the resolving power, obtained by increasing the mass of the illuminating particles. It would then be possible to examine the internal structure of atoms. This hypothesis seems to be experimentally possible since electrostatic lenses have properties independent of the mass of the particles. In the table on page 6[illegible] are shown calculated resolving powers for increasingly heavy particles which could be used in the ion source of the microscope. Optimum aperture of the beam has been indicated to show the possibilities of the hypothesis. It is seen that a microscope utilizing xenon would have a resolving power of 0.24 ×

Illuminating Particle	*Resolving Power* (10^{-8} *cm*)	*Optimum Aperture* $\times 10^3$
electron	25	2
proton	1.5	0.8
deuteron	1.16	0.75
helium	0.9	0.67
neon	0.5	0.55
argon	0.38	0.51
krypton	0.29	0.46
xenon	0.24	0.44

10^{-8} cm. This would not be far from the diameter of the most external shells of the atom. From this, one might think that some day we would be able to see the details of the atom, but, although aberrations caused by ellipticity of lenses, by the adjustments of the latter and by electrostatic repulsion of beam ions can be overcome, de Broglie has shown (*22, 23, 24*) this to be impossible.

Calculated below (by de Broglie's method) is the recoil of a very small object of mass M, which will impinge on the object carrier of the microscope when struck by a proton. After the impulse, the momentum of the scattered particle will be p' and that of the object P_x. We then have

$$(P_x)_{max} = p' \sin \alpha \qquad (28)$$

α being the objective aperture. Since p' differs little from p and since α is small, we can write

$$(P_x)_{max} = p\alpha; \qquad P_x = MV_x; \qquad p = mv \qquad (29)$$

V and v being, respectively, the velocity of the object of mass M and that of the particle of mass m. We then have

$$(V_x)_{max} = \frac{\alpha}{M} mv = \frac{\alpha}{M} \frac{h}{\lambda} = \frac{h}{2M} \frac{I}{d_{min}} \qquad (30)$$

since $\lambda = \dfrac{h}{mv}$ and $d_{min} = \dfrac{\lambda}{2\alpha}$

Here, we encounter an idea which is the basis of Heisenberg's calculation: the more λ is increased to increase the resolving power, the more the velocity V_x of the object will increase. In fact, to obtain a good image of the whole object, this object must scatter into the microscope a great number of incident particles. If $\bar{\tau}$ is the time interval which separates the average arrival of two consecutive particles at the object, the product $V_x \times \bar{\tau}$ must be very small compared to the average size l of the object; if not, there would be considerable movement of the object in the object plane during the time interval between two successive impulses. The image would thus be imperfect.

Evaluation of $\bar{\tau}$ gives us

$$\bar{\tau} = \frac{e}{il^2} \qquad (31)$$

where e is the charge of the particle, i the current density of the flux of the illuminating particles, and l^2 the object area. We then obtain

$$(V_x)_{max} \times \frac{e}{il^2} \ll l \qquad (32)$$

or

$$\frac{h}{2M} \times \frac{I}{d_{min}} \times \frac{e}{il^2} \ll l \qquad (33)$$

From this expression, we can estimate the minimum size of the object as far as convenient recoil is concerned. If we assume a current density of 1 ma per mm^2, and use the estimates $d_{min} = \dfrac{l}{10}$ and $M \approx l^3$, we get $l \gg 10$ mμ. In fact, the statistical distribution of recoils could make this limit less approximate. On the other hand, objects are never free from, but adhere to or are a part of, a more complex structure; thus the recoil effect is limited. This should be true only for particles moving in rarified gas.

To the imperfections of images caused by the recoil of small objects struck by the illuminating particles must be added the imperfection caused by thermal agitation of the objects. In fact, for an absolute temperature T, small objects will have a thermal agitation as if their velocity V_x were about $\sqrt{\dfrac{kT}{M}}$, where k is the Boltzmann constant. To obtain a perfect image, we must have, as before,

$$\sqrt{\frac{kT}{M}} \times \frac{e}{il^2} \ll l \qquad (34)$$

With the same hypothesis as above, we might have

$$T \ll 10^{52} \times l^3$$

For $l = 10$ mμ, extraordinarily low temperatures would be necessary to obtain perfect images.

For objects with dimensions less than 10 mμ, thermal agitation, as a recoil effect, causes imperfection in the image. If the object, instead of being free, is a part of the structure, the effect of thermal agitation is less noticeable and the limits given above are more accurate.

To free an atom which is part of a solid or of a liquid, an energy of a fraction of an ev is required. To remove an electron from a shell of an atom, a maximum energy of a hundred thousand ev is necessary. The equations of conservation of energy and momentum of an incident particle, with the atom considered as the object, show us that, with an aperture angle of α, the maximum value of energy taken by the object from the particle in recoil is

$$W_{max} = \frac{h^2}{2M} \frac{\alpha^2}{\lambda^2} = \frac{h^2}{2M} \frac{I}{(d_{min})^2} \qquad (35)$$

For an atom of mass M between 10^{-22} and 10^{-24} gm and a resolving power of 10^{-9} cm, W_{max} would be about an electron volt. The atom will then be drawn off and an image made impossible because the former would vanish at the first impulse.

For an electron of 10^{-27} gm mass, with the same resolving power, W_{max} will equal 100,000 ev and the electron will be removed from its orbit.

Therefore, because of recoil and thermal agitation, it is impossible to obtain an image in corpuscular microscopy for object dimensions less than 20 or 30 Angstroms. For atoms bound to a structure, or for periphery electrons, these phenomena are completed by an ejection.

We have thus arrived at the point (from the Heisenberg principle) where we realize that it is impossible to see the internal structure of atoms with corpuscular microscopes. In brief, the proton microscope, and eventually microscopes using heavier ions, will permit us to observe objects whose sizes are compatible with a resolving power of 1.5×10^{-8} cm and less. We think that they will be very useful for the examination of complex molecules (in biological chemistry) which are now out of the range of electron microscopes. The domain of investigation will certainly be more limited than that for electron microscopes, the latter being compared with those using light. However, the improvement in resolving power justifies this research. As de Broglie has shown, even with success, an upper limit will be reached, the one which, for atomic sizes, results from the Heisenberg principle.

BIBLIOGRAPHY

1. A. Ertaud, L'optique electronique, published under the direction of L. de Broglie, p. 103 (*Rev. optique*, Paris, 1946)
2. E. Brüche, O. Scherzer, "Geometrische Elektronoptik," (J. Springer, Berlin, 1934)
3. P. Chanson, A. Ertaud, C. Magnan, *Compt. rend.* **221**, 233 (1945)
4. O. Scherzer, *Z. Physik* **1**, 602 (1936)
5. P. Chanson, Thèse de Doctorat ès Sciences, 1947, p. 52 Masson Edit.
6. P. Chanson, A. Ertaud, C. Magnan, *Compt. rend.* **218**, 912 (1944)
7. F. Bertein, E. Regenstreif, *Compt. rend.* **224**, 737 (1947)
8. C. Magnan, p. 30, ref. *1*
9. P. Grivet, p. 128, ref. *1*
10. H. Mahl, special publication of the Allgemeine Elektrische Gesellschaft Forschung, Vol. **2**, No. 1, S. 11 (1940)
11. C. Magnan, p. 18, ref. *1*
12. H. Boersch, *Naturwiss.* **30**, 711 (1942)
13. P. Chanson, p. 73, ref. *5*
14. "Handbuch der Physik," Vol. **58**, Part 2 (1933)
15. E. Bloch, *Z. Physik* **81**, 363 (1933)
16. P. Chanson, p. 77, ref. *5*
17. H. Heil, *Z. Physik* **120**, 212 (1944)
18. M. von Ardenne, *Physik. Z.* **43**, 91 (1942)
19. A. T. Finkelstein, *J. Sci. Instr.* **11**, 94 (1940)
20. J. G. Rutherglen, J. F. I. Cole, *Nature* **160**, 545 (1947)
21. M. von Ardenne, "Elektronen Ubermikroskopie," p. 11 (J. Springer, Berlin, 1940)
22. L. de Broglie, *Compt. rend.* **222**, 1017 (1946)
23. L. de Broglie, *Compt. rend.* **223**, 490 (1946)
24. L. de Broglie, *Compt. rend.* **224**, 1743 (1947)

GAMMA-RAY WELL LOGGING

Industry acceptance of radioactivity well logs to locate new sources of petroleum is plainly illustrated by the fact that 18,000 gamma-ray curves have already been logged in U.S. wells alone. In this first of two articles, the physical science behind successful gamma-ray well logging is discussed

By ROBERT E. FEARON
Well Surveys, Inc., Tulsa, Oklahoma

JUST AS A NAVIGATOR refers to the records of a journey of his craft as a ship's log, well drillers have come to call sequence of data recorded in the downward journey of a drill bit *a well log*.

If it is to be of maximum value in carrying out the purpose the well will serve, the well log must contain information that comprises various kinds of data. Chips of broken rock, torn off by the bit, are often sufficiently large to be valuable as a source of information. Cores may be recovered and cohesive samples of rock thus brought from the bottom of the hole to the geologist's microscope. Rate of drill-bit progress under given drilling conditions is a useful addition to the information to be entered on a well log.

Several new procedures have recently been added to the older methods of building up a well log. Unlike other geophysical prospecting methods, they are carried out in the borehole instead of on the surface of the earth. The uniformity which often prevails in drilled wells generally favors processes of a scanning nature, in which an instrument that is sensitive to the desired rock properties consecutively passes the strata, usually from the bottom up. Automatic records are made possible by providing an insulated cable over which a quantitative electrical indication of the desired property is continuously transmitted, through slip-rings on the cable drum, to the recorder. Progress of paper or film through the recorder may be correlated with depth to provide a quantitative depth axis on the record. This is easily accomplished by passing the cable over a measuring wheel, with which the paper drive is synchronized.

Radioactivity Logs

Many properties of the strata are and can be used to contribute to the total amount of information in a well log (*1*). The information in a related group of these processes is sometimes referred to as a special type of well log. For example, the total information obtained by means of penetrating radiations derived from nuclear processes is often called a radioactivity log. The individual records of measured data are referred to simply as curves, as, for example, the gamma-ray curve, which is discussed in this paper, or the neutron curve, which is to be treated in the second article on this general subject to be published in NUCLEONICS.

Gamma-ray well logging is the business of measuring, and deriving information from, the intensity of the gamma rays naturally emitted into a well bore by any given succession of strata. The means of obtaining such measurements, the significance which may be attributed to them, once they

are obtained, and how they serve to augment the total value of the well log, comprise the subjects covered.

For the purpose of simplification, it will at first be assumed that sections of a long narrow borehole may be taken as equivalent to completely enclosed cavities in uniform strata (we shall neglect ends). Also, we shall limit our attention to the case of radiations for which the mass absorption coefficient may be regarded as constant for the elements common in sedimentary rocks (oxygen, silicon, aluminum, calcium). The detector of radiation will be assumed to be an ionization chamber. Geiger counters have been successfully used (*2*). However, their treatment is more complex, and contributes little to the general understanding of this subject.

Thin-walled Ionization Chamber

We shall consider first the thin-walled ionization chamber containing a dense gas of mass considerably exceeding secondary electron range in any direction, but much less than primary gamma-ray range.

By a careful analogy with reasoning applied to cavity radiation in thermodynamics, we can conclude that, if the ratio of energy of radiation of a given kind, emitted per gram of substance, to the mass absorption coefficient in that substance is everywhere a constant in a large mass of material, then the radiation in any cavity in such a mass will be isotropic, and independent of the distribution of density or the shape or size of the cavity. We shall not be satisfied with analogy, however.

In Fig. 1, consider the point P, within a cavity, the periphery of which is S. An element of solid angle in the direction PQ intersects S at r_1 and encounters a region from r_2 to r_3 having density D_2, differing from the density prevailing from r_1 to r_2, D_1. From r_3 to infinity, density is assumed to be D_3. An element of volume, such as ϵ_r, emits $\rho r^2 d\phi dr$ ergs of radiant energy per second, in all directions where ρ is the emitting power per unit mass (assumed to be constant for all the bodies in the vicinity of the periphery S), where $d\phi$ is an element of solid angle lying in the close vicinity of PQ.

The intensity of the radiation received at P from an element of volume between r_1 and r_2 is, therefore

$$dI = \frac{1}{4\pi r^2} \rho r^2 d\phi dr e^{-(r-r_1)K_0 D_1}$$

where K_0 is the coefficient by which density is converted to mass absorption coefficient. However, if the emitting power ρ is always the same per unit mass, as assumed, then $K_1 D_1 = \rho$, where K_1 is a natural constant of the system.

It follows that:

$$dI = \frac{d\phi dr}{4\pi} \rho e^{-\frac{rK_0\rho}{K_1}} e^{\frac{r_1 K_0 \rho}{K_1}}$$

Gathering the constant terms:

$$dI = \left(\frac{d\phi dr}{4\pi} e^{\frac{r_1 K_0 \rho}{K_1}}\right) \rho e^{-\frac{rK_0\rho}{K_1}}$$

$$\int_{r_1}^{r_2} I dr = \left[-\frac{d\phi K_1}{4\pi K_0} e^{\frac{r_1 K_0 \rho}{K_1}} e^{-\frac{rK_0\rho}{K_1}} \right]_{r_1}^{r_2}$$

For the lower limit, the product of the exponentials equals 1. Because the integrand is negative, the lower limit has a positive sign. The definite integral is, therefore:

$$\int_{r_1}^{r_2} I dr = \frac{K_1 d\phi}{4\pi K_0} \left(1 - e^{\frac{(r_1 - r_2)K_0\rho}{K_1}}\right)$$

$$\frac{dI}{d\phi} = \frac{K_1}{4\pi K_0} \left(1 - e^{\frac{(r_1 - r_2)K_0\rho}{K_1}}\right)$$

The second term above would vanish if $r = \infty$. If we were now to perform an integration between r_2 and r_3, the first term of such integration would exactly cancel the second term of the above. The second term of the integral from r_2 to r_3 would be smaller than the second term of the above. In any succeeding integration, intervening terms would similarly cancel, giving, as

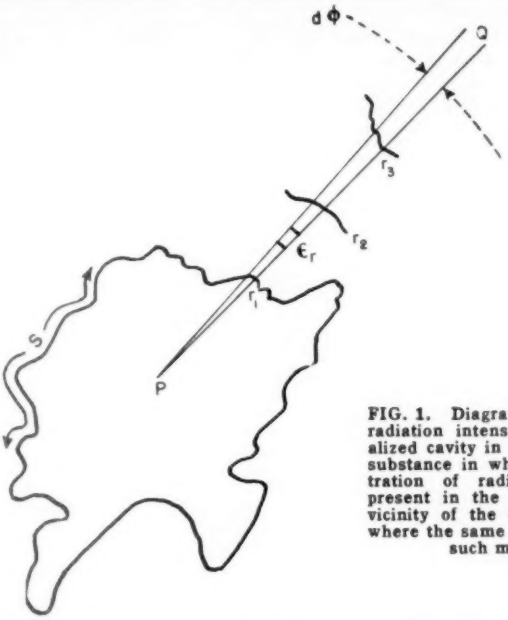

FIG. 1. Diagram for computing radiation intensity in a generalized cavity in a heterogeneous substance in which the concentration of radioactive emitter present in the material in the vicinity of the cavity is everywhere the same per unit mass of such material

the net result of any number of such integrations, always one last term (which might be made as small as we wished if we were to proceed far enough) and the constant term $K_1/4\pi K_0$. Now $\mu = K_0 D$ and $\rho = K_1 D$. Therefore, $dI/d\phi = \rho/4\pi\mu$.

A corollary of the above proposition, which we shall not take the space here to demonstrate, is that: In an extensive heterogeneous medium made up of particles of different density which have the same mass absorption coefficient for gamma rays, and for which the concentration of a given kind of radioactive matter in activity per unit weight is the same for all particles, each portion absorbs exactly as much radiant energy as it emits.

Now, if we suppose a cavity to contain a detector of radiation, and if the detector of radiation is considered to be part of a heterogeneous medium, in which it is one phase, and the uniform rock layer surrounding it is the other phase, then the above corollary will hold if the radioactive composition of the radiation detector is the same as that of the rock. If, also, the detector as a whole is thin compared with the ranges of the radiations considered, it may be regarded as a negligible inhomogeneity. In such a case, it will make no appreciable difference if we allow its radioactive content to be zero, since there will be but little disturbance in the radiation field in its neighborhood caused by the small loss of radiation in the detector.

From these arguments, there is an important conclusion: A relatively thin-walled, but pressure-filled, ionization chamber, in a cavity in the rock strata, will, if of reasonable dimensions, experience a liberation of radiant energy in its gas contents which will be the

same as the energy emitted by a quantity of surrounding rock having the same weight as the contained gas.

From this, if we know the average energetic cost of an ion pair in the contained gas, calculating the saturated ionization current from the radioactive assay of the rock is a simple matter.

With these factors in view, it is relatively easy to establish weighting factors for the variables observed in well logging, when logging is done in uncased holes, and with an ionization chamber such as above described. Table 1 is a list of these factors.

Sampling in a Long Cylindrical Bore

Sampling is a term used in geological investigations to describe the ability to recognize how some property of the earth is weighted throughout the portion of the earth being studied in a given test.

In a cylindrical borehole, the weighting factor falls off radially and is a function of the absorption coefficient of the rays which are emitted by the source radioelement present. The weighting factor may be computed, for a stationary measurement, and for any particle in the vicinity of the detector, by a calculation of the probability of radiation originating from the given particle. This probability is made up of three factors:

1) The solid angle subtended by the detector, with the particle as a vertex.
2) The average absorption factor which prevails for radiation lying in the given solid angle.
3) The efficiency of the detector for radiation coming in from the direction of the particle.

The weighting factor, computed as described above, falls off continuously with distance away from the nearest surface of the detector, nowhere falling abruptly to zero. Nonetheless, at considerable distances, the weighting factor is so near zero that the neglect of all matter beyond a rather thick shell would cause a negligible influence on the measurement.

TABLE 1

Substance	*Relative concentration, grams of radioelement per gram of rock, to produce a given ionization current in a thin-walled chamber*
Radium and series	1.43×10^{-11}
Thorium and series	6.41×10^{-5}
Potassium (Natural Isotopic Mixture)	0.1

Data on total energy fluxes of gamma rays appear to be somewhat in doubt, as reflected in the literature. It has been assumed here that:

Potassium emits 3.6 quanta per second of 1.55-Mev gamma rays per gram.

Radium and series emit 3.0×10^{10} quanta per second of 1.81-Mev gamma rays per gram.

Thorium and series emit 1.38×10^{9} quanta per second of 2.6 Mev gamma rays per gram.

For the purpose of creating a better analogy with chemical sampling, which has a weighting factor of 1 in the sample taken, and zero outside it, we shall speak of the sample measured in gamma-ray well logging as the material lying inside a surface of constant weighting factor. The surface which we arbitrarily choose is the one for which the weighting factor is $1/e$ of the value for material at a point in contact with the ionization chamber at its center. Although it is somewhat inaccurate to do so, we have frequently adopted, for thin-walled chambers, a practical expedient of defining the sample as extending from the wall of the borehole into the rock by an amount equal to the reciprocal of the absorption coefficient in the rock for the radiations from the element being measured, and as having a length equal to that of the

ionization chamber plus well diameter (for end effect).

Nonstationary measurements are easily reasoned from the stationary ones as being merely a succession of stationary states, integrated over time, with a factor in the integrand representing the time response of the instrument to radiation.

In Table 2, prepared in accordance with this arbitrary manner of computing the sample, we have taken rock density as 2.7, and assumed a borehole diameter of 7 inches. Absorption of radiations by any fluid in the hole has been neglected.

It will be seen that the sampling accomplished by gamma-ray well logging is considerably more extensive, for a given length of borehole, than that accomplished by coring. Gamma-ray well logging, therefore, enjoys a relative advantage for the study and correlation of sequences of strata consisting of heterogeneous rocks, for which a 3-inch core might not provide a sufficiently representative sample.

Speed of Logging and Length of Sample

The length of the sample for nonstationary measurements must be considered together with the time of response of the measuring and recording equipment. For accurate measurements of the strata, the time of response must be appreciable, *i.e.*, of the order of seconds if refined comparisons are being made between weakly radioactive strata. This is true because of the necessity of indicating a statistically sufficient number of quanta for good accuracy. So that the length of the sample will not be increased unreasonably, it is necessary to limit the speed in all gamma-ray well logging processes. The desirable maximum speed is that value which corresponds with a progress of not over one sensitive length of the scanning (logging) instrument in the time corresponding to the exponential time constant for the time response of the instrument to a Heaviside unit function of radiation intensity.

TABLE 2

Radioelement predominantly responsible for radiation	*Weight of sample*	*Weight of 3-inch diameter core of equal length*
Radium and series	370 lb	25 lb
Thorium and series	560 lb	25 lb
Potassium-40	160 lb	25 lb

The author was guided by Gleditsch and Graf in regard to hardness of gamma rays of potassium [*Phys. Rev.* **72,** 640 (1947)].

Restating this matter: If the growth or decay of the reading, subsequent to a sudden change of radiation intensity, proceeds to its new value on an exponential proportional to $e^{-(t/t_0)}$, then t_0 is the time in which the instrument should not advance more than one sensitive length.

When the response curve is not exponential, a designation of proper well-surveying speed is more complex, as can readily be seen. Proper speeds differ from one province to another over the earth, in correspondence with the general level of radioactivity of the rocks. The permitted speed will be a function of the accuracy of the measurement which the geological problem demands. Less accuracy, more speed. If we permit representative strata to be measured with a probable error twice as large, we can shorten the response time of the equipment, and go four times as fast, with satisfactory sampling, but less accuracy.

Accordingly, from one region to another, the response time and speed of logging is varied to suit the particular need.

To increase speed, sensitive detectors are employed, involving high pressure gases of very appreciable density (*3*). Crystal scintillation counters, and other

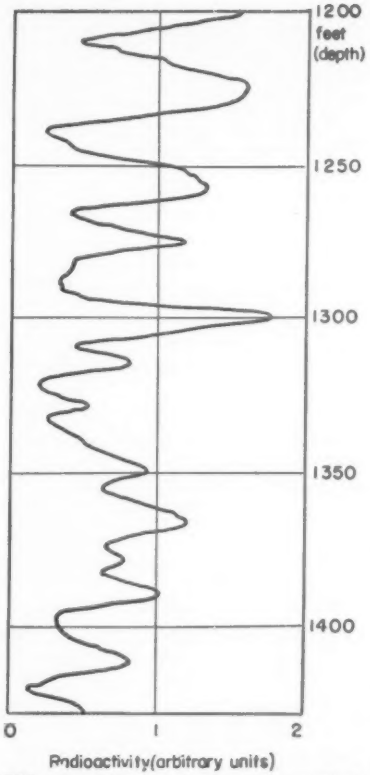

FIG. 2. This section of a practical gamma-ray curve for a well of sub-sea depth (from a sea level datum plane) in Ellis County, Kansas, illustrates satisfactory sensitivity, accuracy, sampling, and speed. The sequence of strata is particularly simple. Shales, which are radioactive, are indicated by throws to the right; limestones, which are non-radioactive, are indicated by minima. Courtesy of Lane-Wells Company, Los Angeles, California

highly sensitive devices have also received attention (*4*). The latter, however, have not as yet been adapted to the operating conditions which prevail in a well.

In view of the progress that is being made toward increasing the speed of gamma-ray well logging, it would seem unwise to set down values, for they would surely be obsolete in a short time. For present-day operations, speeds of gamma-ray logging which provide satisfactory results range from 1,000 ft per hr, in unfavorable cases, to 4,800 ft per hr in favorable circumstances, or where the geological problem is of an undemanding nature. Figure 2 shows a practical gamma-ray curve that illustrates acceptable sampling and adjustment of speed.

TABLE 3

Thickness of absorbing layer ($\mu = 1.5$ *in.*$^{-1}$)	*Ratio of intensity of rays transmitted perpendicularly to intensity transmitted at 45° incidence*
0.5 inches	1.35
0.75 "	1.59
1.00 "	1.86
1.5 "	2.54
2.0 "	3.47

Thick-walled Ionization Chamber

For a thick-walled ionization chamber, there is a "collimating" effect which causes it to prefer rays entering perpendicularly to its walls. For the ionization chamber of cylindrical design, as employed in well logging, this amounts to a preference for rays entering in the equatorial plane. Table 3 illustrates this collimating effect.

It is a consequence of Table 3 that, for a radiation detector thickly lined with very strongly absorbing material, the end effect is less, and the sample measured in a stationary measurement is more nearly reduced to the length of the chamber.

Thin-walled vs Thick-walled Detectors

The thin-walled chamber is better able to admit rays from nearby strata in directions not parallel to its equatorial plane. Rock appreciably dis-

tant from the wall of the borehole can efficiently emit, into the borehole, only radiation that is parallel to the equatorial plane. This is so because of the "thick-wall" effect of the intervening rock, which, for the remote portion of the sample, constitutes a cylindrical shield around the radiation detector. The thin-walled detector, therefore, can give greater weight to the rocks closely neighboring the hole than the thick-walled detector can. The end effect of a thin-walled detector, likewise, corresponds with shallow sampling, in terms of radial depth, out perpendicularly from the bore. Accordingly, detectors of reasonable length, several times borehole diameter, are generally used. Also, if sufficient sensitivity and logging speed can be retained, a thick-walled chamber, being sensitive only to equatorial radiations, gives a larger and more representative sample. Fig. 3 illustrates these considerations.

Spectral Selectivity of a Thick-walled Chamber

A thick-walled chamber exercises a preference in respect to the radiations it observes. The hardest radiations of the thorium series are given greater weight when the thick walls are made of an element of low or medium atomic number. When the walls are constructed of substances of higher atomic number, on the other hand, the spectral selectivity of a thick-walled gamma-ray detector is relatively less important. Use of very large wall thicknesses might give better discrimination. However, this is at present impractical for design of well-logging instruments because of prevailing well diameters and decreased sensitivity brought about by the absorption due to such thick walls.

Gamma Logging in a Cased Borehole

Where a long cylindrical opening in the earth has been lined with a steel pipe, the effect is much the same as

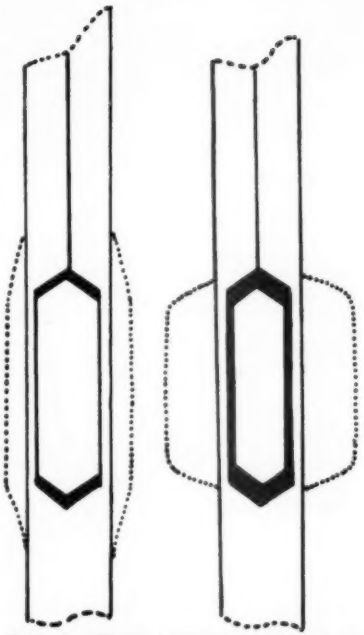

FIG. 3. These diagrams show, in an exaggerated way, the difference in sampling caused by choice of wall thickness of the ionization chamber. The dotted lines indicate, in section, an approximate surface over which the weighting factor for detection of a given radioelement in the rock would be a constant. Practical construction corresponds with very thick ends. Radiation must, therefore, be considered to enter largely through the side walls. See Table 3 for directional influence of thick walls, as shown by right-hand diagram

that observed with a thick-walled gamma-ray detector, provided the pipe has not been cemented in place with Portland cement where it passes through the sequence of rock strata about which information is to be obtained by gamma-ray well logging.

When the steel pipe is held in place by Portland cement, new factors enter. The cement is made by calcining together limestone and shale rock, and grinding the heated aggregates very

TABLE 4

Shale formation	*Radioactivity concentration, units of 10^{-12} grams radium equivalent per gram of rock*
Sylvan (Okla.)	12.6 ± 1.6
Chattanooga (Tenn.)	42.1 ± 1.7
Bandera (Okla.)	158 ± 3.6
Upper Tarouba (Calif.)	6.3 ± 1.8
Black (Okla.)	21.2 ± 2.2

finely. The radioactivity of the cement is contributed by the shales, since, ordinarily, limestones have a nearly negligible radioactivity (*5*). W. L. Russell has given values of the radioactivities of several shales derived from sedimentary sequences found in oilfields (*5*). Values of several representative shales are quoted in Table 4.

Since many of these shales appear at the surface, where they can be open-pit mined, it is not impossible that there may be on the market Portland cement containing any of them.

If the borehole is of a uniform diameter, making the cement outside the casing have a constant thickness, the effect of cement on the curve is:

1) to raise the base value corresponding with weakly radioactive strata,
2) to decrease the amplitude of difference between weakly radioactive strata and stronger ones,
3) to impair the accuracy with which the radioactivity of rock strata are compared.

If a borehole is of nonuniform diameter, making cement outside the casing have a variable thickness, the influence is much more serious. For this, there are two cases:

1) Highly competent sandstones.
2) Poorly cemented and mechanically incompetent sandstones.

In the first instance, the largest hole will be at places where the boring passes through shale bodies. In that circumstance, the Portland cement will cause no very grave errors of interpretation of results, since the Portland cement is, itself, generally similar to a shale.

In the second instance, the errors which may result will be very grave. If the radioactivity of the cement is sufficient, and the excess of erosion from the borehole walls of the sandstone large, the cement may totally mask the presence of the sandstone, which is very often identified by, among other things, low radioactivity. Failure to recognize sandstone may amount to a failure to discover a source of petroleum, often found in the interstitial spaces of sandstones. Such a failure would negate one of the chief ends of the gamma-ray well-logging art, to aid the discovery of petroleum.

When it is expected that borehole diameter varies considerably and, accurate gamma-ray logs through casing are desired, these three courses are open:

1) Withhold cement.
2) Use feebly radioactive cement.
3) Caliper the entire length of the hole, and use cement of known radioactivity, so that corrections may be made for the effect of cement.

Quite often, feebly radioactive cement is a preferred choice. Even in old wells, some data along the line of the caliper method may be obtained, or satisfactorily estimated.

Thus, in spite of the mentioned deficiencies, gamma-ray well logging can be applied in all but a few rare cases, and the curve will be found to be highly informative regarding the type and sequence of subterranean strata penetrated by the borings.

Problems which have no answer in the gamma-ray well-logging art are those of wells strongly contaminated in an unexpected manner with highly

radioactive materials. Such unfavorable wells can usually be successfully logged by the technique of neutron well logging.

Artificially Contaminated Wells

Tracer methods have been applied, to a considerable extent, chiefly in cement location.

Processes have been described for studying permeability of adjacent strata by introducing radioactive fluids into the well, and measuring the amount that goes into sandstones and porous limestones. In such instances it is desirable to remove the radioactive fluid from the open space of the borehole since, with variations in hole size, it interferes with the proper logging of the tracer. Cost of displacing well fluid is considerable, constituting an obstacle to use of these techniques. Colloids normally present in drilling mud are generally similar in adsorptive properties to the rock strata, making tracer work based on selective adsorption an art fraught with considerable difficulty.

Conclusions

Together with a collaborator, the author some time ago expressed an opinion that living things in the ocean may be responsible for concentrating radioelements in fine sediments (*6*). While this may be true of black marine shales, settled out of anaerobic seas, there is reason to doubt the above conclusion in other cases. Even for the black shales, the concentration may have been a sulfide precipitation. For other shales, a combination of factors seems to play a part of which most are essentially physical chemistry. Recent thinking on the subject strongly suggests that aluminosilicate complexes are to be thought of as base exchange adsorbers, with a selectivity for polyvalent metal ions.

This conclusion is supported by the fact that nearly all shales are richer in heavy metals than are pure sandstones and limestones. Fortunately for gamma-ray well logging, fine sediments seem to exercise a preference for potassium as well, preferring it over sodium. Were it not for this happy chance, it would be very doubtful whether the value of gamma-ray well logging in correlating and helping identification of strata would be anywhere near as great as it is.

Along this line, the reader may wonder why so much study has been put on such an apparently simple physical process as the one described in this article. The economic reason is best explained by the fact that, as this goes to press, approximately 18,000 gamma-ray curves have been run in wells in the United States, exclusive of foreign countries, where many wells have also been logged. The tremendous economic contribution to oil finding, by these many runs, is spectacular evidence of the vast new values to be obtained as nuclear physics in its application to the needs of man. These logs represent a totality of many millions of comparisons of rock radioactivities, undoubtedly the greatest body of such data on earth.

The article to follow, on neutron well logging, will explain the physical principles of another nuclear method of aiding the discovery of oil in borings and show how this additional method complements gamma-ray well logging.

* * *

The author expresses his thanks to Well Surveys, Inc., for permission to publish this article, and to Messrs. J. M. Thayer and Arthur Youmans and Mrs. Fearon for reading the manuscript.

BIBLIOGRAPHY

1. U. S. Patents 2,39 255; 2,179,593; 2,398,800; 2,398,868; 2,396,935
2. Lynn G. Howell, Alex Frosch, *Geophysics* **4**, No. 2, 106 (1939)
3. U. S. Patent 2,349,225
4. U. S. Patent 2,351,028
5. W. L. Russell, *Geophysics* **9**, No. 2, 180 (1944)
6. W. G. Green, R. E. Fearon, *Geophysics* **5**, No. 3, 272 (1940)

NUCLEONIC EVENTS

NORMAN R. BEERS NAMED EDITOR OF "NUCLEONICS"

Normal R. Beers, leader of the Meteorology Group, Brookhaven National Laboratory, has resigned to become editor of NUCLEONICS, effective April 15. At Brookhaven, he was particularly concerned with problems involved in atmospheric disposal of radioactive wastes, and his paper on that subject appears in this issue.

Mr. Beers received his B.S. in E.E. from the University of Missouri in 1933, and his M.A. in Mathematical Physics there the following year. He attended Oxford University as a Rhodes scholar, where he took his B.Sc. in Astrophysics in 1937. From 1937–41 he was with the McGraw-Hill Book Co., Inc., and then resigned to enter the U. S. Navy. His naval experience (1941–46) was largely in meteorology, but he spent ten months at the Naval Air Station, Jacksonville, Fla., in charge of the basic-phase Aviation Machinist Mate School, and four months with IFF airborne radar maintenance in the Bureau of Aeronautics. He left the Navy as a lieutenant-commander to become associate professor of Aerological Engineering at the Postgraduate School in Annapolis during the year 1946–47. Since that time he has been at Brookhaven.

Mr. Beers is co-author of the "Handbook of Meteorology," and has published research papers in the *Transactions* of the American Geophysical Union, in the *Journal of Meteorology* of the American Meteorological Society, and in USAF reports. He is a member of a number of technical societies, including the two mentioned above.

Mr. Beers will continue as a consultant for the Nuclear Reactor Project at Brookhaven. Keith Henney will continue with NUCLEONICS as consulting editor.

FRENCH AEC DESCRIBES OPERATION OF NEW PILE

On December 15, 1948, "Zoe" the first atomic pile built in France began operation at Chatillon. A review of the work leading to the completion of the pile is contained in the February, 1948, issue of *Atomes*, a popular French journal devoted to atomic energy.

Frederic Joliot-Curie, High Commissioner of the French Atomic Energy Commission, points out that French efforts began with an almost total lack of trained personnel and materials. There were only four Frenchmen available with experience in England or Canada. The pile just completed is to be only the first step in an ambitious program planned by the French commission; plans are already made for the construction of a larger pile and the development of a center of nuclear studies at Saclay, to be completed by 1953. Joliot-Curie looks forward to the eventual establishment of a center for nuclear power. During the next five years, French efforts will be directed toward: 1) the training of personnel and the production of radioisotopes for biological and industrial research; 2) the construction of the Saclay Center of Nuclear Studies, where scientists can use the projected pile and high-energy accelerators for research; and 3) the exploitation of natural sources of atomic energy in France and French overseas territories.

The French pile, the dimensions of which are not given, consists of a cistern of heavy water in which are placed aluminum cans containing uranium oxide (UO_2). There are several safety rods of cadmium or boron, mounted vertically, which can be either completely submerged in the heavy water or completely removed. Two minutes are needed to raise them, four seconds to lower them. Outside the cistern, there are regulating plates to control the level of operation. Constructed of a neutron-absorbing material, they are raised or lowered by servomotors. As an emergency precaution, the heavy water can be drained out of the cistern. Outside the regulating plates, there is a graphite reflector of great purity and a concrete shield surrounding the entire structure. The shield contains several holes for the ionization chambers needed in the control mechanism, and a few for experimental purposes. The power level apparently lies between 1 and 10 kw.

The French originally planned to use a uranium metal and graphite-moderated pile but were forced to turn to UO_2 and heavy water in the summer of 1947 because sufficient quantities of pure uranium were not available. Starting with the large quantity of U_3O_8, which Joliot-Curie had obtained before the war and which was hidden in Morocco during the occupation of France, UO_2 was obtained in the following manner: U_3O_8 was reduced to uranyl nitrate and, by an ether and water extraction process, the nitrate transformed into UO_4, which, in turn was calcined at 300° C to obtain UO_3 and reduced again with hydrogen at 650° C, to form the final product, UO_2. The UO_2, however, was in the form of a powder of insufficient density to sustain a chain reaction. By compression in a neutral or reducing atmosphere and a temperature between 1,000° C and 1,600° C, sufficient density, stability, and a uniform grain were obtained.

The articles in *Atomes* were written by L. Kowarski, technical director of the French commission; Eugene LeMeur, chief of mechanical engineering; Maurice Surdin, chief of electrical engineering; Andre Ertaud, chief of pile physics; Bertrand Goldschmidt, chief industrial chemist; and J. A. Stohr, director of the Chatillon center.

CANCER RESEARCHERS TO GET FREE ISOTOPES

All radioisotopes used in cancer research have been made available without charge to qualified cancer research workers in the United States, according to an announcement by the Atomic Energy Commission.

A sum of $450,000 has been set aside to defray the cost of the new program during its first year of operation. The only charge to be made by the AEC will be a nominal $10 for handling—covering the cost of packaging, monitoring, accounting and billing—plus the actual cost of transportation. The materials themselves will be free. In those cases where the isotopes are synthesized into a chemical compound, the user will be required to pay for the cost of synthesizing the compound, but not for the radioisotopes.

The free isotopes will be allocated for the following purposes: (1) cancer investigations involving animal subjects, (2) research programs studying basic cellular metabolism of cancerous cells, and (3) experimental programs designed to evaluate the therapeutic use of radioactive materials.

The same careful controls over the distribution program now in effect will be continued. Applicants for materials must fulfill the requirements of the AEC for users of radioactive materials and must offer assurance that there will be no resale or charges to patients for the isotopes procured under the program. Applications for radioiso-

topes for use in human subjects must be approved by the Subcommittee on Human Applications of the Commission's Committee on Isotope Distribution.

INDIA REPORTS ON NUCLEAR PHYSICS WORK

The recently issued annual report for the year 1947–48 of the Tata Institute of Fundamental Research in India contains descriptions of the institute's program in the field of nuclear physics. The following is taken from this report:

A high-energy accelerator, capable of producing particles of energy above 200 Mev and of creating mesons, is planned. A team of ten scientists will work on this project. . . . The intensity of cosmic radiation at high altitudes is being measured by means of radiosonde balloons. A tape recorder and four-fold coincidence counter circuits have been developed for sending up with the balloons. . . . Photographs are being obtained with the Wilson cloud chamber, and the scattering of mesons has been measured in a lead plate. . . . The problems of the azimuthal effect of cosmic radiation and the precision measurement of the absorption spectrum of cosmic rays are being studied. . . . Two different portable G-M counter sets with three different sensitivities for geological prospecting have been developed. An ionization chamber of the type used in the Canadian and British piles is being constructed. . . . The scattering of mesons in a Coulomb field and the diffusion of neutrons in a pile are being investigated.

A large number of selfquenching Geiger-Müller tubes has been made. These tubes have been tested for their plateaus, which extend over 300 volts. In addition to the standard-size tubes, the following special tubes were built as an experiment: 10 mm dia. Pyrex glass, plateau 100 volts; 40 mm (1 ft), 40 mm (2 ft) Pyrex glass, plateau 600 volts; 35 mm, Pyrex glass coated with aquadag, plateau 50 volts; 60 mm, soft glass coated with aquadag instead of copper plate, plateau 600 volts.

Wilson cloud chamber. The Wilson chamber room has been air-conditioned and it has been found possible to maintain the temperature of the room constant at 70° F (variation 4° F), which is necessary for the successful operation of the chamber. Considerable improvements in the design, release mechanism of the chamber and the application of the clearing field have been effected. Two new cameras have been designed and constructed and are now being used for taking stereoscopic photographs. Two hundred pictures at a time can be taken without re-loading. The whole chamber works automatically for several hours without any attention.

Mesons, capable of penetrating 5, 15, 25 and 35 cms of lead, and scattered in a 2 cm lead plate inside the chamber, have been photographed. About one thousand such stereoscopic pictures have been obtained, and are, at present, under analysis.

Some of the photographs, incidentally, throw light on various types of phenomena. The quality of almost all the pictures obtained is good. One particularly interesting photograph has been obtained. A neutral particle has knocked out a heavy particle from the lead plate. This neutral particle on top is accompanied by electrons which have produced cascades in the lead, and by mesons which have gone right through without appreciable scattering, thereby showing their high energies. This photograph is unique in the sense that it is the only one so far published (at time of report) which shows the production of a doubly charged ionizing particle by some neutral radiation at sea level.

High altitude measurements of cosmic radiation. A considerable amount of development work in connection with the balloon flights has been done at the Institute. A receiving unit consisting of two short-wave receivers with a self-recording system has been constructed especially for the purpose. A short-wave transmitter sends pressure signals from this meteorograph at regular short intervals of pressure. The signals received on the superheterodyne receiver accordingly change their audio notes. The coincidence cosmic-ray pulses sent by two short-wave transmitters are received by the receivers on a moving paper tape. The resolving time of the receiving set is such that 50 to 60 events per minute can easily be distinguished from each other.

The complete program envisages a series of thirty-two flights at four stations at different latitudes. At each station it is proposed to have eight flights, four of which will be for the measurement of the total intensity of cosmic radiation, and

the remaining four for the measurement of the intensity of cosmic radiation penetrating a known thickness of lead.

Studies of the azimuthal effect of cosmic radiation at Bombay. Since azimuthal studies of cosmic radiation at intermediate latitudes are of fundamental importance in determining the sign and the energy spectrum of the primary cosmic rays, it was decided to determine the azimuthal measurements at Mexico City and at Lahore. The measurements at Bombay will also extend the energy spectrum to slightly higher energies than those covered by the experiments at Mexico and Lahore.

The apparatus was designed and installed to record variations of cosmic-ray intensity at different zenith and azimuthal angles. The apparatus consists of a twin counter telescope pointing in two diametrically opposite directions mounted on a turntable so as to measure the intensity at the desired azimuthal and zenith angle. A single vertical counter telescope is also provided to record vertical cosmic-ray intensity. The north-west and south-west quadrants have already been covered for a fixed angle of 60°. The results are in agreement with those obtained at Lahore.

$1,000,000 GIFT TO CORNELL LABORATORY

A gift of securities estimated in value at approximately $1,000,000 has been made to the Cornell University Laboratory of Nuclear Studies by Floyd R. Newman, Cleveland petroleum industrialist. In recognition of the gift, the Cornell board of trustees has voted to name the laboratory, which was opened last October, the Floyd Newman Laboratory of Nuclear Studies.

BOOKS

HISTOPATHOLOGY OF IRRADIATION FROM EXTERNAL AND INTERNAL SOURCES, edited by William Bloom, M.D. (University of Chicago), lithographed by Edwards Brothers, Ann Arbor, Mich., published by McGraw-Hill Book Co., Inc., New York, 1948, 808 pages, $8.00. *Reviewed by Roberts Rugh, Assoc. Prof. of Radiology, Columbia University.*

This volume was the first readied for publication from a total of about sixty volumes that will comprise the National Nuclear Energy Series (Manhattan Project Technical Section).* It is Vol. 22I of NNES Division IV, the division devoted to reports of the Plutonium Project.

The book carries a "Foreword" by David E. Lilienthal, chairman of the AEC, and a "Preface" by the Editorial Advisory Board in which is outlined the editorial program for the entire series, a "Plutonium Project Record Foreword" by Arthur H. Compton, an "Introductory Note on the Plutonium Project Record" by Robert S. Mulliken, Editor-in-Chief, Plutonium Project Record, a "Preface to the Health Volumes in the Division IV of the National Nuclear Series" by Raymond E. Zirkle, and an "Editor's Preface" in which Dr. Bloom explains the processes by which this material was made available.

This volume represents the collected works of a large staff of investigators and assistants at the Health Division Metallurgical Laboratory of the University of Chicago, and Dr. Bloom had the able assistance of 11 different chapter editors in organizing the mass of accumulated data.

Available to the staff during the 2½ years of intensive work were a profusion of animals, liberal amounts of old and new radioactive materials, and excellent technical facilities. Because of the

* The National Nuclear Energy Series (NNES) is a record of scientific achievements arising from researches conducted during the war by emergency research organizations and continued by the Atomic Energy Commission. See NUCLEONICS **2**, No. 4, 79 (1948); also **4**, No. 1, 60 (1949).

exigencies of war, there was an imperativeness combined with an overworked staff, in spite of which the main contributions of this book probably will be substantiated by future verification.

The external radiations used were X-rays, beta rays from phosphorus-32, gamma rays from radium and the Clinton pile, fast neutrons, and slow neutrons from the Clinton Pile. Internal radiations were from the various isotopes emitting alpha, beta and gamma rays, and these were administered intramuscularly, intravenously, intracardially, intraperitoneally, and by inhalation.

The material is presented in 18 chapters and a summary chapter by Dr. Bloom. There is an Appendix which gives detailed data on "Experiments Listed by Agent, Animal Species, and Mode of Administration" which should be an aid in cutting short the exploratory procedures in other laboratories. Most of the sections are concerned with specific organs or tissues, and the authors first present the effect of one type of radiation (*e.g.*, X-radiation) and then compare with this the effects, on the same tissue, of other radiations. A similar procedure is followed for the internally administered radioactive substances. Frequent section or chapter summaries aid the reader in pulling the mass of data together.

The report is as scientifically complete as it is possible to be, so that one can repeat the experimental conditions and check the end histological results against an abundant series of photographic illustrations.

In critically evaluating the data *per se* of this book, it is impossible to keep one's opinion from being colored by the constant realization that here is the entire story, unglossed and somewhat unedited. The reviewer intends no criticism here of Dr. Bloom's stupendous task, but rather suggests that the editor has chosen (and properly) to put these data into the hands of an eager public at an early date at the expense of some editorial refinement. The reader must do his own culling of minor data.

Too few species were used to draw many generalizations. Unirradiated controls are generally presented but it is not always clear that they were genetically equivalent to litter mates of the same age and stage of development, although this was probably true. Any deviations from the histological picture of the controls were ascribed to radiation effects. One might have wished for better evidence that all other environmental variables were incontrovertibly eliminated. The investigators were limited to small exposures and doses, due to the hazards involved and certain technical limitations. It may have been profitable to use small doses of localized and directed radiations.

With these more-or-less minor criticisms enumerated, one can turn to the fact that this is a major contribution to the mounting volume of radiation literature, a book which should be at the elbow of all histologists interested in radiation effects. The dosimetry is always given accurately and the radiations used were various.

There is in this book a profusion of illustrations which include some six hundred photographs of tissues and radioautographs, a dozen camera lucida drawings, and about twenty-three drawings in color of cells and tissues, the latter executed by Esther Bohlman. The color illustrations are the most accurately reproduced and, while lithographic reproductions of photographs leave much to be desired, most of the illustrations are functional. Nothing is lost by having the text lithographed. No doubt this method of publishing has put the book into the hands of interested research workers many months before it would be possible otherwise.

It is a "must" reference book for all radiobiologists.

PRODUCTS and MATERIALS

END-WINDOW COUNTER

N. Wood Counter Laboratory, Chesterton, Ind. This mica end-window counter has a $1\frac{1}{16}$ in. window, 2–3 mg/cm² thick, sealed to a stainless steel cathode by means of fused glass. The seal is designed so as not to be affected by heat

or filling vapors and remains tight since there are no gaskets or resins to cause leakage. These counters are claimed to have long, flat plateaus, very low backgrounds and a long lifetime.

ALPHA-BETA-GAMMA METER

Precision Radiation Instruments, Inc., 1101 N. Paulina St., Chicago 22, Ill. The model 102 portable G-M counter is designed to measure low-energy beta

particles and alphas, as well as gamma and X-rays. The tube is self quenching, with its threshold at approximately 825 volts and a plateau of 200 volts. It has a mica window 1.5 mg/cm². The entire probe assembly and cable is mounted on a box $5\frac{1}{4}$ in. × $6\frac{1}{2}$ in. × $4\frac{1}{2}$ in. and weighs about 7 lbs.

DIRECTIONAL COUNTER

Radiation Counter Laboratories, Inc., 1844 W. 21 St., Chicago 8, Ill. This G-M tube is designed to detect only

that beta-gamma radiation which enters the counter through a forward (or backward) cone, the apex angle of which is about 35°. The counter is physically similar to any bubble window counter except that several insulating beads are so placed on the center wire that a discharge along the anode occurs only if radiation enters from an endwise direction and forms primary ion pairs all along the long axis of the counter.

ELECTRON MULTIPLIER

Electric and Musical Industries, Ltd., Hayes, Middlesex, England. The type VX5019 single stage thermionic electron multiplier tube has been designed for use at frequencies up to 100 megacycles. It is essentially a tetrode type in which

the anode is replaced by a secondary electron emitter with an accompanying anode. The emitter-anode section is electrostatically shielded from the other tube elements so that the interelectrode capacity is extremely small. A large fraction of the anode current is supplied by the secondary emitter, resulting in only a slight reaction of the anode current on the cathode and grids. The tube has a very high mutual conductance and a noise level about 50% above that of a normal pentode.

PROPORTIONAL COUNTER

Nuclear Instrument & Chemical Corp., 223 W. Erie St., Chicago 10, Ill. The model D45 methane flow proportional counter is designed to count alpha

particles in the presence of high beta activity with 50% geometry and low coincidence losses. The counter chamber has a highly polished cylindrical cathode. The 0.002 in. tungsten anode is mounted between glass insulators.

HIGH-VACUUM APPARATUS

Central Scientific Co., 1700 Irving Park Rd., Chicago 13, Ill., has issued a booklet on its various high-vacuum apparatus. Included in this 48-page pamphlet are suggestions for planning a high-vacuum system; information on pumping speed; explanation of merit factor, connections and speed of evacuation, low pressure technique, and other data, together with a complete listing of Cenco mechanical pumps, D-P diffusion pumps and Cenco gages, oils, traps and other vacuum accessories.

HEVIMET ALLOY

General Electric Co., Chemical Dept., Pittsfield, Mass. Hevimet alloy was developed as a high density material for use as a gamma-ray absorber. It has a density 50% greater than that of lead and the tensile strength of high-grade steel. Containing tungsten, nickel and copper in varying proportions, Hevimet is produced by powder metallurgy and is said to be readily machinable. It is highly resistant to atmospheric salt water corrosion, is easily plated with cadmium, chromium, or nickel, and can be silver-soldered and brazed by standard methods.

NEW COMPANY

Heinicke Instrument Corp., 315 Alexander St., Rochester 4, N. Y., was formed recently. It is preparing a nuclear physics teaching kit for distribution to colleges and universities. The company is also distributing Eastman Kodak nuclear track plates and is growing anthracene crystals. Officers of the company are K. J. Heinicke, president, and W. H. Bidlack, vice president.

"TAGGED" FORMALDEHYDE

Oak Ridge National Laboratory, Isotopes Division, Oak Ridge, Tenn. A limited amount of formaldehyde labeled with C^{14} is now available. This compound is, at present, distributed as formalin, a 0.5–30% aqueous solution of formaldehyde, in which 3–6% of the carbon atoms are radioactive. The cost of the labeled compound is $250 per millicurie. On a request, the compound formaldehyde and "Item LC-2" under items 5 and 8, respectively, of "Application for Radioisotopes Procurement," should be specified.

ERRATA

In a recent issue of NUCLEONICS [3, No. 6, 43 (1948)], there appeared the article, "Design of an Improved-Yield Discharge Tube," by Jaroslav Pachner. This paper was translated for NUCLEONICS from the Czechoslovakian journal, *Elektrotechnicky Obzor*, by E. Gros of England. A number of errors appeared in the translated version which were not present in the original.

Dr. John Kronsbein, Evansville College, Ind., has pointed out the following: On page 45, the result of the integration, $\int \frac{d(x^2)}{\ln (x^2)}$, is not a natural logarithm, $\ln (x^2)$, but a logarithmic integral, li $(x^2) = -as +$ const.; Eq. 6 therefore reads

$$\text{li}\left(4\frac{m_e}{m_2}\frac{E_2(s)}{J}\right)^2 = \text{li}\left(4\frac{m_e}{m_2}\frac{E_2(0)}{J}\right)^2 = \frac{E_0^2}{J^2} \times N\sigma \times \frac{32}{Z_1} \times \mu^2 \frac{m_e}{(m_2)^3} \times s$$

Mr. Pachner and Mr. Gros have pointed out the following corrections:

In the first equation following Eq. 3*a*, on p. 45, the reduced mass μ in the right-hand side of the equation should be μ^2.

In Eq. 16, and the one preceding it, on p. 47, and in Eq. 24 on p. 48, the symbol w_R should appear as W_R.

In Eq. 26 on p. 48, the numerator should read $(F + E_R)$ and not $(F + F_R)$.

In the diagram on p. 51, the angle ω between the foil plane and the tube axis has been omitted.

If the target is grounded (p. 51), the current for the ion source has to be produced by an insulated synchronous generator at the potential of the ion source, which is driven by a grounded motor through an insulated shaft.

* * *

In the reports on the IRE-AIEE Instrumentation Conference which were published in the January issue, the abstract of the paper, "Cloud Chambers," by G. C. Baldwin, General Electric Company, Schenectady, N. Y., contained a number of errors. Dr. Baldwin has called these errors to the attention of the editors of NUCLEONICS and has submitted the following corrected abstract:

Because cloud chambers give the spatial distribution of ions formed by a nuclear particle, they give more fundamental information than do other detectors; however, where statistically accurate data are required, other detectors are preferable. In a cloud chamber, ions are "amplified" by preferential condensation of moisture from a supersaturated vapor upon them, rather than by "electronic" means. The ions in a track of a fast particle are formed by transfers of momentum from the passing particle to atomic electrons with a probability proportional to the square of its charge divided by the square of its velocity. Thus the density of ions in a track permits this function of charge and velocity to be determined.

The tracks formed in the gas of the chamber, which may be air with a mixture of water vapor and alcohol, are photographed using xenon-filled flash lamps, an f-2 lens and Super-X film through a mirror arrangement that gives a stereoscopic view. The negatives are then reprojected through the same optical system to produce an oriented image in space that can be located by properly tilting a ground glass to obtain the exact direction of the track. In this way precise determinations of track characteristics can be made.

This equipment at the General Electric Research Laboratory is arranged by automatic controls to go through its cycle once a minute. Eight seconds before expansion, a magnetic field of 4,000 gauss is applied for the duration of the exposure. In cosmic-ray work, it is common practice to control the chambers by coincidence counters mounted on either side of the chamber to actuate it when a particle arrives. Special chambers have been built for high or low pressure or for high speed, in which case helium is used as the gas to permit reaching thermal equilibrium quickly after each expansion.

In evaluation of measurements on a track, the following relationships are used:

(1) The density of drops along the track is proportional to the square of the ratio of charge to velocity.

(2) The radius of curvature multiplied by the magnetic flux density is equal to the particle's momentum/its charge.

(3) The length of the track, or range, is the distance that the particle must go to expend all its energy by forming ions at a rate given in (1) above.

By simultaneously solving the three equations resulting from the above relations one can determine the mass, charge and velocity of the particle. In tracks of collisions or nuclear disintegration processes the application of the laws of conservation of energy and momentum permits uncharged particles to be revealed despite the fact that, being uncharged, they leave no tracks.

ABSTRACTS

CHEMICAL PUBLICATIONS

Nucleonics, C. L. Gordon (Natl. Bur. of Standards, Washington, D. C.), *Anal. Chem.* **21,** 96–101 (1949). A review of recent work in the analytical phases of nucleonics. Under the subject of types of procedure are discussed tracers, induced radioactive excitation, differential absorption, and neutron absorption. Various counters, photographic techniques, neutron sources, and health hazards are discussed. A bibliography of 120 references is given.

Gamma rays from the disintegration of boron by slow neutrons, B. Rose (Natl. Research Council of Canada, Chalk River, Ont.), *Can. J. Research* **26A,** 366–378 (1948). Boron in the form of BF_3 in a proportional counter was irradiated with slow neutrons from a Ra-Be source. Coincidences were counted between alpha particle pulses in the BF_3 proportional counter and γ-ray pulses in an adjacent Geiger-Müller counter. The quantum efficiency of the latter was determined by calibration with standard sources. The ratio of the α-γ coincidence rate to the α-rate, corrected for the efficiency of the γ-ray counter, gave a value of 0.90 ± 0.08 for the number of quanta per boron disintegration. The absorption coefficient of the γ-rays in lead was measured, and the energy of the γ-rays was found to be 0.48 ± 0.015 Mev. The results support the disintegration scheme for $B^{10}(n,\alpha)Li^7$ in which 93% of the disintegrations go to the excited Li^{7*}, and only 7% to the ground state.

Search for a 3.20-Mev γ-ray in the disintegration of thorium C″, R. E. Bell, L. G. Elliott (Natl. Research Council of Canada, Chalk River, Ont.), *Can. J. Research* **26A,** 379–385 (1948). According to one of the proposed distintegration schemes for ThC″, 73% of the β-disintegrations take place to an excited state of ThD having an excitation energy of 3.20 Mev; de-excitation takes place by the emission of two successive γ-rays of energies 0.58 and 2.62 Mev, respectively. A search was made for γ-rays of 3.20 Mev from sources of radiothorium in equilibrium with its products. The secondary electrons ejected from thin radiators of lead and uranium were studied using a thin magnetic-lens β-ray spectrometer. No photoelectrons ejected by a 3.20-Mev γ-ray were observed. If the γ-ray occurs, its intensity is less than 0.2% of the 2.62-Mev γ-ray intensity.

Attempt to detect an $(n,2n)$ reaction in deuterium, L. G. Elliott, E. P. Hincks, A. N. May (Natl. Research Council of Canada, Montreal Laboratory) *Can. J. Research* **26A,** 386–403 (1948). Careful experiments were carried out to detect an $(n,2n)$ reaction in deuterium. A Po-α-Be source was placed at the center of a hollow aluminum sphere which was surrounded by an effectively infinite uniform medium of paraffin oil, and the neutron-intensity outside the sphere was measured with a small BF_3 counter. Total integrated neutron densities were determined with the sphere empty and filled with deuterium. After all corrections, it was found that the fraction of neutrons contributing to a $(n,2n)$ reaction is $0.1 \pm 2.7\%$.

The emission of L-radiation following internal conversion of γ-radiation in heavy elements, B. B. Kinsey (Natl. Research Council of Canada, Chalk River, Ont.), *Can. J. Research* **26A,** 404–420 (1948). Computations were made of the fluorescence yields resulting from the internal conversion of γ-radiation in the L-levels of the heavy elements, and of the distribution of the energy in the spectrum. It was found that the total fluorescence yield for elements in the vicinity of tantalum, resulting from excitation by internal conversion, is appreciably less than the yield measured for fluorescence excitation; however, for the heavier elements, the yields are comparable. In the case of fluorescence excitation, the observed and calculated total fluorescence yields are in agreement.

The emission of L-radiation in the disintegration of ThC and RaD, B. B. Kinsey (Natl. Research Council of Canada, Chalk River, Ont.), *Can. J. Research* **26A,** 421–450 (1948). Measurements were made of the amount of L-radiation resulting from the K-conversion of γ-radiation emitted in the disintegration of ThB, and of the yields of L-radiation resulting from the L-conversion of the low energy γ-radiation emitted in the disintegrations of ThC and of RaD. The results were found to be in general agreement with calculations (see preceding abstract) in the case of ThB, but were too high for ThC and too low for RaD. The results are discussed in detail.

The effects of high energy radiations on water and aqueous systems, F. H. Krenz (Natl. Research Council of Canada, Chalk River, Ont.), *Can. J. Research* **26B,** 647–656 (1948). The primary act of absorption of high energy particles and quanta is thought to result in the production of hydrogen atoms and hydroxyl radicals, which then react to give secondary decomposition processes. Any chemical changes that occur upon the absorption of energy from X- or γ-rays must occur at the vibrational level, since this is the only level involving excitation of chemical bonds. Higher forms of atomic excitation must be degraded within the atom itself. Evidence obtained from dilatometer measurements of the expansion of water irradiated with γ-rays indicates the production of long-lived activity in the irradiated water. This may be attributed to vibrationally excited "polymers" of water. A study was made of the oxidation of ferrous ion in dilute aqueous solution by γ-radiation. At concentrations of ferrous ion greater than about 5×10^{-5} mole per liter, the energy absorbed is used to oxidize the ferrous ions; at lower concentrations, the energy is dissipated in some other way.

Exchange reactions in the uranyl-uranous system, R. H. Betts (Natl. Research Council of Canada, Chalk River, Ont.), *Can. J. Research* **26B,** 702–710 (1948). The rate of exchange of uranium atoms between U^{4+} and UO_2^{++} in sulfuric acid solutions of constant ionic strength was measured. The method comprised labeling UO_2^{++} with U^{233}, mixing it with natural uranium as U^{4+}, and measuring the subsequent changes in specific activity of the two species. The effect of *p*H, temperature, and U^{4+} and U^{6+} concentrations were studied over a narrow range. The exchange took place readily, although the rate in the dark was only about 5% of that for the corresponding photocatalyzed reaction. The observed rate of exchange (with illumination) ranged from 1–2 $\times 10^{-4}$ mole per liter per min; the corresponding energy of activation is 8,400 to 8,500 cal per mole. The order of the reaction was found to be 0.30. The correlation between the electrochemical behavior of the system and the observed rates of exchange is discussed.

Determination of the maximum energy of the β^- radiation of S^{35}, L. Yaffe, K. M. Justus (Natl. Research Council of Canada, Chalk River, Ont.) *Can. J. Research* **26B,** 734–736 (1948). Using a S^{35} source of high specific activity and various aluminum absorbers, the range of the β^- radiation of S^{35} was found to be 32.2 $\pm$ 0.3 mg per cm^2. With the aid of various range-energy relationships taken from the literature, the maximum energy was calculated to be 169 $\pm$ 5 kev.

The chemistry of element 43, E. Jacobi (Physical Institute, Zürich, Switz.), *Helv. Chim. Acta* **31,** 2118–2123 (1948). A procedure was worked out for the rapid separation of element 43 from proton-bombarded molybdenum, with only 0.3 to 2 mg of carrier. The dependence of time and hydrochloric acid concentration on the adsorption of element 43 by Re_2S_7 and CuS was studied. Speed is necessary because of the short half-life (53 minutes) of element 43; the separation required about 40 minutes.

The chemical behavior of radioactive materials in unweighable mixtures by precipitation reactions; E. Jacobi (Physical Institute, Zürich, Switz.), *Helv. Chim. Acta* **31,** 2124–2127 (1948). A classification of methods is given for the separation of radioelements from the starting materials from which they arose.

Oxidation of glucose by yeast, studied with isotopic carbon, S. Weinhouse, R. H. Millington, K. F. Lewis (Temple Univ., Philadelphia, Pa.), *J. Am. Chem. Soc.* **70,** 3680–3683 (1948). Experiments were carried out on the oxidation of glucose by yeast in the presence of either magnesium acetate, labeled with C^{13} in the carboxyl carbon, or sodium bicarbonate-C^{13}. It was found that at least half and probably more of glucose undergoing complete oxidation passes through the intermediate stage of acetate. Intermediates in the fermentation process in yeast are not in equilibrium with acetate. The results are in agreement with the postulates that the conversion of glucose to acetate, and then to components of the tricarboxylic acid cycle, is a major oxidative pathway of carbohydrates in yeast, and that fermentation and oxidation of glucose diverge at acetaldehyde. The assimilation of carbon dioxide was found to occur, but seems relatively unimportant in the formation of succinate from glucose.

Chemical degradation of isotopic succinic and malic acids, A. A. Benson, J. A. Bassham (Univ. of California, Berkeley), *J. Am. Chem. Soc.* **70,** 3939 (1948). Succinic and malic acids containing C^{14} were isolated from plant extracts using silica gel partition chromatography, and co-crystallized with carrier acids. The

succinic acid was chemically degraded to ethylenediamine dihydrochloride and carbon dioxide, thus making it possible to determine the activity of the methylene carbon atoms without interference from any carboxyl carbon activity. Only 2.6% of the succinic acid activity was found in the methylene carbon atoms. The malic acid was oxidized with chromic acid to carbon dioxide and acetic acid, and the activity of each product was determined. Such unequivocal degradations are of value in determining the path of carbon in photosynthesis.

The separation of nuclear isomers of bromine on silver plates, W. S. Koski (Los Alamos Scientific Lab., Los Alamos, N. Mex.), *J. Am. Chem. Soc.* **70,** 4251–4252 (1948). Irradiated with slow neutrons, *n*-butyl bromide contains 34-hr Br^{82}, 4.4-hr Br^{80*} and 18-min Br^{80}. Some such irradiated bromide was dissolved in acetone, and a silver foil, charged or uncharged, was immersed in the solution for 15 sec, then removed, washed, dried, and measured for activity. It was found that the electrode had adsorbed radioactivity, and a study of the decay curve showed that there was an appreciable enrichment of the 18-min isotope over the equilibrium value. Roughly the same separation efficiencies were obtained with charged and uncharged foils, indicating that the separation effect is mainly chemical.

Cation exchange studies on the barium citrate complex and related equilibria, J. Schubert, J. W. Richter (Argonne Natl. Laboratory, Chicago, Ill.), *J. Am. Chem. Soc.* **70,** 4259–4260 (1948). The following data were derived from cation exchange studies in which elution was effected with citric acid adjusted to various *p*H values with ammonium hydroxide: (1) The dissociation constants of barium (and strontium) citrate; (2) The effect of *p*H on the adsorption of Ba^{140} and La^{140}; and the cation exchange constants for the reactions where Ba^{140} and Sr^{89} in ammonium chloride solutions are adsorbed by the ammonium form of a cation exchanger.

The ion-exchange separation of zirconium and hafnium, K. Street, Jr., G. T. Seaborg (Univ. of California, Berkeley). *J. Am. Chem. Soc.* **70,** 4268–4269 (1948). An ion-exchange technique is described for separating zirconium from hafnium. To measure the efficiency of the separation, 65-day Zr^{95} and 46-day Hf^{181} were used as tracers. Starting with a mixture of 15 mg of hafnium oxide and 35 mg of zirconium oxide, 10 mg of hafnium oxide containing ~ 0.1% zirconium oxide were obtained.

Compilation of thermal properties of hydrogen in its various isotopic and ortho-para modifications, H. W. Woolley, R. B. Scott, F. G. Brickwedde (Natl. Bur. of Standards, Washington, D. C.), *J. Research Natl. Bur. Standards* **41,** 379–475 (1948). The available, and some new thermal data for H_2, HD, and D_2 in solid, liquid and gaseous states are given. Included are the properties of ortho and para forms of H_2 and D_2, together with an extensive bibliography.

On the existence of an excited state of the deuteron, S. Nakagawa (The Scientific Research Inst., Ltd., Tokyo). *J. Sci. Res. Institute (Tokyo)* **43,** 10–20 (1948). An investigation was carried out of the effects of an excited state of the deuteron, using Flügge's interaction potential, on the properties of the two-particle neutron-proton system. The values of total cross sections of various neutron-proton interactions agreed fairly well with the experimental values, when the range of nuclear force was taken as 2.3×10^{-13} cm and an excited state $^3P_1$ at 0.8 Mev was assumed.

. . . I. W. RUDERMAN

LIFE SCIENCE PUBLICATIONS

Determination of circulating red blood cell volume with radioactive phosphorus, R. Nieset, B. Porter, W. Trautman, Jr., R. Bell, W. Parson, C. Lyons, H. Mayerson (Lab. of Biophysics, Dept. of Medicine, Tulane Univ., New Orleans, La.), *Am. J. Physiol.* **155,** 226–231 (1948). A method is presented for directly determining total circulating red blood cell volume by the isotope dilution technique using radiophosphorus. The exposed cells take up radiophosphorus rapidly and release it slowly. The results obtained agree closely with results obtained by different techniques.

Comparison of results of measurements of red blood cell volumes by direct and indirect techniques, H. Mayerson, C. Lyons, W. Parson, R. Nieset, W. Trautman, Jr., (Dept. of Medicine, Tulane Univ., New Orleans, La.). *Am. J. Physiol.* **155,** 232–238 (1948). Simultaneous determinations of red cell mass and plasma volume were made using the P-32 tech-

nique and the T-1824 method. There was satisfactory agreement. A comparison of the peripheral and body hematocrites also showed good agreement.

Effect of the administration of adrenalin on the circulating red cell volume, W. Parson, H. Mayerson, C. Lyons, B. Porter, W. Trautman, Jr. (Dept. of Medicine, Tulane Univ., New Orleans, La.), *Am. J. Physiol.* **155,** 239–241 (1948). No uniform or significant changes in the plasma or red blood cell volumes due to subcutaneous injection of adrenalin was detected by either the P-32 or T-1824 techniques.

Fifty years of radium, E. Quimby (Coll. of Physicians and Surgeons, Columbia Univ., N. Y.), *Am. J. Roentgenol. Radium Therapy* **60,** 723–730 (1948).

The achievement of radium in the fight against cancer, S. Cade (Westminster Hosp. and the Radium Inst., London), *Am. J. Roentgenol. Radium Therapy* **60,** 731–740 (1948).

Effective dosage levels in interstitial radium therapy, B. Jolles (Radiotherapy Dept., General Hosp., Northampton, England), *Am. J. Roentgenol. Radium Therapy* **60,** 745–749 (1948). A quantitative method is given for determining effective tolerance dose levels in interstitial radiotherapy of malignant growths.

A concept of the clinical use of radium, A. Arneson (Washington Univ. School of Medicine, St. Louis, Mo.), *Am. J. Roentgenol. Radium Therapy* **60,** 741–744 (1948).

Application of artificial radioactive isotopes in therapy—I. Cobalt, W. Myers (Coll. of Medicine, Ohio State Univ., Columbus) *Am. J. Roentgenol. Radium Therapy* **60,** 816–823 (1948).

Preparation of *p*-dimethylaminoazobenzene containing isotopic nitrogen, W. Fones, J. White (National Cancer Institute, Bethesda, Md.), *Arch. Biochem.* **20,** 118–124 (1949). *p*-Dimethylaminoazobenzene labeled with N^{15} in all three possible positions has been prepared.

The effect of age on calcium binding in mouse liver, A. Lansing, T. Rosenthal, M. Kamen (Dept. of Anatomy, Washington Univ., St. Louis, Mo.), *Arch. Biochem.* **20,** 125–130 (1949). A study was made of the distribution of Ca^{45} in livers of old and young mice. Free calcium was separated from bound calcium by ultrafiltration. In young tissue calcium uptake is low and is subject to rapid turnover. In old tissue calcium uptake is high and is subject to slow turnover. It is suggested that intracellular calcium may be largely associated with a lipide and a ribonucleoprotein.

The effect of substrates on the endogenous metabolism of living yeast, J. Reiner, H. Gest, M. Kamen (Washington Univ. School of Medicine, St. Louis, Mo.), *Arch. Biochem.* **20,** 175–177 (1949). "Endogenous" metabolism in yeast is accelerated by the presence of substrate. The existence of a reserve of metabolic intermediates common to both "endogenous" and "exogenous" metabolism and the ease of exchange between cell fractions show that the manometric correction used in assimilation experiments cannot be directly obtained from data on isotopic exchange.

The cutaneous absorption of radon from naturally carbonated mineral water and plain water baths, W. McClellan, C. Comstock (Albany Med. Coll., Saratoga Springs, N. Y.), *Arch. Phys. Med.* **30,** 29–36 (1949). Experiments performed indicate that radon is absorbed through the skin and is absorbed in greater amounts from water containing carbon dioxide than from plain water. The elimination of radon is rapid and complete in three hours. The beneficial effects of baths containing radon is due to the absorption of radon through the skin and inhalation of radon from air over the tub.

The response of the thyroid gland in normal human subjects to the administration of thyrotropin as shown by studies with I^{131}, M. Stanley, E. Astwood, (Joseph H. Pratt Diagnostic Hosp., Boston, Mass.), *Endocrinology* **44,** 49–60 (1949). With radioiodine, studies were made of the effects of a single dose of thyrotropin upon the rate of uptake by the thyroid. For the first 8 hours following injection there was no detectable change. Thereafter a marked increase reaching a peak at 24 to 48 hours was noted. The turnover rate returned to normal in four to five days. It was not possible to detect any loss of stored thyroid hormone.

Ionizing radiation injury. Its diagnosis by physical examination and clinical laboratory procedures, E. Cronkite (Naval Research Inst., Bethesda, Md.), *J. Am. Med. Assoc.* **139,** 366–369 (1949). A single excessive serious exposure to ionization radiation is evidenced by marked lymphocytopenia followed by a characteristic sequence of events in the other

leukocyte members. The diagnosis of repeated exposures to lesser amounts of ionizing radiation requires blood studies and differential counts of radiation in urine, fecal, and nasal secretions. The principal protection from ionizing radiation is physical control of radiation intensities by establishing monitoring procedures and prevention of contamination of personnel by radioactive materials.

Tracer studies on the role of acetic acid and carbon dioxide in the fermentation of lactate by clostridium lacto-acetophylum, J. Bhat, H. Barker (Div. of Plant Nutrition, Univ. of California, Berkeley), *J. Bact.* **56,** 777–779 (1948). Bacteria in enrichment cultures of clostridium lacto-acetophylum convert carbon dioxide to acetic and butyric acids. In pure culture, carbon dioxide is not reduced by the organism but it can oxidize lactate to acetate and then convert it to butyrate.

The metabolism of thiocyanate in the rat and its inhibition by propylthiouracil, J. Wood, E. Williams, Jr., (Dept. of Chemistry, Univ. of Tennessee, Memphis), *J. Biol. Chem.* **177,** 59–67 (1949). Thyroid gland protein fixes thiocyanate sulfur to a greater degree than does any other tissue protein. This ability is impaired by propylthiouracil treatment. Water-soluble compounds containing radioactive sulfur accumulated in the thyroid but not in liver, muscle, adrenals or plasma. Propylthiouracil treatment inhibited the formation of these products. The thiocyanate level in all tissues decreased as the plasma level decreased. These and other findings are interpreted in terms of a metabolic antagonism of thiocyanate for iodide.

The production of radioactive cystine by direct bombardment in the pile, E. Ball, A. Solomon, O. Cooper (Dept. of Biol. Chem., Harvard Med. School, Boston, Mass.), *J. Biol. Chem.* **177,** 81–89 (1949). Various degradative procedures show that all of the radioactivity in cystine bombarded by the pile was due to the sulfur atom. The cystine obtained has a specific activity of 112,000 counts per millimole per minute.

Distribution and metabolism of iodo-α-estradiol labeled with radioactive iodine, S. Albert, R. Heard, C. Leblond, J. Saffran (Dept. of Anatomy and Biochemistry, McGill Univ., Montreal, Can.), *J. Biol. Chem.* **177,** 247–266 (1949). The most noteworthy aspect of the metabolism of the iodinated α-estradiol in male and female mice is the accumulation of labeled substances in the gastrointestinal tract, entry into which occurs predominantly via the liver and bile. Much of the material is excreted in the feces. The highest concentration of radioactivity was found in the mammary glands especially during pregnancy when the accumulation is markedly increased. Only a small part if any of the radioactivity is combined in a conjugated form in the small intestine, liver, mammary glands and urine.

Excretion of radioactive carbon dioxide by rats after administration of isotopic bicarbonate, acetate, and succinate, R. Gould, F. Sinex, I. Rosenberg, A. Solomon, A. Hastings (Dept. of Biol. Chem., Harvard Med. School, Boston, Mass.), *J. Biol. Chem.* **177,** 295–301 (1949). After four hours the cumulative excretion of carbon dioxide was 95% for bicarbonate, 87% for acetate and 86% for succinate. For the first sixty minutes the excretion of $C^{14}O_2$ appeared to be first order. The rates of change of specific activity of the carbon dioxide were interpreted in the light of the metabolic reactions of the injected substances.

Note on the synthesis of succinic acid labeled in the carboxyl position with radioactive carbon, Y. Topper (Dept. of Biol. Chem., Harvard Med. School, Boston, Mass.), *J. Biol. Chem.* **177,** 303–304 (1949). C^{14}-succinic acid was prepared from isotopic barium carbonate via acetelynedicarboxylic acid in 11% over-all yield.

The metabolism of curium in the rat, K. Scott, D. Axelrod, J. Hamilton (Div. of Radiol. and Med., Univ. of California, Berkeley), *J. Biol. Chem.* **177,** 325–335 (1949). Approximately five-sixths of the curium is absorbed from the site of injection during the first 16 days. Curium is primarily deposited in the liver and skeleton and eliminated from the soft tissues of the body primarily via the gastrointestinal tract. It is retained by the skeleton for long periods of time. Curium and americium are similarly metabolized by the rat.

Hemin synthesis in rabbit bone marrow homogenates, K. Altman, K. Salomon, T. Noonan (School of Medicine and Dentistry, Univ. of Rochester, New York), *J. Biol. Chem.* **177,** 489–490 (1949). Experiments indicate that rabbit bone marrow can synthesize hemin from methylene-C^{14}-labeled glycine. Whether or not globin synthesis occurs is uncertain.

Genetic differences in methionine uptake by surviving tissue, R. Rutman, E. Dempster, H. Tarver (Div. of Biochem., Med. School, Univ. of California, Berkeley), *J. Biol. Chem.* **177,** 491–492 (1949). Two inbred strains of rats were compared for their ability to incorporate methionine into surviving liver slices. The results show a consistent and markedly large difference between the two strains.

Orotic acid, a precursor of pyrimidines in the rat, S. Bergström, H. Arvidson, E. Hammarsten, N. Eliasson, P. Reichard, H. Ubisch (Biochem. Dept., Karolinska Institutet, Stockholm), *J. Biol. Chem.* **177,** 495 (1949). Orotic acid containing N^{15} has been synthesized. It is shown that orotic acid was utilized in the biosynthesis of both uracil and cytosine.

The biologic decay periods of sodium in normal man, in patients with congestive heart failure, and in patients with the nephrotic syndrome as determined by Na^{22} as the tracer, S. Threefoot, G. Burch, P. Reaser (Tulane Univ. School of Medicine, New Orleans, La.), *J. Lab. Clin. Med.* **34,** 1–13 (1949). Studies were made of the rates of elimination of isotopic sodium in normal man and in man suffering from chronic congestive heart failure or chronic glomerulonephritis of the nephrotic type. Compared to that of normal man, the time necessary to reduce the serum concentration to one half of the initial level after establishment of equilibrium was three times as long in patient with chronic congestive heart failure and five times as long in presence of nephrotic syndrome.

Theoretical considerations of biologic decay rates of isotopes, G. Burch, S. Threefoot, J. Cronvich (Tulane Univ. School of Medicine, New Orleans, La.), *J. Lab. Clin. Med.* **34,** 14–30 (1949). Treated mathematically are the influence of variation of intake and output of nontracer substances and of the size of its compartment upon the concentration of a tracer substance administered in a single dose within an organism and its elimination from the organism. The importance of controlling factors which affect the rate of elimination and the size of the compartment of the nontracer substance is stressed.

Biological studies with arsenic^{74}—II. Excretion and tissue localization, H. Ducoff, W. Neal, R. Straube, L. Jacobson, A. Brues (Dept. of Biology, Argonne Natl. Lab., Chicago, Ill.), *Proc. Soc. Expertl. Biol. Med.* **69,** 548–554 (1948). Comparison studies were made of arsenic excretion in man, rabbits and rats. Data are given for arsenic distribution in various organs. The rat retains most of the injected dose in the blood stream for a considerable period of time. Arsenic distribution is altered by the presence of transplanted tumor. The effect of the presence of substances containing sulfhydryl groups on arsenic distribution are discussed.

Metabolism of C^{14}-labeled urea, E. Leifer, L. Hempelman (Los Alamos Scientific Lab., Los Alamos, N. Mex.), *Science* **108,** 748 (1948). A total of 20.8% of the injected isotope of urea appeared in the exhaled carbon dioxide at the end of 48 hours. C^{14} was distributed in tissue uniformly on a weight basis within 25% in liver, heart, spleen, muscle, brain and blood. Kidneys contained a markedly high proportion of the isotope. The mechanism of carbon dioxide formation has not been established.

Oxidation of parenterally administered C^{14}-labeled tripalmitin emulsions, S. Lerner, I. Chaikoff, C. Entenman, W. Dauben (Dept. of Chemistry, Univ. of California, Berkeley), *Science* **109,** 13 (1949). Palmitic acid labeled in the sixth carbon was administered intravenously in the form of its glycerol ester into fasting rats. The exhaled carbon dioxide was collected and its isotopic content determined. At the end of 24 hours approximately one half of the radioactivity was expired. The maximum rate of exhalation was observed during the second and fourth hours. About 50% of the injected labeled fatty acids recovered in the liver were incorporated into phospholipids at the end of 24 hours. From these data it is concluded that emulsified fat introduced directly into the blood stream pursues a normal metabolic path.

The zone of localization of anti-mouse-kidney serum as determined by radioautographs, D. Pressman, R. Hill, F. Foote (Sloane-Kettering Inst. for Cancer Research, New York), *Science* **109,** 65–66 (1949). Mice were injected intravenously with a radioiodinated globulin fraction of anti-mouse-kidney serum and autographs of the kidney tissue were then obtained. A definite accumulation of radioactivity was noted around the cortex, particularly in the glomeruli of the kidney.

. . . BERNARD KANNER

PHYSICAL PUBLICATIONS

The second shower maximum in Au, Hg, and Pb, J. Clay, W. L. Scheen (Univ. of Amsterdam, the Netherlands), *Physica* **14,** 489–494 (1948). The number of two, three, and four-fold coincidences was measured by counters disposed at various angles under various thicknesses of these substances. The resulting shower curves show two maxima. The coincidences between inner and outer pairs of particles also show maxima. It is concluded that the second maximum is due to coincidences between a meson and its knock-on electron. Higher-order coincidences are due to further secondary electrons from the meson, or electrons in cascade with the first.

The production of meson pairs in various materials, J. Clay (Univ. of Amsterdam, the Netherlands), *Physica* **14,** 495–498 (1948). Coincidence measurements on meson pairs produced in water, paraffin, Al, Fe, and Pb and passing through 10 cm of lead indicate that the angle between them is less than 24°. The initiating radiation, 1/16,000 of the meson component of cosmic radiation, is non-ionizing (probably a photon), as indicated by the variation of its absorption in the various materials. No correlation is found between extensive showers and the primary particle for the meson pairs.

The spectrum of the soft, electronic, part of the cosmic radiation, J. Clay (Univ. of Amsterdam, the Netherlands), *Physica* **14,** 499–503 (1948). By using absorbing layers of Pb and Al which are equivalent for mesons, the difference in total absorption gives the number of cosmic-ray electrons between the two energy values corresponding to these thicknesses on the range-energy curve. The energy spectrum so determined had an exponent of −1.27 for Pb-Al layers, and −1.35 for measurements with Fe and C.

Penetration of nucleons through heavy nuclei, G. C. J. Zwanikken (Univ. of Utrecht, the Netherlands), *Physica* **14,** 530–541 (1948). By means of a meson potential well, the collision cross section for fast nucleons and a nucleus represented by a Fermi gas of the neutrons and protons was calculated by using the Born approximation. The probabilities of various energy transfers were also computed, as was the energy distribution of the particles knocked out of the nucleus. The energy loss of the nucleon inside the nucleus was derived, and the results applied to the theory of high-energy stars.

Threshold and resonances in $C^{14}(p,n)N^{14}$ reaction and energy levels of N^{15}, W. E. Shoupp, B. Jennings, K. H. Sun (Westinghouse Research Labs, East Pittsburgh, Pa.), *Phys. Rev.* **75,** 1–7 (1949). Using an electrostatic generator, a thin barium carbonate target containing C^{14} was bombarded with protons and the resulting neutrons counted. The measured threshold sets an upper limit to the neutrino mass. The resonances observed allow the calculation of the N^{15} energy levels. Assuming a certain angular distribution of neutrons, the cross section was calculated.

Total cross sections of nuclei for 90-Mev neutrons, L. J. Cook, E. M. McMillan, J. M. Peterson, D. C. Sewell (Univ. of California, Berkeley), *Phys. Rev.* **75,** 7–14 (1949). The cross sections for nuclei from H to U for a neutron beam of average energy 90 Mev with a 25-Mev half-width were determined by measuring the attenuation of the beam on passing through blocks of various materials, with good geometry. The neutrons were detected by measuring the activity produced in carbon disks by the reaction $C^{12}(n,2n)C^{11}$. An empirical relation for cross section as a function of atomic weight is given, and briefly discussed in relation to the transparent nucleus theory.

On simultaneous beta-gamma emission from nuclei, C. L. Longmire (Univ. of Rochester, N. Y.), *Phys. Rev.* **75,** 15–17 (1949). For very highly forbidden beta decay, a possible alternative is simultaneous emission of a beta particle, a neutrino, and a photon, which avoids the usual selection rules. Though the fact of a compound transition would ordinarily reduce its relative probability by 10^3, the net forbiddenness may be less by enough to allow observation of the phenomenon. The lifetime for a compound transition of this type is estimated at 10^6–10^7 years, and those alternative direct beta transitions which are absolutely forbidden are listed.

The fission of thorium with alpha-particles, A. S. Newton, (Univ. of California, Berkeley), *Phys. Rev.* **75,** 17–29 (1949). The distribution of the fission products for fission of thorium by 37.5-Mev alpha particles was chemically studied. Compared with the curve for slow neutron fission of U^{235}, the two peaks in the curve were lowered, and the elements in the

characteristic dip in the fission yield mass spectrum were increased in abundance. This was related to the excess excitation in the fissioning nucleus. The cross section was 0.6 barns, the threshold about 23 Mev.

Radiations of uranium Y, G. B. Knight, R. L. Macklin (Carbide and Carbon Chemicals Corp., Oak Ridge, Tenn.), *Phys. Rev.* **75,** 34–38 (1949). Absorption measurements in aluminum on UY, a member of the series of U^{235}, with 25.5-hour half-life, indicated a 210-kev beta-ray and a 35-kev gamma-ray 82% converted in the *L* shell.

Experiments on the effect of atomic electrons on the decay constant of Be^7, E. Segrè, C. E. Wiegand (Univ. of California, Berkeley), *Phys. Rev.* **75,** 39–43 (1949). Elements decaying by orbital electron capture should have their decay constants changed by alteration of the atomic electron wave functions, since the probability of decay is proportional to the square of the electronic wave function at the nucleus. By using Be and BeO, the variation due to the difference in chemical structure was found to be about 10^{-4}. A method is described for rapid measurement of fairly long half-lives by balance against a practically constant source in an ionization chamber.

Gamma-rays from deuteron reactions, D. E. Alburger (Yale Univ., New Haven, Conn.), *Phys. Rev.* **75,** 51–56 (1949). The energies of gamma rays given off by various target materials following deuteron bombardment were determined by coincidence absorption of Compton electrons. Compton distributions were also examined by means of a magnetic lens spectrometer in some cases. Certain energy levels are identified with ones previously found by other methods. Moderately high gamma-ray energies predominate.

Isotope shifts in uranium spectra, L. E. Burkhart, G. Stukenbroeker, S. Adams (Carbide and Carbon Chemicals Corp., Oak Ridge, Tenn.), *Phys. Rev.* **75,** 83–85 (1949). The isotopic shift of U^{238}, U^{235}, and U^{233} in the emission spectrum (as taken from the spark spectrum of U_3O_8) was studied, and was sufficient to determine the concentration of the components in a mixture by using spectrographic analysis. The results, compared with those from a mass spectrometer, are of comparable precision.

The electrostatic interaction and low-energy particles in alpha-radioactivity, M. A. Preston (The University, Birmingham, England), *Phys. Rev.* **75,** 90–99 (1949). In an attempt to explain previously reported low-energy groups of alphas, a process by which the asymmetry of the motion of electric charges in the residual nucleus causes an interaction with an alpha particle already emitted is considered. It is found that to reconcile experimental data with this explanation, very improbable assumptions are required.

Measurement of the radioactive decay constant of ThC′ using a coincidence method, F. W. Van Name, Jr. (Yale Univ., New Haven, Conn.), *Phys. Rev.* **75,** 100–103 (1949). Electrons from ThC and alphas from the resulting ThC′ are counted by two different counters next to a source. The output from the electron counter is fed into a coincidence arrangement with the other pulse, after traversing a variable known delay line, while the alpha count encounters a small fixed delay. The coincidence rate as a function of the variable delay gave the half-life of ThC′ as $(2.2 \pm 0.1) \times 10^{-7}$ sec. The resolving time of the coincidence circuit was about 10^{-8} sec. The effect of variation of pulse formation time was considered, and results of the theory were compared with experiment.

The magnetic internal conversion coefficient, S. D. Drell (Univ. of Illinois, Urbana), *Phys. Rev.* **75,** 132–136 (1949). The magnetic internal conversion coefficient for *K*-shell electrons, calculated using the Dirac current for the electron, is shown to be comparable to the electric conversion in importance. The influence of this effect on *K*- to *L*-shell conversion ratios is discussed.

The effect of crystal orientation on the scattering of slow neutrons, G. P. Arnold, V. W. Myers, A. H. Weber (Argonne Natl. Lab., Chicago, Ill.), *Phys. Rev.* **75,** 217–220 (1949). A mechanical velocity selector together with a pile was used to measure cross sections of powdered and extruded graphite. The theory of the effect of nonrandom orientations on neutron scattering with a single symmetry axis was developed, and the results checked with experiment.

Radiations from Cd^{115}, In^{115*}, and Hf^{181}, C. E. Mandeville, M. V. Scherb, W. B. Keighton (Bartol Research Foundation, Franklin Institute, Swarthmore, Pa.), *Phys. Rev.* **75,** 221–226 (1949). The characteristic radiations of these three isotopes were investigated by coincidence-

absorption methods. Cd^{115} has a beta-ray group of 0.46 Mev. Four-hour In^{115*} decays with the emission of a single partially converted gamma ray. Hf^{181} emits 0.52 Mev betas and 0.17 and 0.47 Mev gammas.

Radiations from Hf^{181}, K. Y. Chu, M. L. Wiedenbeck (Univ. of Michigan, Ann Arbor), *Phys. Rev.* **75,** 226–231 (1949). A continuous beta-ray group of maximum energy 0.404 Mev was found, along with four partially converted gamma rays. A disintegration scheme is proposed. Relative intensities of the gamma rays were estimated from Compton and photoelectron intensities.

Evidence for a new isotope of potassium, R. Overstreet, L. Jacobson, P. R. Stout (Univ. of California, Berkeley), *Phys. Rev.* **75,** 231–233 (1949). Bombardment of argon by 40-Mev alpha-particles produces a 22.4-hour half-life. The radioisotope in question decays by emission of 0.8 and 0.25 Mev beta rays (from photographic measurements in a magnetic spectrometer) and a 0.4 Mev gamma ray. The reaction is identified as $A^{40}(\alpha,p)K^{43}$.

Absolute voltage determination of three nuclear reactions, R. G. Herb, S. C. Snowdon, O. Sala (Univ. of Wisconsin, Madison), *Phys. Rev.* **75,** 246–259 (1949). By knowing the analyzer voltage together with the analyzer geometry, an absolute determination of proton energy from the Wisconsin electrostatic generator was made possible. By this method, an absolute voltage determination was made for the $Li^7(p,n)Be^7$ threshold (1.882 Mev), an $Al^{27}(p,\gamma)Si^{28}$ resonance (0.9933 Mev), and a $F^{19}(p,\alpha\text{-}\gamma)O^{16}$ resonance (0.8735 Mev). The uncertainties were all $\sim 0.1\%$.

Screening and relativistic effects on beta-spectra, C. Longmire, H. Brown (Columbia Univ., New York, N. Y.), *Phys. Rev.* **75,** 264–270 (1949). The effect of the atomic electron distribution on the shape of the positron and electron beta spectra is calculated approximately for various values of Z. A more accurate expression for the relativistic Coulomb factor is also evaluated for various cases.

Grain density in photographic plates of heavy particles, M. Blau (Columbia Univ., New York, N. Y.), *Phys. Rev.* **75,** 279–282 (1949). A semi-empirical formula is given for the probability of development of a grain in a photographic emulsion as a function of the slope of the range-energy curve (two experimental constants must be determined). From this a relation between grain density and particle energy is derived, which fits all experimental curves extant for alphas, tritons, protons, π- and μ-mesons.

Radioactivity of C^{10} and O^{14}, R. Sherr, H. R. Muether, M. G. White (Princeton Univ., Princeton, N. J.), *Phys. Rev.* **75,** 282–292 (1949). Proton bombardment of solid targets followed by alcohol flushing of the gaseous products indicated two activities. They were formed by the reactions $N^{14}(p,n)O^{14}$ and $B^{10}(p,n)C^{10}$. O^{14} has a 76.5-sec half-life, and emits a 1.8-Mev positron and a 2.3-Mev gamma ray, probably in cascade. C^{10} has a 19.1-sec half-life and emits a 2.2-Mev positron and a gamma-ray of about 1 Mev. The Coulomb energy difference in mirror nuclei is verified by this case. The ft values are 2,000–3,000 for the transitions to excited states, indicating forbidden spectra for transition to the ground states. This is difficult to reconcile with the spin changes.

The scattering of fast β-particles through large angles by nitrogen nuclei, F. C. Champion, R. R. Roy (Univ. of London, England), *Proc. Phys. Soc.* **61,** 532–535 (1948). A standard cloud chamber was fitted with counter control so that photographs were made only when β-particles were deflected by more than 85°. Elastic large-angle scattering data was thus obtained for β-energies of about 1 Mev. The results agree with Mott's theory.

The penetrating particles in cosmic-ray showers—II. The lightly-ionizing penetrating particles in penetrating showers, G. D. Rochester, C. C. Butler (The University, Manchester, England), *Proc. Phys. Soc.* **61,** 535–541 (1948). Cloud-chamber measurements were made on the momentum spectrum of penetrating particles in showers containing more than one such particle. The momenta were of the order of 10^9 ev/c. Most of these particles were positive, and probably were protons and π- or heavier mesons.

Note on nuclear magnetic resonance, E. E. Schneider (Univ. of Durham, Newcastle-on-Tyne, England), *Proc. Phys. Soc.* **61,** 569–571 (1948). The discrimination against noise is increased by using the frequency selectivity of an oscillating system regeneratively maintained in a nonlinear manner. This has been applied to detection of very weak nuclear resonances.

(Continued on page 94)

HIGH-ACCURACY RADIATION STANDARDS

For calibration of Geiger counters and other instruments, U. S. Radium offers a new type as well as the conventional type

For dependable, accurate calibration of Geiger counters, ionization chamber survey instruments, and radiation dosage meters, the United States Radium Corporation now offers two types of standards. The conventional type consists of hermetically sealed capsules containing a radium salt.

The new type is based on the incorporation of radium, or related element, in foil. This type is available as a point source or as a linear source, calibrated for alpha, beta, and gamma radiations. It offers new latitude in design—makes possible fitting the configuration of the standard to the specific instrument or counter tube. It also makes possible accurate duplication of standards.

VARIOUS SOURCES

While radium is a suitable source of radiation and is used in most of these standards, frequently arrangements can be made to supply standards utilizing a source of either virtually pure beta or gamma radiation alone.

NEED FOR SUCH STANDARDS

The original calibration of instruments for measuring radiation usually becomes altered by mechanical shock, vibration, weakening of the power supply, radioactive contamination of the equipment, aging of the counter tube, and other causes. In time, recalibration is necessary. U. S. Radium Radiation Standards meet the most exacting needs of research, industry, and medicine for recalibration or on-the-spot checking of radiation measuring equipment. We will be pleased to answer your inquiry about them.

US RADIUM

Please address Dept. X-9

UNITED STATES RADIUM CORPORATION

535 Pearl Street New York 7, N. Y.

Nuclear β-spectra of thorium B → C and C → C′, and the intensity of some β-ray lines of thorium (B + C + C″), D. G. E. Martin (Univ. of Liverpool, England), H. O. W. Richardson (Univ. of Edinburgh, Scotland), *Proc. Roy. Soc.* **A195,** 287–300 (1948). The continuous spectrum of ThC → C′, after subtracting the ThC″ → D spectrum, is of the allowed shape down to 0.9 Mev and is probably complex. A possible level scheme, with spins, for ThC′ is given. ThB has a spectrum of two groups. The internal conversion coefficients for the *F* gamma-ray is 0.377.

Orbital stability in a proton synchrotron, R. Q. Twiss, N. H. Frank (Massachusetts Inst. of Technology, Cambridge), *Rev. Sci. Instr.* **20,** 1–17 (1949). The operation of a proton synchrotron is discussed, with emphasis on the oscillations. The problems of injection and stability are considered for the initial betatron acceleration. Application is made to a 10-Bev model.

Improved magnetic focusing of charged particles, L. Kerwin (Laval Univ., Quebec, Can.), *Rev. Sci. Instr.* **20,** 36–41 (1949). The general theory of wedge-shaped magnetic focusing devices is given. Perfect focusing and approximations which lead to aberrations are considered, and a method for eliminating those of second order is derived.

A Geiger-Müller counting unit and external quenching equipment for the estimation of C^{14} in carbon dioxide, W. B. Mann, G. B. Parkinson (Natl. Research Council, Chalk River, Ontario, Can.), *Rev. Sci. Instr.* **20,** 41–47 (1949). To compensate for end effects in counters filled with the gas to be assayed, a long and a short counter are used and the difference in the number of counts measured. A quenching unit based on a multivibrator circuit allows arbitrary variation of counter voltage, and plateaus of about 200 volts are thus obtained.

The statistical theory of the dead time losses of a counter, C. E. Clark (Emory Univ., Emory Univ., Ga.), *Rev. Sci. Instr.* **20,** 51–52 (1949). Derived is the statistical distribution of the actual number of events occurring, when the number recorded by a counter is known. The result approximates a normal distribution, and an approximation is given for the standard deviation.

. . . HAROLD BROWN

Radiation Components New—unique—superfine

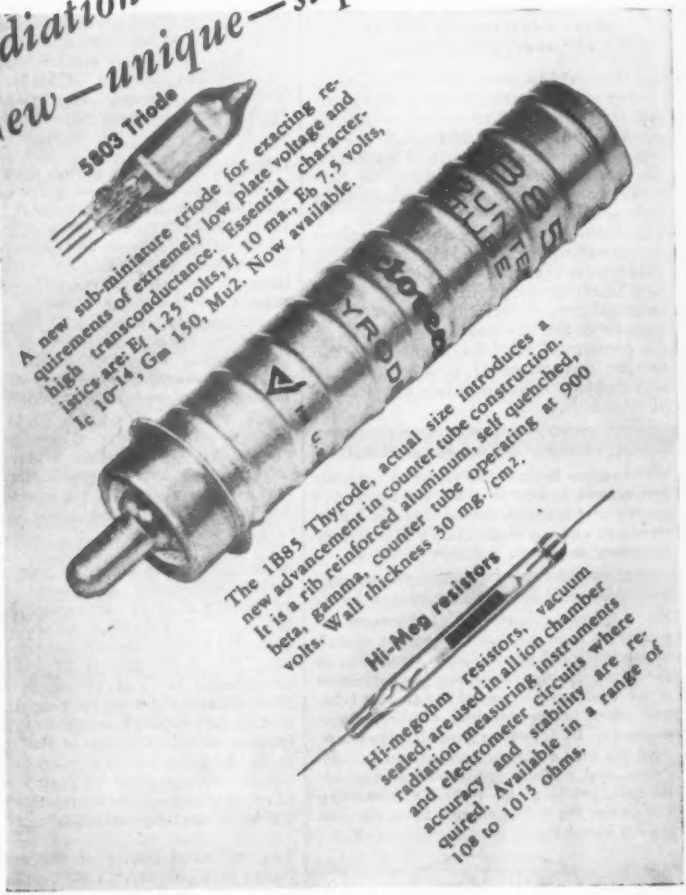
5803 Triode
A new sub-miniature triode for exacting requirements of extremely low plate voltage and high transconductance. Essential characteristics are: Ef 1.25 volts, If 10 ma., Eb 7.5 volts, Ic 10⁻¹⁴, Gm 150, Mu2. Now available.
The 1B85 Thyrode, actual size introduces a new advancement in counter tube construction. It is a rib reinforced aluminum, self quenched, beta, gamma, counter tube operating at 900 volts. Wall thickness 30 mg./cm2.
Hi-Meg resistors
Hi-megohm resistors, vacuum sealed, are used in all ion chamber radiation measuring instruments and electrometer circuits where accuracy and stability are required. Available in a range of 10⁸ to 10¹³ ohms.

Victoreen

5806 HOUGH AVENUE CLEVELAND 3, OHIO